Summer 2020

Synthesis and thermodynamic characterization of free and surface water of colloidal unimolecular polymer (CUP) particles utilizing DSC and TGA

Peng Geng

Department: Chemistry

SYNTHESIS AND THERMODYNAMIC CHARACTERIZATION OF FREE AND SURFACE WATER OF COLLOIDAL UNIMOLECULAR POLYMER (CUP) PARTICLES UTILIZING DSC AND TGA

by

PENG GENG

A DISSERTATION

Presented to the Graduate Faculty of the

MISSOURI UNIVERSITY OF SCIENCE AND TECHNOLOGY

In Partial Fulfillment of the Requirements for the Degree

DOCTOR OF PHILOSOPHY

in

CHEMISTRY

2020

Approved by:

Dr. Michael R. Van De Mark, Advisor
Dr. Chariklia Sotiriou-Leventis
Dr. Jeffrey G. Winiarz
Dr. V Prakash Reddy
Dr. Baojun Bai

PUBLICATION DISSERTATION OPTION

This dissertation consists of the following three articles, formatted in the style used by the Missouri University of Science and Technology:

Paper I, found on pages 11–64, has been published by Polymers.

Paper II, found on pages 65–102, has been submitted to Polymers.

Paper III, found on pages 103–132, has been accepted by Journal of Coatings Technology and Research.

ABSTRACT

Colloidal Unimolecular Polymer (CUP) is spheroidal nanoscale polymer particle (3-9 nm) with charged hydrophilic gruops on the surface and a hydrophobic core. The formation of CUPs involves a simple free radical polymerization and a water reduction process. CUPs are thermodynamically stable in water, molecular weight, particle size and charge density can be designed and controlled. CUPs have a layer of surface associated water, due to the small particle size, the surface water/CUP volume ratio is ultra-high. Therefore, CUP is a very promising candidate to investigate the thermodynamic of surface water characteristics. In addition, CUP solution is free of surfactant and has zero volatile content, which exhibit great potential in coatings applications. DSC evaluation was performed to determine the characteristics of surface water. Surface water thickness varies from 0.427 to 0.766 nm, and it is charge density dependent. The surface water has a larger density than free water and increased with the increase in surface charge density. The specific heat of surface water was found to be 3.04~3.07 J/g·K at 253.15 K and 3.07~3.09 J/g·K at 293.15 K, which was larger than ice but smaller than free water. The average area occupied by carboxylate and ester groups on the CUP surface were determined to be 0.287 nm^2 and 0.374 nm^2. The evaporation rate of CUP solutions was investigated by TGA, results showed that CUP was capable to increase the evaporation rate of free water due to the deformation of air-water interface,caused by electrostatic repulsion. Surface water presented a much slower evaporation rate compared with free water, and did not evaporate until there is no free water. Thus, CUP was able to be used as an additive to give freeze thaw stability, wet edge retention and open time for coatings.

ACKNOWLEDGMENTS

First and foremost, I would like to express my gratitude and appreciation to my advisor, Dr. Michael R. Van De Mark for his continuous guidance, encouragement, and support through the course of pursuing my PhD. His creative and critical thinking has improved my research skills and prepared me for future challenges. I admire his personality, his hard-working attitude, and passion for science and research. It was a great honor for me to be part of his research group.

I want to extend my gratitude to my committee members, Dr. Chariklia Sotirious-Levntis, Dr. Jeffrey G. Winiarz, Dr. V Prakash Reddy, and Dr. Baojun Bai for their support and guidance throughout the completion of my PhD program.

I would like to thank my current and former lab members, Ashish Zore, Dr. Minghang Chen, Dr. Ameya Natu, Dr. Sagar Gade, Dr. Yousef Dawib, and Fei Zheng for their willingness to help and support for my research work. Further, I would like to thank Missouri S&T Coatings Institute and Department of Chemistry for financial support and other resources.

I am grateful to Dave Satterfield, Dr. Nathan D. Leigh, and all faculty and staff in the Department of Chemistry for their help at various occasions.

Last but not least, sincere gratitude and respect to my parents, Jian Geng and Junping Xing, for their unconditional and endless love, inspiration, encouragement, and financial support.

TABLE OF CONTENTS

Page

PUBLICATION DISSERTATION OPTION iii

ABSTRACT iv

ACKNOWLEDGMENTS v

LIST OF ILLUSTRATIONS xi

LIST OF TABLES xiv

NOMENCLATURE xvi

SECTION

1. INTRODUCTION 1

1.1. SINGLE CHAIN POLYMER NANOPARTICLE 1

1.2. TYPE OF SINGLE CHAIN POLYMER NANOPARTICLE 1

1.2.1. Single Rings Polymer Nanoparticle 2

1.2.2. Intramolecular Cross-linking Single Chain Polymer Nanoparticle 2

1.2.3. Pseudo-Globular Single Chain Polymer Nanoparticle 3

1.2.4. Reversible Self-folding Single Chain Polymer Nanoparticle 3

1.3. INTRODUCTION TO CUP 4

1.3.1. What is CUP 4

1.3.2. CUP Formation 4

1.3.3. Characterization of CUP 6

1.3.4. Advantages of CUP 6

1.4. SURFACE WATER..... 7

1.5. OBJECTIVE OF THIS STUDY..... 8

1.5.1. Characterization of Surface Water..... 8

1.5.2. Evaporation Rate of Free Water..... 9

1.5.3. Evaporation Rate of Surface Water..... 10

1.5.4. Application in Coatings..... 10

PAPER

I. THERMODYNAMIC CHARACTERIZATION OF FREE AND SURFACE WATER OF COLLOIDAL UNIMOLECULAR POLYMER (CUP) PARTICLES UTILIZING DSC..... 11

ABSTRACT..... 11

1. INTRODUCTION..... 12

2. EXPERIMENTAL..... 20

2.1. MATERIALS..... 20

2.2. SYSNTHESIS OF POLY(MMA/MAA) COPOLYMER..... 21

2.3. WATER REDUCTION METHOD..... 22

2.4. CHARACTERIZATION OF POLYMERS..... 22

2.4.1. Absolute Molecule Weight of Copolymers..... 22

2.4.2. Density of CUP Solutions..... 23

2.4.3. Density of Dry CUP Polymer..... 23

2.4.4. Acid Number (AN)..... 23

2.4.5. Viscosity of CUP Solution..... 23

2.4.6. Particle Size of CUP..... 24

2.4.7. Differential Scanning Calorimetry 25

3. RESULTS AND DISCUSSION 25

3.1. POLYMER SYNTHESIS AND CHARACTERIZATION 25

3.2. EFFECT OF COOLING RATE AND ICE FORMATION 27

3.3. WEIGHT FRACTION OF SURFACE WATER 35

3.4. SURFACE WATER DENSITY 40

3.5. SURFACE WATER THICKNESS 44

3.6. MELTING POINT DEPREESION 47

3.7. SPECIFIC HEAT ANALYSIS 52

4. CONCLUSION 56

ACKNOWLEDGEMENTS 58

REFERENCES 58

II. INVESTIGATION OF THE EVAPORATION RATE OF WATER FROM COLLOIDAL UNIMOLECULAR POLYMER (CUP) SYSTEMS BY ISOTHERMAL TGA 65

ABSTRACT 65

1. INTRODUCTION 66

2. EXPERIMENTAL 69

2.1. MATERIALS AND SYNTHESIS 69

2.2. THERMOGRAVIMETRIC ANALYSIS 69

3. RESULTS AND DISCUSSION 70

3.1. POLYMER SYNTHESIS AND CHARACTERIZATION 70

3.2. METHOD FOR EVAPORATION RATE DETERMINATION 71

3.3. EVAPORATION RATE OF FREE WATER FROM CUPS..... 73

3.4. EVAPORATION RATE OF SURFACE WATER..... 92

4. CONCLUSIONS..... 96

AUTHOR CONTRIBUTIONS..... 97

FUNDINGS..... 97

ACKNOWLEDGEMENTS..... 98

CONFLICTS OF INTEREST..... 98

REFERENCES..... 98

III. DSC AND TGA CHARACTERIZATION OF FREE AND SURFACE WATER OF COLLOIDAL UNIMOLECULAR POLYMER (CUP) PARTICLES FOR COATINGS APPLICATIONS..... 103

ABSTRACT..... 103

1. INTRODUCTION..... 104

2. EXPERIMENTAL..... 109

2.1. POLYMER SYNTHESIS..... 109

2.2. ABSOLUTE MOLECULAR WEIGHT OF COPOLYMERS..... 110

2.3. DENSITY OF DRY CUPS..... 110

2.4. DENSITY OF CUP SOLUTIONS..... 111

2.5. ACID NUMBER (AN)..... 111

2.6. VISCOSITY OF CUP SOLUTIONS..... 111

2.7. PARTICLE SIZE OF CUP..... 112

2.8. DIFFERENTIAL SCANNING CALORIMETRY..... 113

2.9. PAINT FORMULATION..... 113

2.10. FREEZE THAW STABILITY 113

2.11. WET EDGE RETENTION 114

2.12. PAINT VISCOSITY 114

2.13. THERMOGRAVIMETRIC ANALYZER 114

3. RESULTS AND DISCUSSION 115

3.1. HEAT OF FUSION 116

3.2. FREEZE/THAW STABILITY 121

3.3. EVAPORATION RATE 126

4. CONCLUSIONS 129

ACKNOWLEDGEMENTS 130

REFERENCES 130

SECTION

2. CONCLUSIONS AND FUTURE WORK 133

2.1. CONCLUSIONS 133

2.2. FUTURE WORK 135

BIBLIOGRAPHY 136

VITA 140

LIST OF ILLUSTRATIONS

SECTION Page

Figure 1.1. Scheme for controlled self-folding of single polymer chains induced by metal-ligand complexation....2

Figure 1.2. Scheme for synthesis of Unimolecular Polymeric Janus Nanoparticles and their self-assembly in a common solvent, DMF....3

Figure 1.3. Scheme for THE, DMPA, UV-light irradiation at 300-400 nm, rt, 90 min, [DODT]/[PGA]=1....3

Figure 1.4. Scheme for reversible self-folding of single polymer chains....4

Figure 1.5. Scheme for water reduction process, formation of CUP....6

PAPER I

Figure 1. CUP particles with surface water....13

Figure 2. Comparison of latex, polyurethane dispersion (PUD) and CUP (25.4k)....14

Figure 3. Formation of a typical CUP particle....15

Figure 4. Heat of fusion of 10.03% Polymer 1 with different isothermal time....28

Figure 5. Freezing of Latex polymers....29

Figure 6. Amount of surface water per CUP particle of Polymer 1 at 5.23%, 10.40% and 14.92% at different cooling rates....32

Figure 7. Amount of surface water per CUP particle of Polymer 1 at different weight fraction at different cooling rate....33

Figure 8. Amount of surface water per CUP particle of Polymer 1 at different weight fraction at 0.1 K/min and 10 K/min cooling rate....34

Figure 9. Heat of fusion of Polymer 1 solution at various weight fraction....36

Figure 10. Weight fraction of surface water of different CUPs with different monomer ratio vs weight fraction of each CUP....38

Figure 11. Weight fraction of surface water vs CUP particles of Polymer 1..... 40

Figure 12. Dependence of $1/\rho_s$ on weight fraction of Polymer 1 CUP solution..... 41

Figure 13. Surface water density vs charge density in ions per nm^2..... 43

Figure 14. Surface water thickness vs charge density in ions per nm^2..... 46

Figure 15. Molality of CUPs vs melting point depression..... 49

PAPER II

Figure 1. Evaporation rate of pure water, (a) raw data (b) with running average..... 72

Figure 2. Deviation of evaporation rate of water..... 73

Figure 3. Scheme of Photo of deionized water and CUP wetting and dry on platinum substrate..... 74

Figure 4. Evaporation rate of 5.47% Polymer 1 solution and water..... 75

Figure 5. Segments I, II, III, IV and V during the isothermal process..... 75

Figure 6. Evaporation rate of Polymer 1-6 solutions at various mM..... 76

Figure 7. Comparison of effective distance and interparticle distance for Polymer 1-4... 81

Figure 8. Scheme for deformation of water surface at air-water interface by CUP particles due to charge repulsion..... 82

Figure 9. Scheme for deformation of water at air-water interface by CUP particles due to charge repulsion..... 83

Figure 10. Evaporation rate of Polymer 4 solution at 4.71%, 10.34%, 16.92% and 20.16% in the first 2400 seconds..... 86

Figure 11. Evaporation rate of Polymer 1 and Polymer 4 solutions with different initial %solids concentrations..... 87

Figure 12. Evaporation rate of Polymer 2 (1.83 mmol/L) and Polymer 4 (1.87 mmol/L)..... 89

Figure 13. Evaporation rate at various percent solids for Polymer 1-6..... 91

Figure 14. Scheme for possibilities during surface water evaporation process..... 93

Figure 15. Evaporation rate of water at different solid%, (a) 5.04% Polymer 2, (b) 4.35% Poliymer 6..... 95

PAPER III

Figure 1. Water reduction process, formation of CUP..... 105

Figure 2. CUP with surface water and free water..... 106

Figure 3. Heat of fusion of water..... 116

Figure 4. Heat of fusion of 10.35% Polymer 2..... 117

Figure 5. 1/density vs solid% of Polymer 1..... 119

Figure 6. Heat of fusion of propylene glycol 9.96% in water..... 122

Figure 7. Freezing of Latex Polymers with CUP..... 125

Figure 8. Evaporation rate of water in 10.12% Polymer 1 CUP solution and pure water..... 127

Figure 9. Evaporation rate of water in 10.12 Polymer 1 CUP solution..... 128

LIST OF TABLES

PAPER I Page

Table 1. Polymer synthesis: the amount of materials used.....21

Table 2. Molecular weight, particle size, acid number and density of the polymers..... 27

Table 3. Density of surface water for Polymers 1-7.....42

Table 4. Surface water thickness of each CUP at different concentrations.....45

Table 5. Average area of each carboxylate and ester group on CUPs.....51

Table 6. Specific heat of each components in polymer 1-7 (J/gK)..... 54

Table 7. Specific heat of surface water associated with carboxylate and ester groups at 293.15 K (J/gK)..... 55

Table 8. Specific heat of surface water associated with carboxylate and ester groups at 253.15 K (J/gK)..... 56

PAPER II

Table 1. Molecular weight, particle size, acid number and density of the polymers..... 71

Table 2. Comparison of surface tension and evaporation rate of sodium salts..... 77

Table 3. Comparison of surface tension and evaporation rate of CUP solutions..... 78

Table 4. Diffusion coefficient of CUP particles at 298.15 K ($\times 10^{-6}$ cm^2/s)..... 85

Table 5. Percent solids for CUP Polymer 2&6 for HCP and RCP.....95

PAPER III

Table 1. Polymer synthesis, the amount of materials used.....110

Table 2. Molecular weight, particle size, acid number and density of the polymers..... 115

Table 3. Weight fraction of free water and CUP polymers..... 118

Table 4. Paint formulation of the master batch.....123

Table 5. Weight per gallon, % solids by weight, % solid by volume and PVC of the paint.....124

Table 6. Freeze thaw stability (KU viscosity)..... 124

Table 7. Wet edge retention and open time..... 129

NOMENCLATURE

Symbol	Description
CUP	Colloidal Unimolecular Polymer
DSC	Differential Scanning Calorimetry
THF	Tetrahydrofuran
VOC	Volatile organic content
MMA	Methyl Methacrylate
MAA	Methacrylic acid
AIBN	2,2'-azobis(2-methylpropionitrile)
ASTM	American Society fro Testing and Materials
η	Viscosity
ρ_v	charge density in ions per nm^2
r	radius
M	molecular weight
ρ	density
m	mass
ΔH	heat of fusion
X	weight fraction
N_A	Avogadro constant
ϕ	volume fraction
λ	surface water thickness
b	molality

K_F	cryoscopic constant
V	volume
i	van't Hoff factor
C	specific heat
q	heat flow rate
ϱ	evaporation rate
F	electrostatic repulsion
K_0	Coulomb's constant
E	electrostatic repulsion effect
p	vapor pressure
A	surface area
R	gas constant
α	evaporation coefficient
k	calibration coefficient

1. INTRODUCTION

1.1. SINGLE CHAIN POLYMER NANOPARTICLE

Polymer nanoparticles based on single polymer chain have seen major development over the past two decades. The formation is mainly based on the collapsing or folding of individual polymer chain [1-4], with a particle size ranging from 1 to 20 nm [5]. These nanoparticles are expected to have unique properties and functionalities due to the small particle size, and the wide varieties of chemical compositions. Many scientists have devoted their efforts to control the conformation and dynamics of single chain polymers. However, the surface water associated with these particles in an aqueous system has seen less emphasis. The surface water and the nanoparticles effect on aqueous systems will be the focus of this dissertation. The specific type of single chain nanoparticle here is the Colloidal Unimolecular Polymer particle, CUP, which was developed by the Van De Mark group.

1.2. TYPES OF SINGLE CHAIN POLYMER NANOPARTICLE

There are many different approaches to the formation of single chain nanoparticles. The following represents a few examples of approaches being taken. In addition there are many examples of proteins which exhibit a globular particulate nature. The fullerene type structures as well as graphene are also single molecule particulates. None of the systems can be varied as to size and surface ion content easily nor are their preparation low cost. CUP can be readily varied and are low cost.

1.2.1. Single Rings Polymer Nanoparticle. Barner-Kowollik et al. developed a controlled self-folding single polymer chain, the employing of intra-chain nitrile-imine ligation with the presence of Pd(II) was the crosslinking method, shown in Scheme 1. The ratio of tetra-zole was adjusted to control the particle size and fluorescence properties. The particle size of the single chain metal complexes was reported to be 2.8 to 5.2 nm [6], shown in Figure 1.1.

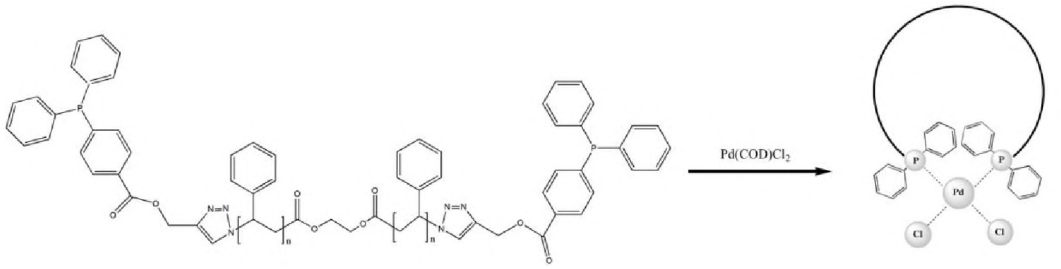

Figure 1.1. Scheme for controlled self-folding of single polymer chains induced by metal-ligand complexation.

1.2.2. Intramolecular Cross-linking Single Chain Polymer Nanoparticle. Zhu et al. formed unimolecular Janus tadpoles in dimethyl formamide. The formation of these Janus tadpoles involved intra-molecular crosslinking of poly(2-vinyl pyridine) (P2VP) using DBB. The intermolecluar crosslink was prohibited by the long end block, polystyrene (PS) and poly(ethylene oxide) (PEO). The particle size of Janus nanoparticle was concentration dependant, about 8.7 nm as unimolecular form at low concentraion (<2.0 mg/ml). When concentration is high, these nanoparticles aggregated into supermicelles, 50-100 nm [7], shown in Figure 1.2.

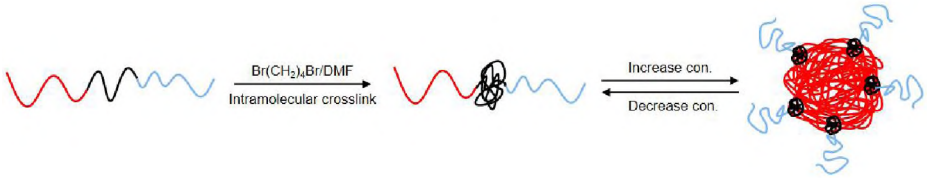

Figure 1.2. Scheme for synthesis of Unimolecular Polymeric Janus Nanoparticles and their self-assembly in a common solvent, DMF.

1.2.3. Pseudo-Globular Single Chain Polymer Nanoparticle. Pomposo et al. developed the synthesis of a nearly globular morphology in solution based on using both photo-activated radical-medicated thiol-yne coupling reaction and crosslinker. The intramolecular crosslinking resulted to the collapse/folding and the global shape. The particle size was 10±3 nm [8], shown in Figure 1.3.

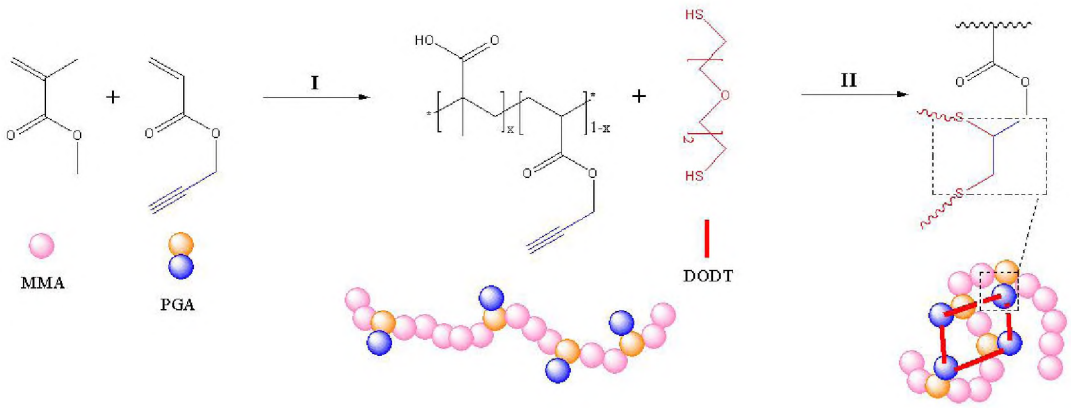

Figure 1.3. Scheme for THF, DMPA, UV-light irradiation at 300-400 nm, rt, 90 min, [DODT]/[PGA]=1.

1.2.4. Reversible Self-folding Single Chain Polymer Nanoparticle. Sawamoto et al. reported a spherical amphilic random copolymer chains that undergo a reversible single chain self-folding in water, and can be unfolded by adding methanol. The polymer

was synthesized by attaching hydrophilic poly(ethylene glycol) methyl ether methacrylate and a group of alkyl methacrylate monomers to a hydrophobic backbone, through a ruthenium catalyzed living radical polymerization. The particle size ranges from 5 to 11.1 nm depending on the alky methacrylate content [9], shown in Figure 1.4.

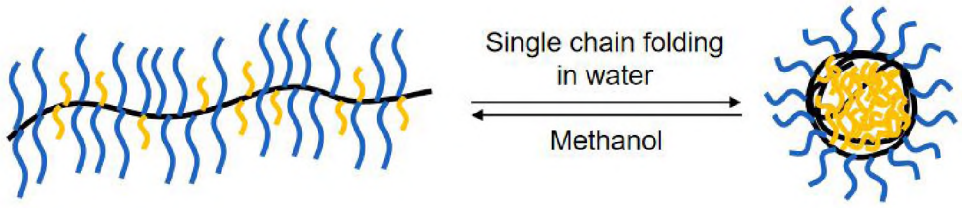

Figure 1.4. Scheme for reversible self-folding of single polymer chains.

1.3. INTRODUCTION TO CUP

1.3.1. What is CUP. Colloidal Unimolecular Polymer (CUP) is a new type of spheroidal particles, the formation is based upon the collapse of a single polymer chain and exists as a solid spheroidal particle in an aqueous media with particle size ranging from 3 to 9 nm depending on the molecular weight. These nanoparticles have hydrophilic groups on the surface and a hydrophobic backbone, and are stabilized in water by ionic repulsive forces. The CUP surface has a layer of surface associated or bounded water, due to hydrogen bonding.

1.3.2. CUP Formation. Cup polymers could be synthesized from any type of monomers by any polymerization method. To be noted, the ratio of hydrophobic and hydrophilic monomers on the polymer chain (HLB value) is very critical. If the polymer is too hydrophilic, the polymer may become soluble or fail to form a spheroid shape, and if the polymer is too hydrophobic, the polymer tends to aggregate [1,10,11]. To date, Van

De Mark et al. have successfully made CUP system from MMA-MAA [12], MMA-AMPS [5], EA-AA [13], quaternary salts, amine hardener, etc.

After purification of the polymer, CUP particle was obtained through a process called water reduction, Figure 1.5. Polymers were dissolved in a low boiling water miscible solvent, like THF, MeOH, EtOH and Me_2O/EtOH have all been used. Stirred overnight to ensure all polymer chains are in a random coil configuration, Structure I. Base was slowly added to the solution to pH 8.5 forming salts and the chains became more extended due to the charge repulsion, Structure II. As pH adjusted water was gradually added, the ions became solvated and separated. The repulsion between adjacent ions increased due to the increasing dielectric caused by the added water and the chain extended toward linearity which increased the viscosity [4], Structure III. At a critical water to solvent ratio the Mark-Houwink exponent reaches the highest value, and the polymer-polymer interaction became greater than the polymer-solvent interaction, the hydrophilic (salt) groups oriented into the water phase, organizing to produce maximum separation of charge. Hence, water released from the polymer backbone increases the entropy and, the hydrophobic polymer chain collapses into spheroidal shape, Structure IV. Finally, the low boiling solvent was stripped off under reduced pressure. The presence of ionic groups on the surface is the driving force to prevent the particles from aggregating through charge-charge repulsion. Once formed, these particles form a thermodynamically stable solution in water.

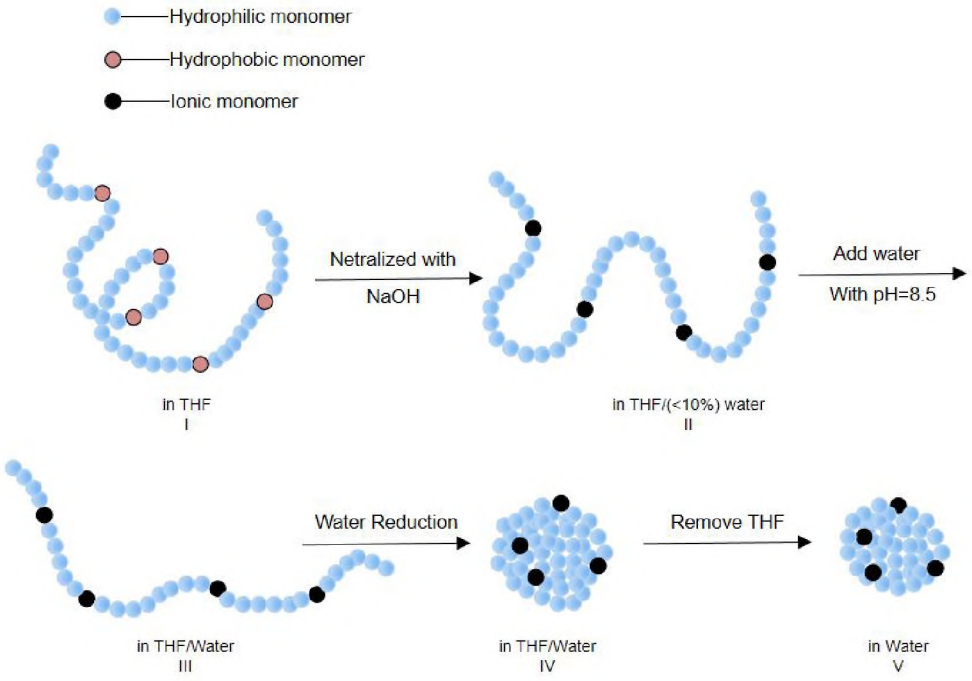

Figure 1.5 . Scheme for water reduction process, formation of CUP.

1.3.3. Characterization of CUP. The characterization involves several parts: absolute molecular weight of the polymer, density of the CUP solution, density of the dry CUP, acid number (AN). viscosity of the CUP solution, particle size of CUP. The diameter and spheroidal shape was confirmed by measurement of particle size with DLS, and correlating with the absolute molecular weight and distribution from SEC [13]. The spheroidal nature is driven by the charges repelling each other and this also prevents the particles from aggregating.

1.3.4. Advantages of CUP. Very few single chain nanoparticles were able to form a spherical shape, and some of which had to involve an intra-molecular crosslinking [7,8,14]. The synthesis of CUP polymers is considered fairly simple and the materials involved are very low cost. No surfactants or additives are in the CUP system making it

better for fundamental scientific studies. Due to the hydrophobic backbone, the particle when formed, organizes the chain much like the bulk polymer with very similar glass transition temperature [12]. In addition, the CUP particle has hydrophilic groups on the surface that associated with a layer of surface water, that presents a similar phenomena as proteins, making CUP an ideal model for surface water studies. Furthermore, CUP's surface charge density and surface functional groups can be varied as well as its surface charge density and charge type, carboxylate, sulfonate or quaternary salt or others as desired, providing more possibilities to endow these particles with function.

1.4. SURFACE WATER

The term " surface water" has been used since 1922 [15]. Previous studies reported that water molecules associated with a solid interface show different properties from free water [16-26].

The structural phenomena of water close to silica/water interface being different from free water was reported by Drost-Hansen et al. by using differential thermal analysis (DTA) [27]. Toney et al. measured the water density profile perpendicular to silver (III) at two voltages by using X-ray scattering, and observed that 1.1 (-0.23 V) to 1.8 (+0.52 V) water molecules per Ag atom for surface water, while the free water should have 0.8 water molecules per Ag atom. Which indicated that the first inner layer of surface water has a greater density compared with free water, due to the hydrogen-boding network [28,29].

Other work stated that the mobility of surface water molecules is lower than free water molecules. Katayama et al. investigated the states of water in a polyacrylamide gel

using spin-lattice relaxation time constant measurements by NMR, and noticed the difference between surface water and free water [30]. Mamnontov used neutron scattering to investigate the vibrational dynamics of surface water in ZrO_2. The rotational diffusion of surface water molecules was found to be slower by about a factor of 2 when compared with free water, and the residence time for translational diffusion of surface water was about 40 times longer than free water [31]. It was also determined that the surface water does not freeze until very low temperature. Berlin et al. studied whey protein systems by using DSC and determined that 0.5 gram of water per gram of whey protein would not freeze at -40 °C [28,32]. Hatakeyema et al. quantitatively calculated that each hydroxyl group of PVA can associate with 1-1.5 molecules of non-freezable water and 5-6 molecules of freezable bound water [33]. Ostrowska-Czubenko et al. analyzed the state of water in chitosan hydrogel membranes, and found that the non-freezable surface water ranged from 0.47 to 0.65 g per gram of dry membrane [34].

1.5. OBJECTIVE OF THIS STUDY

1.5.1. Characterization of Surface Water. The particle size of CUP is very small and can offer a high surface area to volume ratio which makes differentiating surface and bulk water easier. With the spheroidal shape and charged surface, CUP shows a promising potential to investigate the surface water behavior and properties. Knowledge of the characteristics of surface water would contribute to the understanding of proteins, micelles and other materials with water interfaces. Considerable work on CUP surface water has been done by Van De Mark et al. The surface water thickness was estimated to be 0.57 nm based on the rheological behavior [4] , which is similar to the

case of protein [35] and cylindrical nanopores [36]. Spin-lattice relaxation time measurements were performed using NMR to determine the surface water thickness which ranged from 0.19 nm to 0.693 nm and it was found to be both molecular weight and temperature dependent [31].

Differential scanning calorimetry is considered one of the most common thermal techniques. DSC has been widely used to investigate detailed information on the state of water for many water absorbed system [37-43]. This study utilized DSC to determine the amount of surface water utilizing the heat of fusion, the specific heat both above and below the freezing point, the surface water thickness, the density of surface water, the surface charge density, the effect of functional groups both carboxylate and esters, and evaluate the effect of changing the size and charge density as well as concentration. DSC is a simple method but capable of providing a large amount of information.

1.5.2. Evaporation of Free Water. Water evaporation is one of the important fundamental kinetic and thermodynamic characteristics in the applications of aqueous systems. The evaporation rate contributes to many areas, such as: drying of fine chemicals, food drying process, spraying of agricultural fields, the drying of paint, cosmetics, and many others.

Previous work from Van De Mark et al. evaluated dynamic surface tension of CUP solutions using a maximum bubble pressure surface tensiometer. The result indicated that CUPs with more surface charge density tends to have a higher surface tension reduction, and higher molecular weight CUPs required more time to reach the surface tension equilibrium. The effect on surface tension indicates that there may be a change in the evaporation rate when CUPs are present. The lowering of surface tension

may increase the evaporation rate. However, the viscosity of the CUP solution also increases with concentration and at moderate concentrations the system forms a gel. As the concentration increases it may reduce the evaporation rate due to this viscosity increase and gel formation.

In order to have a better understanding about the effect of molecular weight and surface charge density, and concentration effects, an evaporation rate evaluation of water from CUP solutions, was undertaken using TGA under isothermal conditions to follow mass loss for an extended time, 360 min.

1.5.3. Evaporation of Surface Water. Many researchers have discovered that surface water has a much lower mobility compared with free water, due to the association with the surface [32]. In the case of CUPs, the evaporation rate of surface water was expected to be much slower. By using TGA, it is possible to actually distinguish the difference between surface and free water by a different approach, and estimate the steps of how water released from CUP particles.

1.5.4. Application in Coatings. CUP offers a large surface area with a large amount of non-freezable surface water that exhibits great potential for being a freeze thaw stabilizer to replace traditional glycols. The functionalities were demonstrated by measuring the heat of fusion of samples containing CUP versus the traditional glycols. The CUP particles were also used to stabilize a latex paint to protect it from freezing. The effect on the drying behavior of the paint was also evaluated for wet edge and open time.

PAPER

I. THERMODYNAMIC CHARACTERIZATION OF FREE AND SURFACE WATER OF COLLOIDAL UNIMOLECULAR POLYMER (CUP) PARTICLES UTILIZING DSC

Peng Geng, Ashish Zore, and Michael R. Van De Mark*

Department of Chemistry, Missouri S&T Coatings Institute, Missouri University of Science and Technology, Roll, MO 65409, USA; pgkr4@mst.edu (P.G.); aszbnd@mst.edu (A.Z.)

*Corresponding author mvandema@mst.edu

ABSTRACT

Colloidal Unimolecular Polymer, CUP, particles are spheroidal, 3-9 nm, with charged groups on the surface and a hydrophobic core, which offer a larger surface water fraction to improve the analysis of its characteristics. DSC was performed to determine the characteristics of surface water. These properties include the amount of surface water, the layer thickness, density, specific heat of the surface water above and below the freezing point of water, melting point depression of free water, effect of charge density and particle size. The charge density on the CUP surface was varied as well as the molecular weight which controls the particle diameter. The surface water is proportional to the weight fraction of CUP <20%. Analogous to recrystallization the CUP particles were trapped in the ice when rapidly cooled but slow cooling excluded the CUP, causing inter-molecular counterion condensation and less surface water. The density of surface

water was calculated to be 1.023 g/ml to 1.056 g/ml depending on the surface charge density. The thickness of surface water increased with surface charge density. The specific heat of surface water was found to be 3.04 to 3.07 J/g·K at 253.15 K and 3.07 to 3.09 J/g·K at 293.15 K. The average area occupied by carboxylate and ester groups on the CUP surface were determined.

Keywords: Colloidal Unimolecular Polymer (CUP), Differential Scanning Calorimetry (DSC), surface water, density, heat of fusion, thickness, cooling rate, specific heat, melting point depression, counterion condensation.

1. INTRODUCTION

The freezing of water has been an extensively studied thermodynamic property. The freeze thaw of sperm, eggs, cryogenic preservation, crop freezing, food preservation by freezing, paint freeze thaw stability, road and walkway ice and aircraft icing are just a few examples of where ice formation is a critical issue. Surface associated water plays an important role in most of these examples. However, the study of surface water has been difficult due to the low ratio of surface to free water present in a system. Nano particles can offer a significantly enhanced window into surface water due to the high surface water to particle weight ratio.

Colloidal Unimolecular Polymer (CUP) particles are a new class of spheroidal nanoscale polymer particles (3-9 nm) with charged hydrophilic groups on the surface and a hydrophobic backbone [1]. These nano particles can be inexpensively and easily synthesized, particle size can be varied with narrow particle size dispersity by controlling

the molecular weight, and different surface charge density can be designed with both positive and negative charges, this will provide a very predictable, controllable and reproducible system. Also, CUP particles are spheroidal with charges on the surface, but unlike latex particles, CUP solutions are free of surfactant or additives and are zero VOC, making it a promising model for fundamental scientific studies. The CUP surface has a layer of surface associated or bound water, which does not freeze until a much lower temperature than free water [2-6], shown in Figure 1.

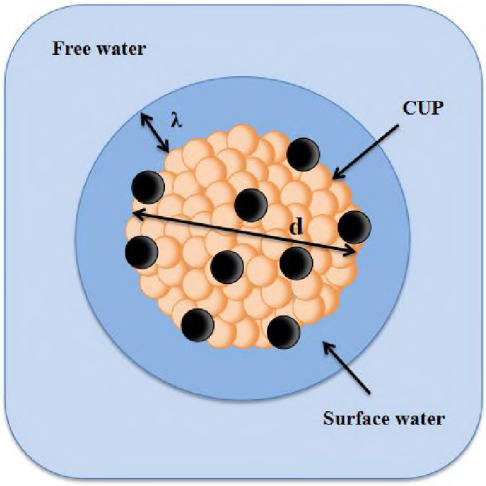

Figure 1. CUP particles with surface water.

Due to the small particle size, CUP's surface area per gram is ultra-high, giving a high surface area to volume ratio and surface functionality [7]. The effect of surface water can be neglected when the size of the particle is very large. The size of a typical latex particle is about 100 nm, and the diameter of water molecule is only 0.28 nm. Assuming that there is one layer of water bounded on the particle surface, the volume ratio of bound water and latex particle is only 1.69%. However, when the particle is as

small as 3.90 nm, the ratio is 49.56% [1], which makes the contribution of surface water much more significant as shown in Figure 2.

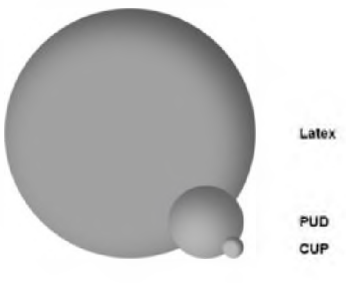

	Latex	PUD	CUP
Particle size (nm)	100	25	3.90
Surface area (m^2) / Mass (g)	48.98	195.92	1255.89
Surface area (nm^2) / Volume (nm^3)	0.06	0.24	1.54
Volum ratio of surface water to polymer (assuming1 layer of surface water)	0.017	0.069	0.50

Figure 2. Comparison of latex, polyurethane dispersion (PUD) and CUP (25.4k).

These facts make CUP an ideal model for surface water studies, offering a huge advantage over proteins which are limited in size, structure, and availability [7]. CUPs can contribute to our understanding of proteins and micelles and also contribute to the study of other materials with water interfaces. Zero VOC CUPs are a very good candidate for future applications including coatings, adhesives, sealants and many others.

The formation of CUP particles is generally accomplished through a water reduction process, according to the Flory-Huggins theory [8]. The process is driven by the polymer-polymer interaction being greater than the polymer-solvent interaction and entropically favored by releasing water analogously to micelle formation. The charged groups repel each other to create the spheroidal shape. Once formed, CUPs are thermodynamically stable in water solution. CUP solutions are made through a water reduction process, as shown in Figure 3. The brown spheres represent the hydrophobic polymer backbone, each sphere is a methyl methacrylate unit (or hydrophobic monomer). While the gray spheres represent the ionizable carboxylic acid side-chain groups (or

methacrylic acid unit). Polymers were dissolved in a low boiling water miscible solvent, like THF, stirred overnight to ensure all polymer chains are in a random coil configuration, Structure I. Base was slowly added to the solution to pH 8.5 forming carboxylate salts and the chains became more extended due to the charge repulsion, Structure II.

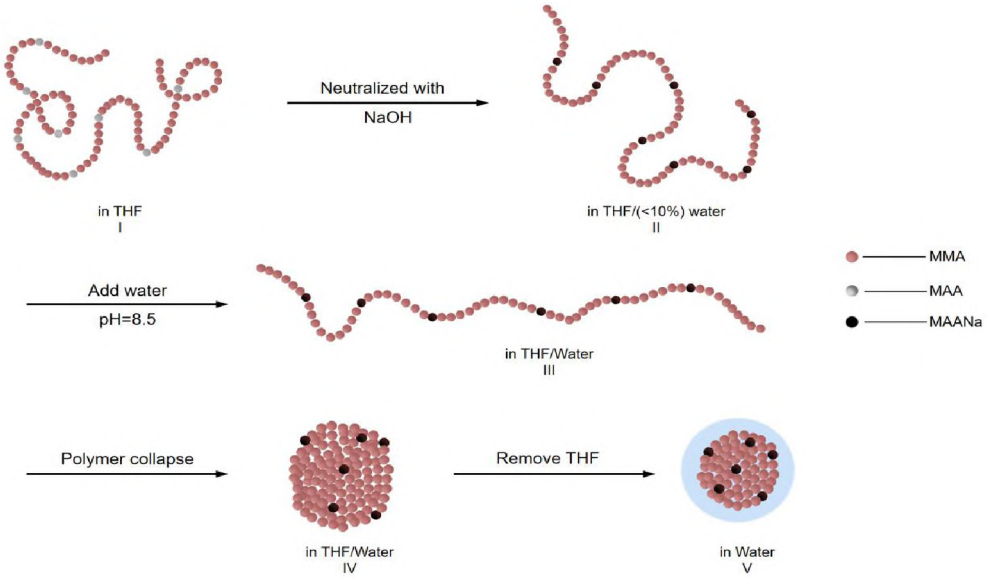

Figure 3. Formation of a typical CUP particle.

As pH adjusted water was gradually added, the sodium carboxylate ions became solvated and separated. The repulsion between adjacent ions increased due to the increasing dielectric caused by the added water and the chain extended toward linearity which increased the viscosity [9], Structure III. At a critical water to THF ratio the Mark-Houwink parameter reaches the highest value, and the polymer-polymer interaction became greater than the polymer-solvent interaction, the carboxylate groups oriented into

the water phase, organizing to produce maximum separation of charge. Hence, water released from the polymer backbone increases the entropy and, the hydrophobic polymer chain collapses into spheroidal shape, Structure IV. Finally, the low boiling solvent, THF was stripped off under reduced pressure. The presence of ionic groups on the surface is the driving force to prevent the particles from aggregating through charge-charge repulsion [10]. Once formed, these colloidal solutions are thermodynamically stable [11]. The ratio of hydrophobic and hydrophilic monomers on the polymer chain (HLB value) is very critical in the unimolecular collapse of the polymer chain during water reduction process. If the chains are too hydrophobic, the collapsed chain tend to aggregate and if the chains are too hydrophilic, the polymer will dissolve or form a more extended or barbell like structure [1,12,13].

The term "surface water" has been used since 1922 [14]. Ever since that, many techniques have been used to investigate the surface water. Previous studies suggest that water molecules were arranged in several layers adjacent to a solid interface changing the properties of the water [15-25]. The state of water has been widely investigated by various techniques.

Van De Mark et al. correlated the surface water with the rheological behavior of CUP particles [10]. They found that from the intrinsic viscosity of the CUP solution, by combining the density and molecular weight of CUPs, the thickness of water layer was estimated to be 0.57 nm, which is similar to the case of protein [2] and cylindrical nanopores [26].

Nuclear magnetic resonance (NMR) is another method which has been used to examine surface water. The mobility of surface water molecules is lower than free water

molecules, therefore NMR probing of the mobility has been used to verify the existence of structured water around colloidal polyvinyl acetate (PVA) with particle size of 0.13 and 0.8 micron used by Clifford et al. By measuring the spin lattice relaxation time constants of protons, they concluded that the total amount of bound water per unit surface area was larger for larger particles [27-29].

Katayama et al. investigated the states of water in a polyacrylamide gel using spin-lattice relaxation time constant measurements, and concluded that the macromolecule must have a hydrophilic substituent to be able to capture surface water, and the amount of surface water remarkably depends on the amount and the nature of the substituents [30]. Van De Mark et al. used the same method to determine the surface water thickness of CUP particles, which ranged from 0.19 nm to 0.693 nm and it was found to be both molecular weight and temperature dependent [31].

Quasielastic neutron scattering (QENS) has been used for both organic and inorganic water-containing materials. Mamnontov used neutron scattering to investigate the vibrational dynamics of surface water in ZrO2. The rotational diffusion of surface water molecules was found to be slower by about a factor of 2 when compared with free water, and the residence time for translational diffusion of surface water was about 40 times longer than free water. It was proposed that there were about two hydration layers on top of the layer of surface OH groups [32].

Toney et al. measured the water density profile perpendicular to silver (III) at two voltages by using X-ray scattering, and found that the first inner layer of surface water has a greater density compared with free water, 1.1 (-0.23 V) to 1.8 (+0.52 V) water molecules per Ag atom for surface water, while they expected 0.8 water molecules per

Ag atom, based on the density of free water. Which indicated that the hydrogen-boding network changed and resulted in very different properties in this layer from those in free water [33,34].

Drost-Hansen et al. studied the water adjacent to silica surfaces by using differential thermal analysis (DTA). They observed thermal property changes in the slope and displacements of the baseline in thermograms and small endothermic peaks in heating curves. These peaks were associated with structural phenomena changes of the water at silica/water interface, indicating the properties of water close to solid interfaces are very different from free water [35].

Velazquez et al. described the interaction of water with hydrophilic materials indicating that a portion of water was firmly bounded to individual sites. By using infrared spectroscopy, the bound water amount on a methylcellulose film was identified. It was reported that the bending vibration mode of bound water shifted toward lower frequency by about 15.5 cm-1. When the humidity increased, the bound water content remained at below 5 % [36].

Differential scanning calorimetry (DSC) has been widely used to investigate detailed information on the state of water by distinguishing the amount of freezable water from non-freezable water for many water absorbed system [37-43], Ross [44], Bushuk et al. [45], and Biswas et al. [46] all concluded that the amount of unfrozen water per gram of solute increased with the increasing dilution, this dependence was more obvious for concentrations smaller than 1 M.

Berlin et al. studied whey protein systems by using DSC and determined that 0.5 gram of water per gram of whey protein would not freeze at -40 °C. And by adding

lactose and salts, the unfreezable water increased as the concentration of lactose and salts were increased, which varied between 0.5 and 1.2 gram of water per gram of solids [47,48]. Hatakeyema et al. quantitatively calculated the amount of bound water in poly(vinyl alcohol) hydrogel using DSC. It was reported that each hydroxyl group of PVA can associate with 1-1.5 molecules of non-freezable water and 5-6 molecules of freezable bound water [49]. Ostrowska-Czubenko et al. analyzed the state of water in chitosan hydrogel membranes, and found that freezable water content increased linearly with the water uptake, while non-freezable water content remained constant beyond critical water content value. The non-freezable surface water ranged from 0.47 to 0.65 g per gram of dry membrane [50]. Muffett et al. investigated the amount of unfrozen water in soy proteins by DSC, and reported that the unfrozen water amount increased in the range of 0.09-0.14 g of unfrozen water per gram of total water, with the increasing of total water [51]. Garti et al. determined the thickness of bound water layer in the n-dodecane/1-pentanol/$C_{12}(EO)_8$ system to be 0.5 nm by using DSC [40]. Kobayashi et al. determined the thickness of fully hydrated dimyristoylphosphatidylcholine to be 3.2-3.4 nm, using DSC, X-ray and densimetry [52].

Many of the previous surface water studies utilizing DSC gives confidence to investigate surface water properties of CUP system. DSC has many advantages over other techniques for evaluating the surface water behavior. First, DSC is the most common thermal analysis technique to obtain heat content change (enthalpy) and heat capacity with ease and speed. Second, DSC can hold a precise temperature with no drift, and it can be used for kinetic studies in a faster and more straightforward way than other methods [53-55]. In this study, using hermetically sealed pans and sample size of 30 mg,

accurate water melting and specific heat data should be readily obtainable for even low weight fraction of CUP solutions.

CUP opens a window to investigate the thermodynamics of surface water and free water for particulate systems. This work presents a primary study of the CUP surface water properties utilizing DSC. It includes: synthesis and production of CUP through water reduction; determination of the thickness of surface water of CUP by measuring the heat of fusion and particle size; determine the actual density of surface water; determine the specific heat of surface water; evaluate the effect of cooling rate on the amount of surface water; determine the average surface area of functional groups on the CUP surface by knowing the melting point depression of CUP solutions.; study the relationship between CUP surface water and molecular weight and charge density in ions per nm^2. This work represents the first comprehensive study of the functionality and size effects on CUP surface water behavior during freeze/thaw conditions.

2. EXPERIMENTAL

2.1. MATERIALS

Methyl methacrylate (MMA), methacrylic acid (MAA), 2,2 ′ -azobis(2-methylpropionitrile) (AIBN), and 1-dodecanethiol were purchased from Aldrich. MMA was purified by washing with a 10% (w/w) solution of sodium bicarbonate, followed by rinsing with de-ionized water, and then brine, and then dried over sodium sulfate and filtered. Copper (I) bromide was added to the MMA as an inhibitor, and simple distillation under nitrogen was carried out. MAA was purified by distillation with copper

(I) bromide under reduced pressure. THF was dried and distilled under protection of nitrogen. AIBN was re-crystallized from methanol, and 1-dodecanethiol was used as received.

2.2. SYNTHESIS OF POLY(MMA/MAA) COPOLYMER

Table 1 shows the component amount for the synthesis of Polymers 1-7.

Table 1. Polymer synthesis: the amount of materials used.

Polymer	Molecular weight (g/mol)	Monomer 1	Monomer 2	Initiator	Chain transfer agent	Solvent
		Methyl methacrylate (mol)	Methacrylic acid (mol)	AIBN (mol)	1-Dodecanethiol (mol)	THF (mol)
1	28,900	2.25	0.25	1.75×10^{-3}	7.61×10^{-3}	10.40
2	59,800	2.25	0.25	1.75×10^{-3}	3.79×10^{-3}	10.40
3	122,500	2.25	0.25	1.75×10^{-3}	1.87×10^{-3}	10.40
4	25,400	2.22	0.33	1.78×10^{-3}	8.62×10^{-3}	10.40
5	73,500	2.30	0.23	1.77×10^{-3}	3.10×10^{-3}	10.40
6	49,700	2.35	0.17	1.76×10^{-3}	4.51×10^{-3}	10.40
7	22,700	2.39	0.13	1.76×10^{-3}	9.46×10^{-3}	10.40

Polymers were synthesized by a free radical polymerization method in tetrahydrofuran (THF) [21]. To a 2 L three neck flask, 10.40 mol of THF was added. Methyl methacrylate (MMA) and methacrylic acid (MAA) were used with various molar ratios. 1-Dodecanethiol was added as a chain transfer agent based on desired molecular weight of polymer. The initiator AIBN was then added, 0.0007 times the total moles of monomers. The reaction was carried out under nitrogen, with condenser and a gas outlet

adapter connected to an oil bubbler to allow a positive flow of nitrogen throughout the polymerization. The mixture was heated slowly to reflux under stirring for 24 hours. The polymer solutions were then cooled to room temperature, and part of the THF removed by rotovap. Finally, the polymer was precipitated in cold deionized water under high shearing rate, and dried in a 323.15 K oven under vacuum for 24 hours.

2.3. WATER REDUCTION METHOD

To a 500 ml Erlenmeyer flask were added 10 g of dry polymer, 40 g of THF and stirred for 12 hours to let the polymer chains fully obtain a random coil configuration. Based on the measured acid number, 1 M NaOH solution was slowly added to neutralize the solution to pH 8.5 by peristaltic pump at the rate of 1.24 g/min. Then 90 g of deionized water modified to pH=8.5 using 1 M NaOH solution was then gradually added by peristaltic pump at the rate of 1.24 g/min. The pH of system was maintained at 8.5 throughout the process of water reduction. Majority of THF was stripped off by rotovap, and the sample was left in vacuum to remove the last trace of THF, giving zero VOC CUP solution. The clear solutions were then filtered through a 0.45 micron filter to remove any extraneous trace particulate contaminants, the typical loss on filtering was less than 0.05% of the solids by weight.

2.4. CHARACTERIZATION OF POLYMERS

2.4.1. Absolute Molecular Weight of Copolymers. Gel permeation chromatography utilized a Viscotek model 305 manufactured by Malvern Corp. system. The GPC was equipped with a triple detector array TDA305: refractive index detector,

low and right-angle light scattering detector, and intrinsic viscosity detector, the column, two PAM-505 from PolyAnalytik with a guard column, the column size is 7.5 mm (ID) × 300 mm (L). Polymer samples were prepared to 2 mg/cc. Injection volume was 100 µl, and THF flow rate was 0.5 ml/min.

2.4.2. Density of CUP Solutions. Densities of CUP solutions were directly measured by density meter (DDM 2911 plus by Rudolph Research Analytical) at various weight fractions at 298.15 K. The accuracy is 0.00001 g/cm^3.

2.4.3. Density of Dry CUP Polymer. The solutions of CUP were dried in a vacuum oven, heated at 323.15 K with the presence of solid sodium hydroxide to absorb carbon dioxide. After the clear crystal-like material formed, the sample was then heated to 383.15 K to constant weight. The densities of the dry CUPs were measured by a gas displacement pycnometer, Micrometritics AccuPycII 1340. The temperature was controlled at 299.04±0.04 K. Twenty five readings were made for each sample, and the results were reported by average and standard deviation.

2.4.4. Acid Number (AN). The acid number of the copolymers were determined by the titration method ASTM D974, and reported in mg of KOH/g of polymer sample. The method was modified by using potassium hydrogen phthalate (KHP) in place of hydrochloric acid and phenolphthalein in place of methyl orange. THF was used as the solvent of the titration.

2.4.5. Viscosity of CUP Solution. Viscosity of CUP solution was measured based on ASTM D445, ASTM-D446 and ISO 3104, 3105. Ubbelohde capillary viscometer J-340 from Cannon instrument company was used to determine the viscosity of CUP solutions at two different temperatures: 298.15 K and 302.15 K. Before each

measurement, CUP solution was transferred to the Ubbelohde capillary viscometer and kept in a constant temperature water bath at 298.15±0.1 K for 20 minutes with plastic wrap covering on top of the viscometer to prevent potential evaporation and carbon dioxide contamination of the solution. A stop watch with 0.01 second precision was used to monitor the elution time and each measurement was repeated for at least three times and the error being less than 0.5%. Absolute viscosity was then calculated by Equation (1).

$$\eta = t \cdot d \cdot c \tag{1}$$

where η is the viscosity of CUP solution (cP), t is the elution time (s), d is the density of CUP solution (g/ml) and c is the Ubbelohde capillary viscometer constant (0.009749 mm^2/s).

2.4.6. Particle Size of CUP. Particle size was measured by dynamic light scattering, using Microtrac Nanotrac 250 particle size analyzer from Microtrac with a laser diode of 780 nm wavelength, and 180° measuring angle. The viscosity of solution was used, due to high weight fraction of CUP having high viscosity that caused by electronic repulsion [10], and low weight fraction of CUP produce very poor light scattering efficiency and a weak signal, because of small particle size, around 5 nm. The CUP solutions were diluted to 10% weight fraction by pH adjusted Mili-Q ultrapure water with resistance of 18.3 MΩ. The particle size was calculated by Stokes-Einstein Equation (2).

$$D = \frac{k_B T}{6\pi\eta r} \tag{2}$$

where k_B is the Boltzman constant, T is the absolute temperature of solution, η is the viscosity of solution and r is the radius of the CUP particle.

2.4.7. Differential Scanning Calorimetry. Differential scanning calorimeter from TA instruments Q2000 was used to measure the heat of fusion, specific heat and freezing point depression of CUP solutions. About 30 mg of CUP samples were sealed in the Tzero Hermetic pan from DSC Consumables Inc., then cooled to the target temperature at a series of cooling rates, isothermal for 10 min, and heated up to 313.15 K at 3 K/min rate. The mass of sealed pan was measured before and after each measurement with the result being considered valid if the mass difference was smaller than 0.001 mg.

3. RESULTS AND DISCUSSION

3.1. POLYMER SYNTHESIS AND CHARACTERIZATION

It was found that polymers with molecular weight lower than 13,000 g/mol tended to be unstable, due to insufficient electrostatic stabilization causing the polymer to aggregate. Polymers with very high molecular weight, higher than 200,000 g/mol might have issue during water reduction process due to chain chain entanglement. At high molecular weight the reduction solution must be very dilute since as the molecular weight increases the chance for chain entanglement increases therefore the solutions must be diluted. Thus, seven polymers with different molecular weights (22,700-122,500 g/mol) and different monomer ratios were synthesized and successfully made into CUP solutions. Polymer 1, 2 and 3 have different molecular weight but the same monomer ratio, 9 mol MMA to 1 mol MAA. In order to investigate the behavior at very low charge density

values, Polymer 6 and 7 were synthesized with a large monomer ratio. To understand the effect of the molecular weight, monomer ratio and ions per nm^2 (surface charge density) effect on the surface water properties, Polymer 4 and 5 were designed to have different molecular weight but same charge density in ions per nm^2 as Polymer 2. The charge density ρ_v was determined by Equation (3).

$$\rho_v = \frac{M_W}{4\pi r^2 (n_1 \cdot M_{MMA} + n_2 \cdot M_{MAA})} \tag{3}$$

where ρ_v is the charge density in ions per nm^2, M_w is the molecular weight of CUP polymer, r is the radius of the CUP particle, n_1 is the moles of MMA and n_2 is the moles of MAA used per average repeat unit, M_{MAA} is the molecular weight of monomer methacrylic acid, M_{MMA} is the molecular weight of monomer methyl methacrylate. Polymer 6 and Polymer 7 were synthesized to have a much higher monomer ratio which was able to investigate the behavior at very low charge density values.

The molecular weight, acid number, particle size and density of the polymers are listed in Table 2. The densities of the dry polymer increased with the increasing of molecular weight, because when molecular weight is larger, the number of polymer chain end groups decrease, result in less free volume and higher density [56]. All polymers had consistent acid numbers with respect to the monomer feed. The polymers were then reduced, the THF removed and the CUP solutions were concentrated. The samples were then measured for particle size and validated as to single chain particles due to a match in particle size with the calculated size and distribution from the absolute molecular weight [2]. The samples were either concentrated or diluted into different weight fractions for DSC analysis.

Table 2. Molecular weight, particle size, acid number and density of the polymers.

Sample	M_n (g/mol)	Monomer ratio	Particle size (nm)	AN (mg KOH/g)	Density of dry CUP, ρ_p (g/ml)	charge density in ions per nm^2
1	28,900	9:1	4.22	56.8	1.2246±0.0018	0.52
2	59,800	9:1	5.38	57.0	1.2311±0.0014	0.66
3	122,500	9:1	6.83	56.9	1.2342±0.0018	0.84
4	25,400	6.8:1	4.04	73.2	1.2243±0.0018	0.66
5	73,500	9.8:1	5.76	52.6	1.2315±0.0018	0.66
6	49,700	14:1	5.06	37.7	1.2307±0.0016	0.42
7	22,700	19:1	3.90	28.2	1.2241±0.0018	0.24

3.2. EFFECT OF COOLING RATE AND ICE FORMATION

The DSC measurements were done using about 30 mg of CUP solution in Tzero hermetically sealed pans. Enough head space was allowed to avoid rupture or leaking during the freeze thaw cycle and large enough to give an accurate measurement. DSC samples were cooled to 233.15 K and held for 10 minutes to ensure all freezable water froze, and then heated to 313.15 K to allow all the ice to melt without causing leakage. It was difficult to precisely obtain accurate area of the ice formation peak due to some super-cooling during the temperature lowering scan. Therefore, the data presented here represents the heating, melting process only. The mass of the DSC pan was measured before and after to ensure that no water had been lost during the cycle, only runs with losses of less than 0. 001 mg were used.

To evaluate the time required to freeze the sample as well as to determine if the surface water will slowly leave the outer surface and freeze, samples of a 10.03% 28.9k

CUP solution, Polymer 1, were cooled to 233.15 K at 10 K/min, isothermal for 10 minutes, then heated up to 313.15 K at 3 K/min. The same sample was also measured following the same protocol, except the isothermal time was changed to 1h, 2h, 4h and 8h, shown in Figure 4.

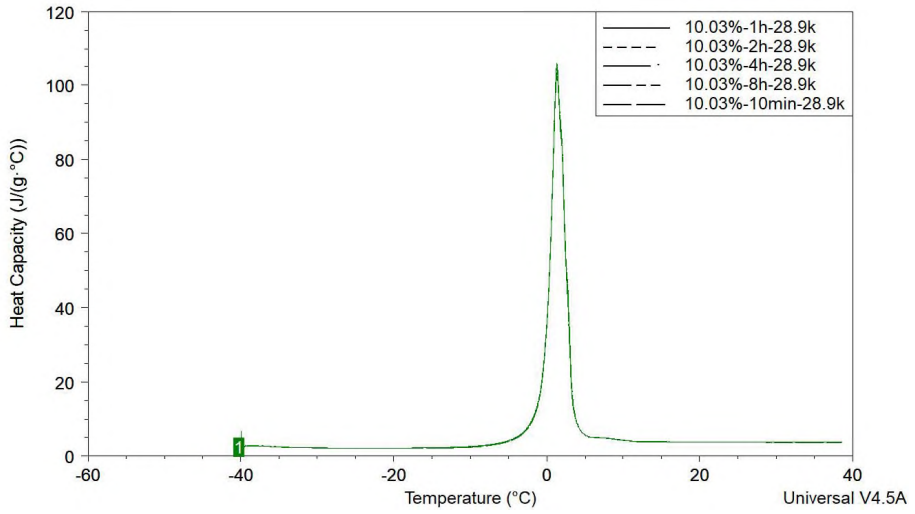

Figure 4. Heat of fusion of 10.03% Polymer 1 with different isothermal time.

The endothermic peaks represented the measured heat of fusion of freezable water. The same area and shape indicated that all freezable water was able to completely freeze within the 10 mins isothermal period. Thus, 10 minutes was chosen as the experimental isothermal time.

Ice forms typically near 273 K, however, the endothermic peak is somewhat broad so is the freezing peak making baseline determinations near 273 K ± 10 K difficult. Evaluation of the lowest temperature needed was evaluated by running scans with 10.40% 28.9k CUP solution cooled to 233.15 K, 243.15 K and 253.15 K at 10 K/min from room temperature, isothermal at each temperature for 10 minutes. Then the sample

was heated up to 313.15 K at the rate of 3 K/min. The heat of fusion was unchanged over this range. Which implied that the 233.15 K isothermal temperature could assure all freezable water froze.

When water-based latex resins are exposed to cold temperature conditions, shown in Figure 5.

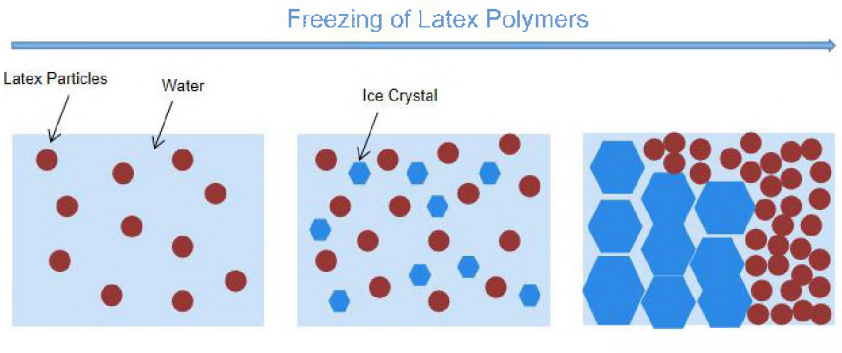

Figure 5. Freezing of Latex polymers

Water will start to freeze and form ice crystals excluding the latex. As the ice crystals grow, there is less and less liquid water existing in the solution and therefore the weight fraction of latex particles increases in the remaining liquid, and the particles are forced close together [57].

Thus, in theory, CUP solutions should perform in a similar way. If the CUP solution was cooled at an infinity slow rate, the distance between each CUP particles will become a minimum, reaching maximum inter-molecular counterion condensation effect and result in the minimum amount of surface water, regardless of initial weight fraction of CUP particles.

In the literature, different freezing methods result in different supercooling effects [58]. For normal protein freeze-drying process, the fastest cooling rate can be obtained by liquid nitrogen freezing with a small volume of sample, that gives the most supercooling; while the lowest supercooling is for the pre-cooled shelf method [59-61].

In order to understand the effect of the cooling rate on the measurement. Variation in the cooling rate was evaluated analogously for Polymer 1. The DSC of CUP solutions were cooled at 0.1 K/min, 0.2 K/min, 0.5 K/min, 1 K/min, 2 K/min, 3 K/min, 5 K/min, 7 K/min and 10 K/min. Eight weight fractions of Polymer 1 CUP solutions were cooled to 233.15 K at different rates, then isothermal for 10 mins and heated to 313.15 K at the rate of 3 K/min. The amount of non-freezable surface water per CUP particle was calculated by Equation (4).

$$m_{SW} = \frac{(\frac{\Delta H_W - \Delta H_{FW}}{\Delta H_W} - X_{CUP}) \cdot M}{N_A \cdot X_{CUP}} \tag{4}$$

where m_{sw} is the mass of surface water per CUP particle in grams, N_A is Avogadro constant, ΔH_W is the heat of fusion of water (333.5 J/g), ΔH_{FW} is the heat of fusion of freezable water in CUP solution, M is the molecular weight of CUP polymer, X_{CUP} is the weight fraction of CUP in the solution.

In order to demonstrate the effect of cooling rate on the amount of surface water, the DSC measurement of Polymer 1 solutions was conducted at 10 K/min cooling rate. Results showed that the amount of surface water was constant at concentrations below where Manning condensation occurs, Figure 6. However, as the cooling rate was reduced the amount of surface water measured decreased and showed a small concentration

dependency. As the concentration of CUP increased the surface water decreased only slightly. During the freezing process, ice nucleates and the crystals grow. In a supercooling situation, when ice nucleation occurs growth is extremely rapid and traps the CUP particles in the crystal matrix before significant diffusion can occur. However, when slow cooled the ice growth was slower and allowed time for CUP diffusion and subsequent Manning condensation to occur [62]. When this charge condensation occurs the amount of surface water drops. At 0.1 degrees per minute and 5.23% CUP, the amount of surface water is 4.64×10^{-20} g per particle but at 10 degrees per minute it was 4.94×10^{-20} g per CUP particle, the drop in surface water was only 6.07%. All the CUPs in this study were polymerized from methyl methacrylate and methacrylic acid, the surface charged groups originated from neutralization of carboxylic acid by NaOH. The effective charge on the surface is subject to the dissociation equilibrium, and there are two counterion condensations that exist in this system, inter-molecular counterion condensation and intra-molecular counterion condensation [63-65]. Inter-molecular counterion condensation occurs between particles when the weight fraction of CUP particles is high, and intra-molecular counterion condensation occurs where the charge density of a single particle is high. Slow cooling rates allowed more time for CUP particles to migrate, when CUP particles were forced to become closer, the inter-molecular counterion condensation effect increased which reduced the number of effective charges on CUP's surface, releasing part of the surface water where it became freezable. The counterion condensation effect was greater for higher concentrations of CUPs. This small difference is likely caused by the increased chance of charge condensation in the more crowded higher concentration.

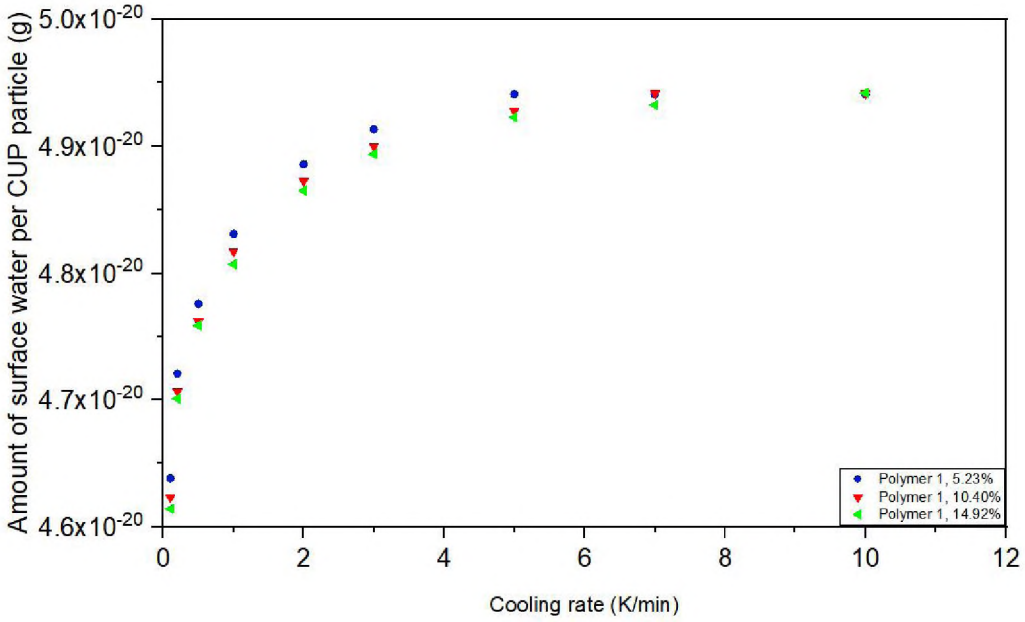

Figure 6. Amount of surface water per CUP particle of Polymer 1 at 5.23%,10.40% and 14.92% at different cooling rates.

Solutions with 21.40% and higher weight fraction CUP showed less surface water per particle at 10 K/min, Figure 7. The cause for this decrease was inter-molecular counterion condensation. When the weight fraction of CUP is high, with short distances between CUP particles, inter-molecular counterion condensation existed even before the cooling process. The inter-molecular counterion condensation also reduced the ice formation driven charge condensation which occurs during slower freezing rates. As the concentration increases the effect of slow freezing is reduced and at about 36% the surface water is a constant being independent of the cooling rate. It is important to note that the viscosity of the CUP solution is concentration dependent and rises rapidly due to the onset of Manning condensation [2, 66]. The ion-ion repulsion reduces the diffusion rate of the CUP particle and thus makes it harder to move away from the advancing crystals of ice being formed and the CUP becomes an inclusion.

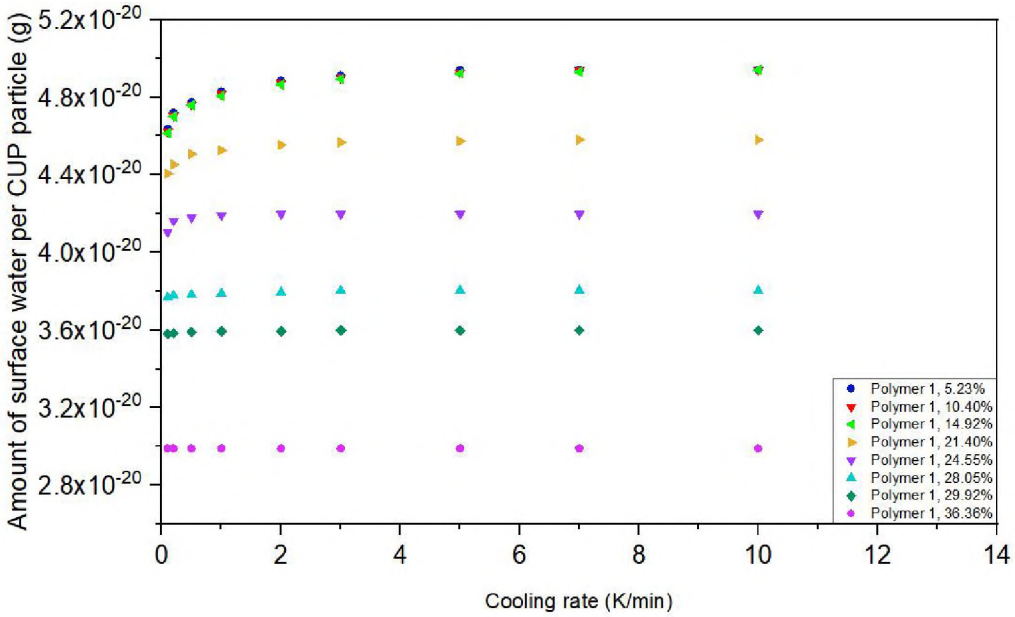

Figure 7. Amount of surface water per CUP particle of Polymer 1 at different weight fraction at different cooling rates.

Direct comparison of the amount of surface water of the solutions with different CUP particle weight fractions are shown in Figure 8. The effect of the cooling rate decreased with the increasing of CUP particle weight fraction, and gradually disappeared. The initial concentration independent region was again below the inter-molecular counterion condensation region. At approximately 20% the contribution due to the inter-molecular counterion condensation and subsequent viscosity effect obviously controlled the system. When the gel point is approached the particles cannot significantly move and the surface water reaches a point where the rate of cooling does not affect the result. Figure 8 illustrates the effect of 0.1 K/min versus 10 K/min cooling rates. At low concentration the surface water per cup was a constant until Manning condensation occurs then as the concentration increases the differences reduce to zero at the gel point.

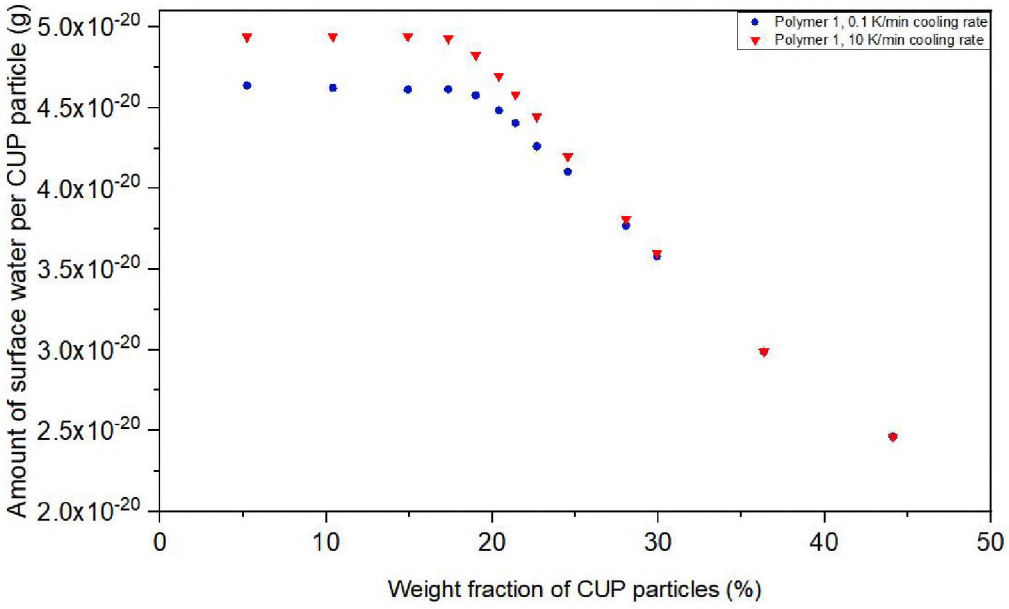

Figure 8. Amount of surface water per CUP particle of Polymer 1 at different weight fraction at 0.1 K/min and 10 K/min cooling rate.

The packing of spheroidal materials is most likely to form either random close packing or hexagonal close packing. The maximum volume fraction 0.634 is for random close packing and for hexagonal close packing it is 0.7405 [67-71]. CUP solution is able to approach hexagonal closing packing with the volume fraction of CUP particle being 0.7405 including surface water. Due to the small particle size and relatively low density the Brownian motion of CUP can help to move the particles to a position where the electrostatic repulsion and Brownian motion reach a balanced stable structure. Based on the previous publication by Van De Mark et al. [2], the weight fraction of CUP particle for each packing model can be calculated by Equation (5-7).

$$\phi = \frac{\rho_s \cdot X_{CUP}}{\rho_p} \tag{5}$$

$$\phi_{\max}(1+\lambda/r)^3 = 0.634 \tag{6}$$

$$\phi_{max}(1+\lambda/r)^3 = 0.7405 \quad (7)$$

where ϕ is the CUP volume fraction, ρ_s is the density of CUP solution, ρ_p is density of CUP particle, X_{CUP} is the weight fraction of CUP, ϕ_{max} is maximum volume fraction, λ is the thickness of surface water, r is radius of the CUP particle.

For CUP solutions of Polymer 1, the weight fraction of CUP particles was 36.16% when reaching random closing packing, which is the gel point, and 43% for hexagonal close packing. When the weight fraction of CUP particles was close to 30%, the cooling rate effect on the amount of surface water was almost gone, due to the very high viscosity and close to maximum inter-molecular counterion condensation. The surface water difference between the two cooling rates approached zero when the weight fraction of CUP particles is close to 43%, at this point and the particle is very difficult to move and any free water will be slow to migrate. It is also the point where CUP particles reaches maximum inter-molecular counterion condensation over the concentration range of 20% to 43%, CUPs the surface water amount drops by 47.55% at 10 K/min and 45.07% at 0.1 K/min. The behavior of CUP solutions were similar to that of latex resins in that as the ice forms the particles are forced together. The higher charge density on the surface and the increased surface area create an increased amount of surface water which does not freeze. The same effects should be observed in globular proteins and other nano scale particles in water as well as in vitro and vivo materials when frozen.

3.3. WEIGHT FRACTION OF SURFACE WATER

In order to minimize the effect of counterion condensation in the remaining portion of this work, all the CUP solutions were cooled at 10 K/min, which is the highest

cooling rate the DSC was capable of. The isothermal time was kept at 10 mins and heated to 313.15 K at the rate of 3 K/min. Furthermore, since the CUP samples were neutralized by NaOH solution, heat of fusion of NaOH modified water sample was measured. Since there was no difference in the heat of fusion and melting point depression between NaOH modified water and deionized water (333.5 J/g), the deionized water was used as the standard. Different molecular weight polymers were made into CUP solutions and were prepared to various weight fractions. The heat of fusion of each solution was measured by DSC.

Figure 9 shows the DSC endothermic peak of Polymer 1 CUP solutions with three weight fractions. It was obvious that with the increasing of the weight fraction, the endothermic peaks shift to lower temperature, this can be explained by Raoult's law [72].

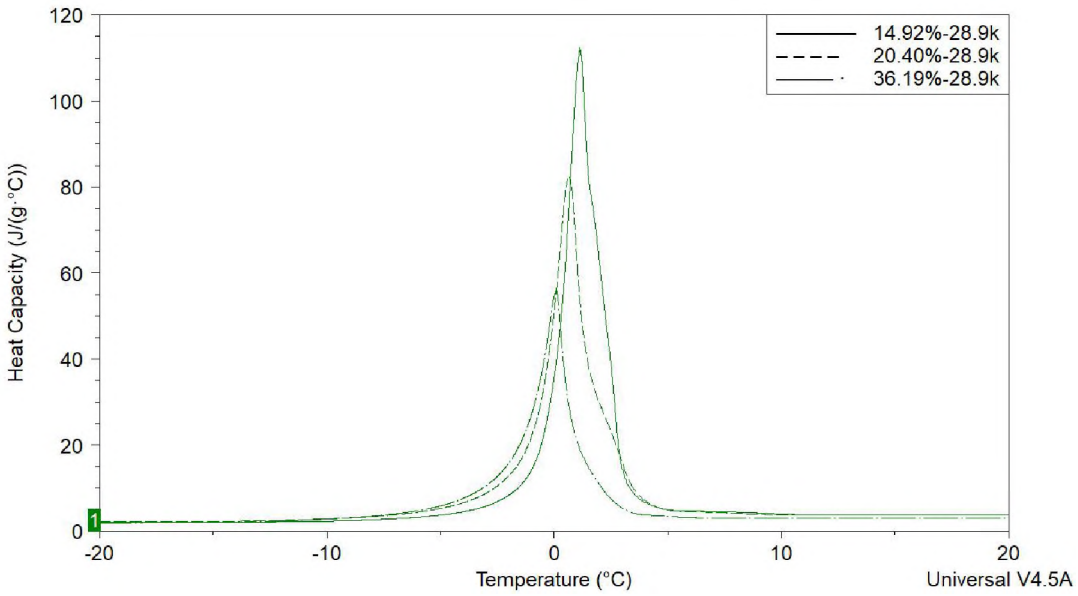

Figure 9. Heat of fusion of Polymer 1 solution at various weight fraction.

CUP solutions contain only CUP particles, free water and surface water. The surface water does not freeze until a very low temperature and the free water which freezes like normal water. The endothermic peak for all the samples exhibited only a single peak. Thus, the observed difference in heat of fusion, between a water sample and a CUP solution, is due to the CUP particles and a fraction of water that does not freeze in the DSC measurement [73]. Therefore it is possible to determine the weight fraction of surface water utilizing the heat of fusion by DSC. For CUP samples, the weight fraction of free water can be determined by dividing the heat of fusion of the CUP solution by that of deionized water, which was used as a standard:

$$X_{FW} = \frac{\Delta H_{FW}}{\Delta H_W} \tag{8}$$

where X_{FW} is the weight fraction of freezable water, ΔH_{FW} is the heat of fusion of freezable water obtained from DSC, ΔH_W is the heat of fusion of water, 333.5 J/g. The surface water weight fraction, XSW can be calculated knowing the weight fraction of CUP, X_{CUP}, and X_{FW}, Equation (9).

$$X_{SW} = 1 - X_{FW} - X_{CUP} \tag{9}$$

combining Equation (8) and (9) to obtain Equation (10).

$$X_{SW} = 1 - X_{CUP} - (\frac{\Delta H_{FW}}{\Delta H_W}) \tag{10}$$

From Equation (8-10), the weight fraction of surface water of each CUP solution was determined. Figure 10 shows the weight fraction of surface water vs weight fraction of the CUP particles.

The results indicate that there was a significant amount of non-freezable water in this system. The amount of water was linearly dependent upon the weight fraction of

CUP over the range shown. Thus, the amount of water was constant per particle. Comparing Polymer 1, 2 and 3, that have a 9:1 MMA:MAA ratio, the higher molecular weight result in a lower slope, due in part to the lower surface area per gram of polymer. However, there is another variable, the charge density of ions on the CUP surface. As the molecular weight increases at a constant MMA:MAA ratio the surface charge density increases since all the charged groups will attempt to be on the surface. It would be expected that more charge density the more surface water should be observed.

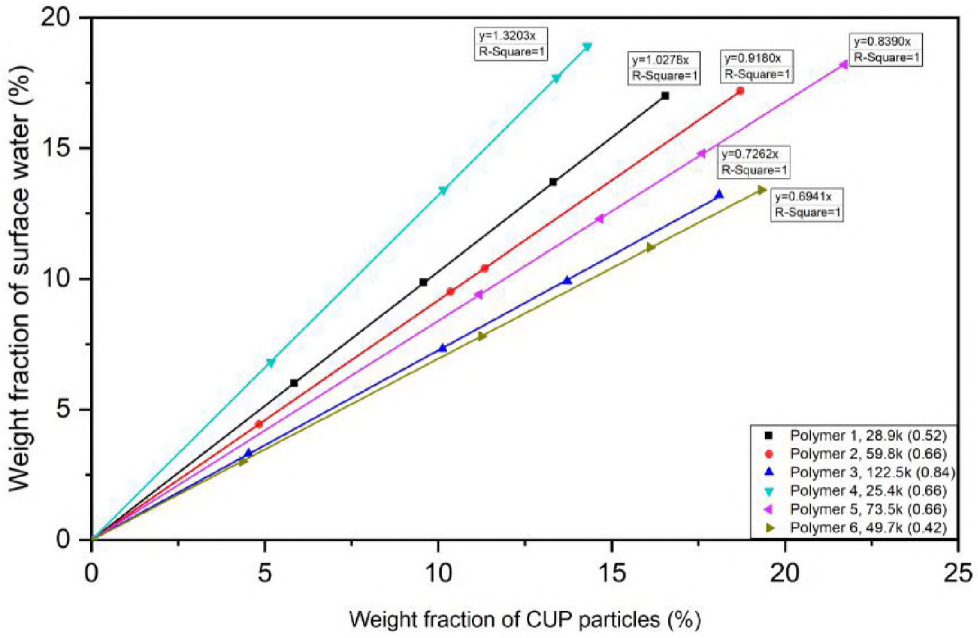

Figure 10. Weight fraction of surface water of different CUPs with different monomer ratio vs weight fraction of each CUP.

Note: The box legend is Polymer, molecular weight and charge density.

Molecular weight of Polymer 4 is slightly larger than Polymer 1, the weight fraction of surface water should have been similar if the surface water is only dependent

upon surface area and not on charge density. However, the charge density of Polymer 4 is much higher than polymer 1 and the surface water was significantly higher. This increase indicates that the surface water is dependent upon charge density. In addition, by comparing Polymer 2 and 5, with similar charge density, Polymer 2 has smaller molecular weight, so that it has more surface area and also more surface water. The conclusion can be made that both molecular weight and charge density play important roles in affecting the weight fraction of surface water. As for the same monomer ratio, larger molecular weight CUP particles will have higher charge density, and if the monomer ratio is different, with similar molecular weight, the surface water weight fraction is proportional to the ions per nm^2, and higher charge density gives a higher surface water weight fraction. When the charge density is the same, higher molecular weight CUP has less surface water weight fraction i.e. the surface area defines the surface water weight fraction.

All the CUP solutions discussed in Figure 10 are below the concentration where Manning condensation occurs. Polymer 1 was used to evaluate higher concentrations as is shown in Figure 11. At concentrations above 20% the weight fraction of water begins to plateau at about 35%. Increasing the concentration causes an increase in the inter-molecular counterion interaction as the distance between ions becomes shorter. This interaction causes Manning condensation and reduces the effective charge on the surface. With less charge, the hydration layer decreases. Looking at Figure 10 and 11, the linear behavior at low concentration can be used to define when Manning condensation becomes significant by noting where the plot becomes non-linear.

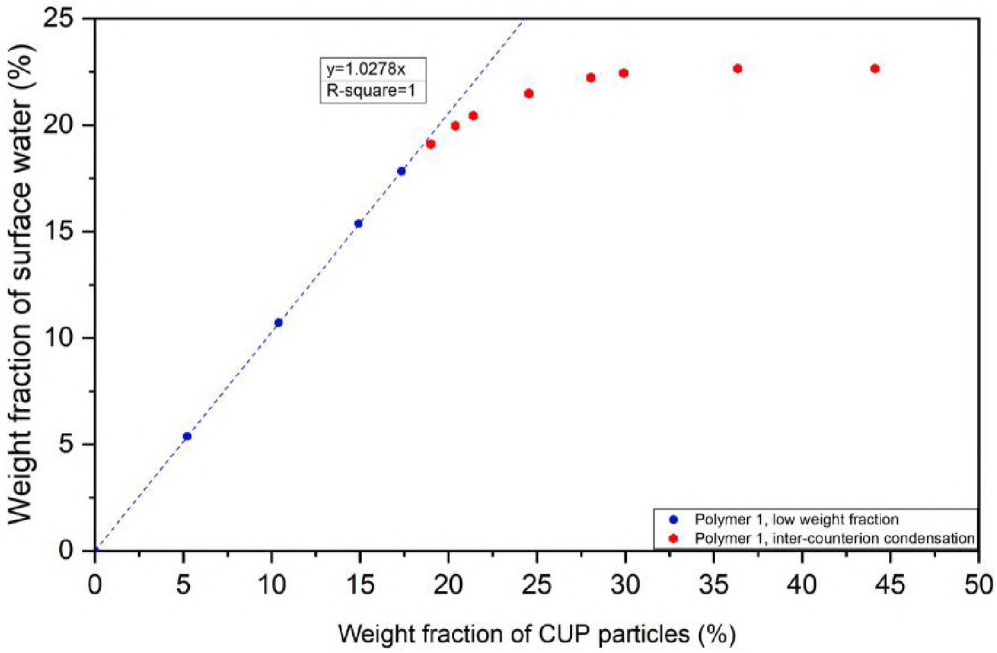

Figure 11. Weight fraction of surface water vs CUP particles of Polymer 1.

3.4. SURFACE WATER DENSITY

Surface water has been found to have a greater density than bulk or free water [10,33,34]. To gain a deeper understanding of CUP surface water, the density of the CUP solutions were measured by high precision density meter at various weight fractions of CUP particles. Values of $1/\rho_s$ were plotted against weight fraction of CUP particles. The reciprocal of density of CUP solution was found to have a linear relationship with the weight fraction of CUP particles at low concentration [8].

Figure 12 shows polymer 1 as an example. It was observed that with the increasing of weight fraction of CUP particles, the reciprocal of density had an excellent linear regression fit up to about 20%. However, at higher concentrations the data deviated from linearity. This deviation can be explained by the increased weight fraction of CUP particles shortening the distance between the charged particles causing inter-molecular

counterion condensation. The condensation reduces the amount of bound water per particle and thus alters the observed density. Higher concentrations could not be accurately measured for density due to their high viscosity.

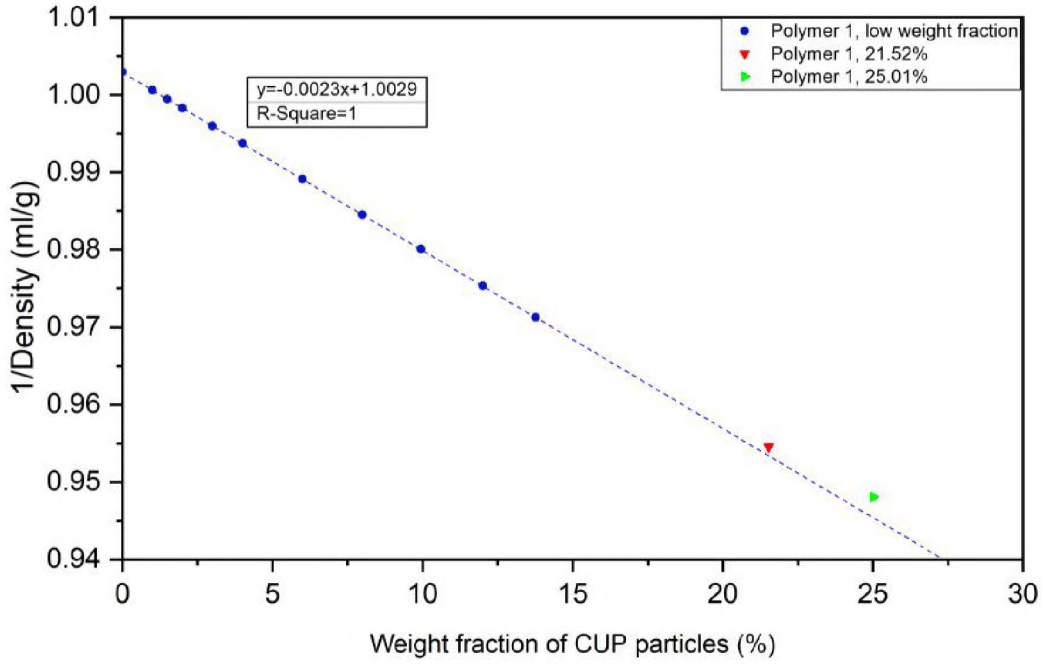

Figure 12. Dependence of $1/\rho_s$ on weight fraction of Polymer 1 CUP solution.

In a given CUP solution, there are three components: free water, surface water and CUP particles. The combination of volume of CUP solid, volume of surface water and volume of free water is equal to the volume of the solution. By knowing the weight fraction of surface water, free water and CUP solids, as well as the density of CUP solid, free water and solution, the density of surface water can be determined by Equation (11).

$$\frac{1}{\rho_S} = \frac{X_{FW}}{\rho_{FW}} + \frac{X_{SW}}{\rho_{SW}} + \frac{X_{CUP}}{\rho_{CUP}} \tag{11}$$

where ρ_s is the density of CUP solution, ρ_{sw} is the density of surface water, ρ_{FW} is the density of free water, ρ_{CUP} is the density of CUP particle.

For each polymer, the surface water density was found to be constant at low weight fraction of CUP particles, and when the weight fraction was high enough to cause inter-molecular counterion condensation the density of surface water drops due to the decreased effective charge density as shown in Table 3.

Table 3. Density of surface water for Polymers 1-7.

CUPs	X_{CUP}	ρ_{sw} (g/ml)	CUPs	X_{CUP}	ρ_{sw} (g/ml)
1 28.9k (0.52)	5.85%	1.0413	3 122.5k (0.84)	4.53%	1.0544
	9.57%	1.0411		10.12%	1.0560
	13.32%	1.0412		13.72%	1.0564
	16.55%	1.0412		18.10%	1.0563
	25.01%	1.0358			
2 59.8k (0.66)	4.83%	1.0511	4 25.4k (0.66)	5.18%	1.0500
	10.35%	1.0508		10.15%	1.0500
	11.35%	1.0509		13.41%	1.0502
	18.72%	1.0507		14.30%	1.0501
5 73.5k (0.66	11.19%	1.0491	6 49.7k (0.42)	4.35%	1.0335
	14.67%	1.0502		11.25%	1.0354
	17.62%	1.0506		16.11%	1.0357
	21.72%	1.0512		19.32%	1.0360
7 22.7k (0.24)	5.00%	1.0231			

When comparing the densities of surface water of CUP solutions with different molecular weights, as it is shown in Figure 13, Polymer 2, Polymer 4 and Polymer 5 have

same charge density (0.66 charges per nm^2) and the densities of surface water are the same. CUPs with higher charge density have higher surface water density. All the CUP polymers except Polymer 3 fit a linear regression relationship of surface water density to surface charge density. Polymer 3 has the largest molecular weight and highest charge density which results in intra-molecular counterion condensation reducing the surface effective charge. This condensation leads to the actual effective charge density being smaller, thus resulting in a slightly smaller surface water density than expected by the linear relationship. When extrapolating the linear function to zero, where there is no charge on the surface, the surface water density is 1.0075 g/ml, which is slightly larger than free water (0.997043 g/ml) [74]. This zero point should also represent the association with the ester groups which is the other group capable of hydrogen bonding interaction with water.

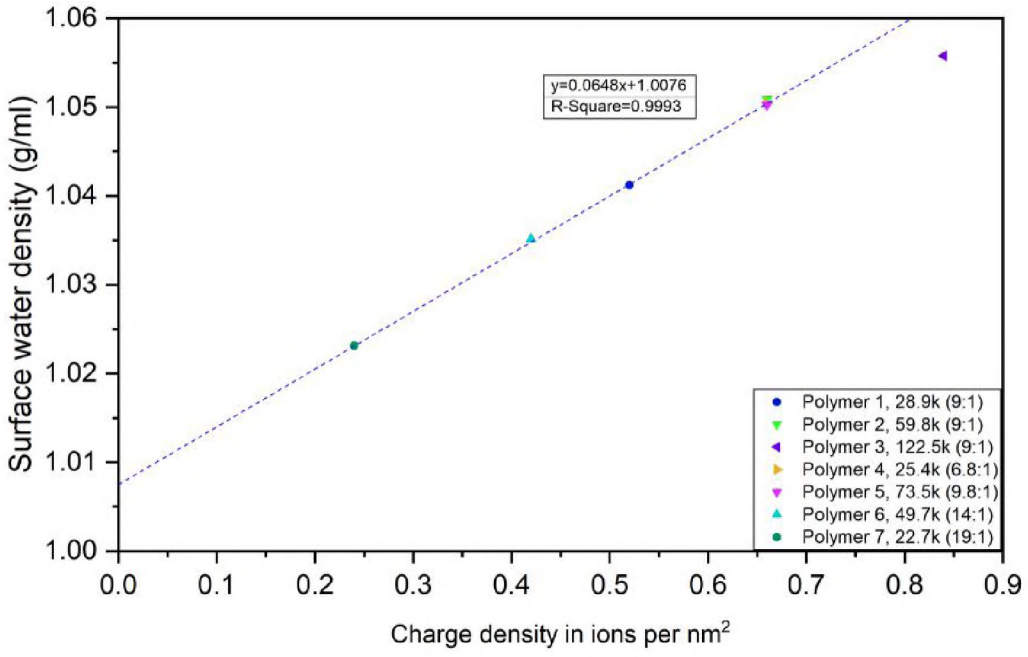

Figure 13. Surface water density vs charge density in ions per nm^2.

The density of the surface water can be related to the hydrogen bonding of water to the carboxylate and the ester groups on the surface. The carboxylate groups form up to six strong hydrogen bonds and the esters four weaker. Therefore, since the carboxylate groups form a stronger interaction the density would be higher than with the ester groups. As the charge density increases, the number of carboxylates increase as does the density [75].

3.5. SURFACE WATER THICKNESS

To gain a deeper understanding of CUP surface water, it is important to relate our results to a structural model for the calculation of the surface water layer thickness. The total surface area of the CUP particles was calculated based on the measurement of the diameter of the CUP particle. The densities of surface water were determined, by knowing the weight fraction of surface water and number of CUP particles, the thickness of each sample was determined by Equation (12) [8].

$$\frac{4}{3}\pi\left(\lambda+\frac{d}{2}\right)^3-\frac{4}{3}\pi\left(\frac{d}{2}\right)^3=\frac{X_{SW}M}{X_{CUP}N_A\rho_{SW}} \tag{12}$$

where λ is the thickness of surface water, d is the diameter of CUP particle, X_{SW} is the weight fraction of surface water, X_{CUP} is the weight fraction of CUP particle, M is the molecular weight of CUP, N_A is Avogadro constant, ρ_{sw} is the density of surface water.

Table 4 shows the surface water thickness of each CUP at different weight fractions. The thickness of CUPs ranges from 0.43 to 0.77 nm, which is about two to four water molecules thick. While previous studies have been suggested that surface water is as thick as from a few water molecules to several dozens of water molecules depending

on the particles surface properties [76,77]. The thickness is likely to be primarily controlled by the charge density of the CUP particle surface and any hydrogen bonding groups at the surface. Charges will hold the water in a more bound state than water more loosely held at more hydrophobic surface groups.

Table 4. Surface water thickness of each CUP at different concentrations.

CUPs	X_{CUP}	λ (nm)	CUPs	X_{CUP}	λ (nm)
Polymer 1 28.9k (0.52)	5.85%	0.635	Polymer 3 122.5k (0.84)	4.53%	0.766
	9.57%	0.637		10.12%	0.766
	13.32%	0.636		13.72%	0.765
	16.55%	0.636		18.10%	0.766
	25.01%	0.564			
Polymer 2 59.8k (0.66)	4.83%	0.733	Polymer 4 25.4k (0.66)	5.18%	0.732
	10.35%	0.735		10.15%	0.735
	11.35%	0.734		13.41%	0.734
	18.72%	0.735		14.30%	0.735
Polymer 5 73.5k (0.66)	11.19%	0.734	Polymer 6 49.7k (0.42)	4.35%	0.556
	14.67%	0.733		11.25%	0.556
	17.62%	0.734		16.11%	0.557
	21.71%	0.732		19.32%	0.556
Polymer 7 22.7k (0.24)	5.00%	0.427			

Comparing Polymer 1, 2 and 3, it can be concluded that the larger particle has the thicker surface water layer due to it having more carboxylate groups at the surface per unit area. A higher charged surface will form a thicker electrical double layer, giving more counterions and associated more water molecules. This result agrees with the

findings of Chen et.al [66]. While Polymer 4 has a lower molecular weight but the same ions per nm^2 as Polymer 2, the thickness of surface water are the same. By looking at Polymer 1, the thickness of surface water is 0.636 nm when the weight fraction is small, and the thickness decreases to 0.564 nm when the weight fraction is 25% due to the increased inter-molecular counter-ion condensation. This again implies that, the thickness of surface water is proportional to ions per nm^2, which also corresponds to the finding of weight fraction of surface water.

Figure 14 shows the plot of surface water thickness and charge density in ions per nm^2. When the charge density increases on a single CUP particle, the intra-molecular counterion condensation occurs on itself, reducing the effective charges on the surface, resulting in a thinner surface water layer.

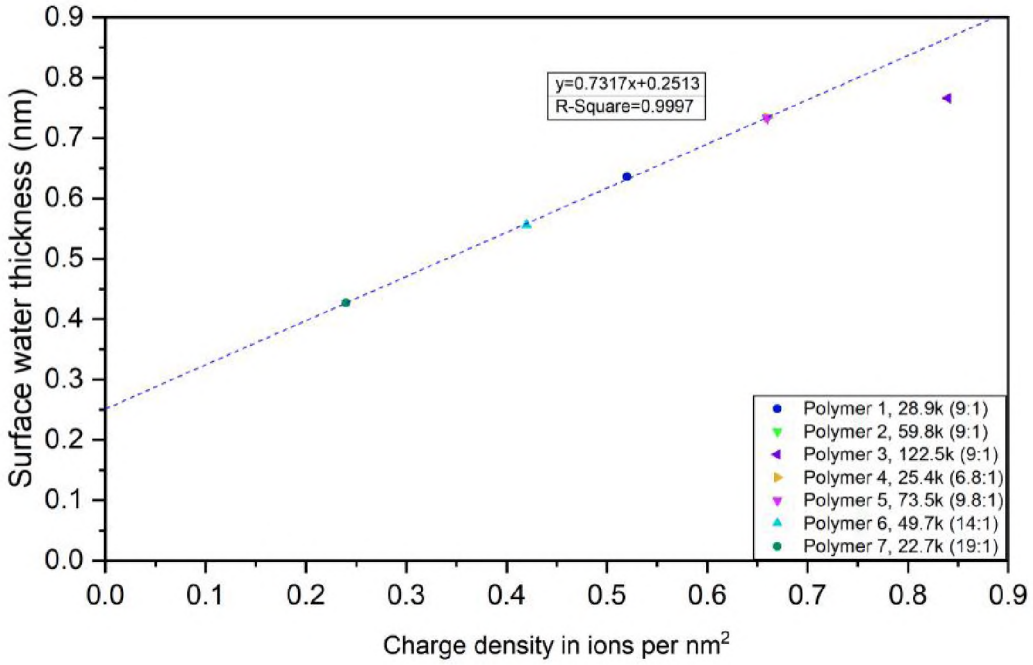

Figure 14. Surface water thickness vs charge density in ions per nm^2.

As can be seen in Figure 14, when charge density was smaller than 0.66 nm, surface water thickness increases with the increasing of charge density, and when charge density is higher, surface water thickness increases but less than expected due to the inter-molecular counterion condensation. Extrapolation of the line to zero shows that when there is no effective charge on CUP surface, there is still a 0.2513 nm surface water layer, which is approximately a monolayer of water [78-80].

3.6. MELTING POINT DEPRESSION

The melting point depression of CUP solutions can also offer potential information. DSC was used to accurately measure the heat flow associated with thermal transitions in CUP solutions. As is well known, by adding a non-volatile solute, the melting point of a solvent decreases [81]. If we consider the solution is ideal, the freezing/melting point depression can be described by Equation (13).

$$\Delta T_F = K_F \cdot b \cdot i \tag{13}$$

where ΔT_F is the melting point depression in K, K_F is cryoscopic constant (1.853 K·kg/mol), i is van't Hoff constant, b is the molality of solute in mol/kg.

Since the CUP solutions were modified by NaOH to pH=8.5, it's important to know if the Na^+ might contribute to the temperature depression, which might affect the van't Hoff factor in Equation (13). The molality of Na^+ in CUP solutions was calculated by Equation (14). The measured melting point depression of water and NaOH modified water was obtained by DSC, there was no difference between pure and pH modified water. By knowing the molality of Na^+, the melting point depression, contributed by

sodium ion in solution, was calculated to be 1.1755×10^{-5} K, obtained from Equation (14), which was negligible.

$$b_{Na} = \frac{10^{pH-14} \cdot V}{m_{solution} - m_{NaOH}} \tag{14}$$

where b_{Na} is the molality of sodium ions, V is the volume of solution, $m_{solution}$ is the mass of solution, m_{NaOH} is the mass of NaOH.

Knowing the molality $b=(n_{solute}/m_{solvent})$, the molality of CUP particles was calculated from Equation (15),

$$b_{CUP} = \frac{X_{CUP}}{(1-X_{CUP}) \cdot M_W} \tag{15}$$

where b_{CUP} is the molality of CUP particle, M_W is the molecular weight of CUP, X_{CUP} is the weight fraction of CUP.

By using Equation (15), the molality of CUP can be calculated, the relation between the molality of CUP and melting point depression was plotted in Figure 15. The molality of CUP being equal to 0.001 mol/kg was picked, the corresponding ΔT_{CUP} was determined from Figure 15. Rearranging Equation (13), the van't Hoff factor can be described as Equation (16).

$$i = \frac{\Delta T_{CUP}}{b \cdot K_F} \tag{16}$$

In each CUP particle, the number of repeat units (n_{rep}) was calculated by dividing the molecular weight of CUP by the molecular weight of each repeat unit. So that the number of effective groups that contributed to van't Hoff factor can be expressed as Equation (17,18).

$$n_{rep} = \frac{M_W}{n \cdot M_{MMA} + M_{MAA}} \tag{17}$$

where n_{rep} is the number of repeat unit in one CUP particle, M_{MMA} is the molecular weight of MMA monomer, M_{MAA} is the molecular weight of MAA monomer, n is the molar ratio of monomer MMA/MAA.

$$n_{eff} = \frac{i}{n_{rep}} \tag{18}$$

where n_{eff} is the number of effective groups in each repeat unit.

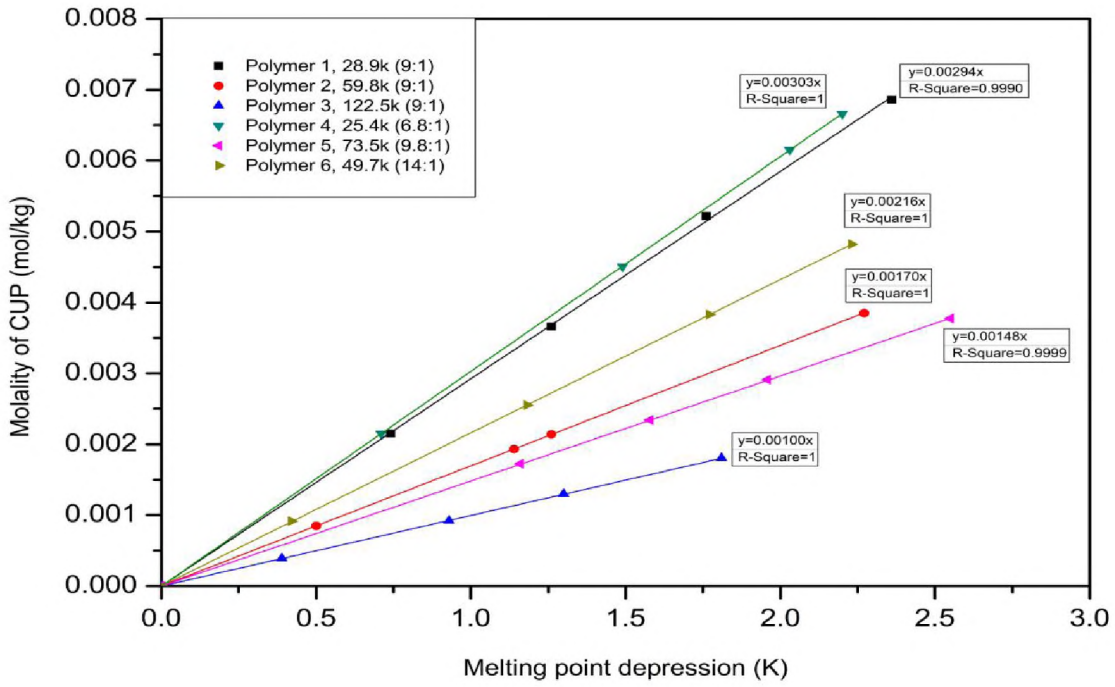

Figure 15. Molality of CUPs vs melting point depression.

The van't Hoff factor, which is the number of ions per individual molecules of solute. As it was well known, van't Hoff factor is equal to 2 for NaCl, and 3 for $BaCl_2$ as an example. In each repeat unit, there is one carboxylate group and several ester groups.

Each carboxylate group was neutralized by NaOH, thus sodium ion may or may not be taken into account, shown in Equation (19) and (20).

$$n_{ester} = n_{eff} - n_c \tag{19}$$

$$n_{ester} = n_{eff} - 2 \cdot n_c \tag{20}$$

where n_{acid} is the number of carboxylate group in each repeat unit, which equals to 1, n_{ester} is the number of ester group in each repeat unit.

The surface area of the CUP particle can be expressed as $A_{CUP}=4\pi r^2$, average area of each repeat unit on CUP was determined.

$$A_{rep} = \frac{A_{CUP}}{n_{rep}} \tag{21}$$

where A_{CUP} is the surface area of one CUP particle.

Since the surface area of CUP was taken by carboxylate and ester groups, in each repeat unit, there is one carboxylate group and several ester groups. Using Equation (22), the average area of each ester group and carboxylate group were determined by using different molecular weight CUP particles.

$$A_{rep} = A_c + n_{ester} \cdot A_{ester} \tag{22}$$

where A_c is the average area of one carboxylate group occupied on CUP surface, A_{ester} is the average area of one ester group occupied on CUP surface.

The calculation indicated that sodium ion did contribute to the van't Hoff factor value, the average area of a carboxylate group on CUP surface was 0.374 nm^2, while average area of a carboxylate group is 0.287 nm^2. If assuming each group is a plane circle, the radius of carboxylate group is 0.244 nm, the radius of carboxylic acid group is

0.213 nm. Which is similar to the total of the length of C=O and O-H bond. The number of carboxylate groups varies upon different molecular weight of CUP particles. Results are shown in Table 5 [82,83].

Table 5. Average area of each carboxylate and ester group on CUPs.

CUPs	ΔT_{CUP} (K)	b_{CUP}	i	n_{rep}	n_{eff}	A_{rep} (nm^2)	A_e (nm^2)	A_c (nm^2)	n^*_c/n^*_e
1 (0.52)	0.344	0.001	185.645	29.276	6.341	1.911	0.375	0.284	29.3/126.3
2 (0.52)	0.589	0.001	317.863	60.579	5.247	1.501	0.374	0.285	60.6/196.7
3 (0.52)	1.010	0.001	545.062	124.096	4.392	1.181	0.375	0.285	124.1/296.8
4 (0.52)	0.330	0.001	178.090	33.121	5.377	1.548	0.373	0.289	33.1/111.9
5 (0.52)	0.674	0.001	363.734	68.869	5.282	1.513	0.374	0.286	68.9/226.0
6 (0.52)	0.462	0.001	249.325	33.406	7.463	2.408	0.372	0.290	33.4/182.5
7 (0.52)	0.262	0.001	141.392	11.417	12.397	4.185	0.375	0.290	11.4/118.7

ΔT: melting point depression in K. b_{CUP}: molality of CUP particles. i: van't Hoff factor. n_{rep}: number of repeat unit in each CUP particle. n_{eff}: number of effective groups per repeat unit. n_{ester}: number of ester groups in each repeat unit. A_{rep}: area of one repeat unit. A_e: average area each ester group takes (in equation $\Delta T=i\cdot K_F\cdot b$, consider i=2). A_c: average area each carboxylate group takes in equation $\Delta T=i\cdot K_F\cdot b$, consider i=2). n^*_c/n^*_e: number of carboxylate and ester groups on one CUP particle surface.

Polymer 1, 2 and 3 have the same monomer ratio, with the increasing of molecular weight of CUP, the number of ester groups per repeat unit decreases. Because higher molecular weight CUP has more of hydrophobic groups on the inside, leaving more hydrophilic charged groups on the surface, giving higher ions per nm^2. Polymer 2, 4 and 5 have similar ions per nm^2 but different molecular weight, the number of ester groups per repeat unit are fairly close. This again indicates that the number of ester groups on the surface is dependent on the charge density with the carboxylates taking surface positions over esters during the formation of CUPs. The implication is that the

area of the surface minus the area needed by the carboxylates leaves the remainder to be filled in by the esters with most esters being on the particle interior.

3.7. SPECIFIC HEAT ANALYSIS

Specific heat is also an important thermodynamic component. The specific heat measurement at a given temperature were also gathered from the DSC measurement, however, in order to obtain proper and critical measurement, the zeroline has to be measured separately and subtracted from the measured curve before evaluation.[84] An empty DSC pan was used to determine the heat flow rate of the zeroline ϕ_0 (T), and a calibration substance of a known behavior, water, was placed into another DSC pan with similar mass, using the same experimental procedure. The precise specific heat CS can be calculated by simply subtracting the calibrated heat flow rate zeroline and combing with the known substance, shown in Equation (23).

$$C_S = \frac{q_S - q_0}{q_{ref} - q_0} \cdot \frac{m_{ref}}{m_S} \cdot C_{ref} \tag{23}$$

where C_S is the specific heat of sample, C_{ref} is the specific heat of reference, q_s is the heat flow rate of the sample, q_0 is the heat flow rate of empty DSC pan, q_{ref} is the heat flow rate of reference, m_{ref} is the mass of reference, ms is the mass of sample.

If considering the mass difference of two DSC pans used for zeroline calibration and actual measurement, it is possible to further make routine calculation, Equation (24). However, the DSC pan correction result in an error smaller than 1%, which is negligible.

$$C_S = \frac{q_S - q_0}{q_{ref} - q_0} \cdot \frac{m_{ref}}{m_S} C_{ref} + \frac{m_{Cr,ref} - m_{Cr,S}}{m_S} \cdot C_{Cr} \quad (24)$$

where $m_{Cr, ref}$ is the mass of reference DSC pan, $m_{Cr, S}$ is the mass of sample DSC pan.

The dry polymer is a fine powder with low thermal conductivity, in order to have better thermal conductivity, the dry polymer was put in an open cap DSC sample pan, and heated to 453.15 K to get rid of the moisture and let the polymer melt to have better contact with the pan. The pan was then sealed, cooled to 233.15 K, isothermal for 10 mins, heated to 313.15 K. Two temperatures were picked for measurement, 253.15 K and 293.15 K, because at 253.15 K, the free water is in its ice form, while at 293.15 K, free water is liquid. Also, at these two temperatures, the baseline is strait, there is no overlapping with the endothermic peak and for one sample at a fixed temperature, the specific heat of dry CUP and surface water are constant. The specific heat of CUP solution is the total of the specific heat of free water (ice), dry CUP and surface water. The specific heat of each component at 263.15 K and 293.15 K was obtained from DSC measurement. Knowing the weight fraction, the specific heat of surface water was determined by Equation (25) and (26).

$$C_{P(s)} = aC_{P(ice)} + bC_{P(CUP)} + cC_{P(sw)} \quad (25)$$

$$C_{P(s)} = aC_{P(Fw)} + bC_{P(CUP)} + cC_{P(sw)} \quad (26)$$

where $C_{P(s)}$ is the specific heat of CUP solution, $C_{P(ice)}$ is the specific heat of ice, $C_{P(CUP)}$ is the specific heat of CUP particle, $C_{P(sw)}$ is the specific heat of surface water, $C_{P(Fw)}$ is the specific heat of free water, a, b and c represent the weight fraction of each component in the CUP solution.

The specific heat of each component in Polymer 1-7 were calculated, surface water specific heat is about 3.07 to 3.09 J/g·K at 293.15 K and 3.04 to 3.07 J/g·K at 253.15 K, which exhibit a small dependency on charge density, Table 6. The values exhibit only a small decrease in going from liquid water temperatures to well below freezing for water. The specific heat of surface water was independent of concentration for the range studied, which were all below the point of Manning condensation. The data for surface water at 293.15 K indicates that the water has more freedom than ice but less than liquid water. The small lowering of the specific heat with a 40 degree drop was similar to many materials not undergoing a phase change or other transition in mobility.

Table 6. Specific heat of each components in polymer 1-7 (J/g·K).

CUPs	Weight fraction	CUP solid (253.15 K)	Surface water (253.15 K)	Ice (253.15 K)	CUP solid (293.15 K)	Surface water (293.15 K)	Free water (293.15 K)
Polymer 1 28.9k (0.52)	5.85%	1.235	3.055	1.943	1.321	3.081	4.182
	9.57%	1.235	3.052	1.943	1.321	3.078	4.182
	13.32%	1.235	3.053	1.943	1.321	3.082	4.182
	16.55%	1.235	3.053	1.943	1.321	3.080	4.182
Polymer 2 59.8k (0.66)	4.83%	1.230	3.047	1.943	1.315	3.073	4.182
	10.35%	1.230	3.051	1.943	1.315	3.076	4.182
	11.35%	1.230	3.049	1.943	1.315	3.072	4.182
	18.72%	1.230	3.049	1.943	1.315	3.074	4.182
Polymer 3 122.5k (0.84)	4.53%	1.195	3.042	1.943	1.305	3.067	4.182
	10.12%	1.195	3.041	1.943	1.305	3.068	4.182
	13.72%	1.195	3.040	1.943	1.305	3.065	4.182
	18.10%	1.195	3.041	1.943	1.305	3.066	4.182
Polymer 4 25.4k (0.66)	5.18%	1.235	3.050	1.943	1.322	3.073	4.182
	10.27%	1.235	3.049	1.943	1.322	3.075	4.182
	13.52%	1.235	3.050	1.943	1.322	3.074	4.182
	14.47%	1.235	3.051	1.943	1.322	3.076	4.182
Polymer 5 73.5k (0.66)	11.23%	1.228	3.048	1.943	1.311	3.074	4.182
	14.67%	1.228	3.047	1.943	1.311	3.075	4.182
	17.62%	1.228	3.049	1.943	1.311	3.074	4.182
	21.71%	1.228	3.048	1.943	1.311	3.075	4.182
Polymer 6 49.7k (0.42)	4.35%	1.231	3.059	1.943	1.316	3.086	4.182
	11.25%	1.231	3.058	1.943	1.316	3.087	4.182
	16.11%	1.231	3.059	1.943	1.316	3.086	4.182
	19.32%	1.231	3.061	1.943	1.316	3.086	4.182
Polymer 7 22.7k (0.24)	5.00%	1.237	3.066	1.943	1.324	3.093	4.182

Surface water associated to the carboxylate and ester groups on CUP surface, known the specific heat of surface water at 293.15 K and 253.15 K, as well as the number of each functional groups, the specific heat of water associated to the carboxylate and ester could be estimated by Equation (27).

$$C_{P(sw)} = \frac{n_{acid}}{n_{acid} + n_{ester}} \cdot C_{P(swa)} + \frac{n_{ester}}{n_{acid} + n_{esetr}} \cdot C_{P(swe)} \quad (27)$$

where $C_{P(swa)}$ is the specific heat of water associated to carboxylate groups, $C_{P(swe)}$ is the specific heat of water associated to ester groups.

Table 7 shows the specific heat due to the ester and the carboxylate groups on the surface.

Table 7. Specific heat of surface water associated with carboxylate and ester groups at 293.15 K (J/g·K).

CUPs	$Cp_{(SW)}$ of acid (293.15 K)	$Cp_{(SW)}$ of ester (293.15 K)
1 (0.52)	2.979	3.103
2 (0.66)	2.979	3.103
3 (0.84)	2.984	3.102
4 (0.66)	2.965	3.107
5 (0.66)	2.975	3.105
6 (0.42)	2.960	3.109
7 (0.24)	2.978	3.104

This estimation of the effect of each group gives a relatively consistent average value which could be used to define a new polymer based on a group contribution basis.

Table 8 shows the specific heat of surface water associated with carboxylate and ester groups at 253.15 K.

Table 8. Specific heat of surface water associated with carboxylate and ester groups at 253.15 K (J/g·K).

CUPs	$Cp_{(SW)}$ of acid (253.15 K)	$Cp_{(SW)}$ of ester (253.15 K)
1 (0.52)	2.965	3.073
2 (0.66)	2.954	3.078
3 (0.84)	2.953	3.078
4 (0.66)	2.956	3.078
5 (0.66)	2.965	3.073
6 (0.42)	2.954	3.078
7 (0.24)	2.956	3.077

4. CONCLUSION

This work discussed the thermal properties of CUPs with different molecular weight, monomer ratio and CUP surface charge density (ions per nm^2), based on the heat of fusion, specific heat and melting point depression aspects. It was found that surface water occupied a significant amount of volume in CUP solutions. Rapid cooling of CUP solutions will result in larger amount of surface water due to more rapid ice crystal growth and less time for CUP particles to migrate and undergo Manning condensation. The effect of cooling rate is less on the higher weight fraction solutions due to charge charge repulsion which lowers mobility. The density of surface water was calculated and ranged from 1.023 g/ml to 1.056 g/ml depending on the charge density. The thickness of

surface water was calculated, showing a trend of increasing with the increasing surface charge density. The molecular weight had no effect on the thickness of the surface water layer. However, as the weight fraction of CUP particles increased above approximately 20%, inter-molecular counterion condensation occurs and decreases surface water layer thickness. The melting point depression was found to linearly dependent upon molality of CUPs with the slope being related to the number of ions on the surface of CUPs. Using the melting point depression data, the average area of carboxylate and ester groups were determined, and its results are independent of the molecular weight. The specific heat of surface water was found to be 3.07 to 3.09 J/g·K at 293.15 K and 3.04 to 3.07 J/g·K at 253.15 K, which was between ice and free water and exhibited a small dependency with the surface charge density. CUPs are true nanoscale spheroidal particles with the molecular weight and surface charge being easily designed and synthesized. The findings can be readily extended and utilized in many fields including biochemical and life sciences. Therefore, CUP particles offer an excellent model to investigate the behavior of surface water, which can be of fundamental importance to protein, micelle, hydrogel and material science. In addition, CUP solution is zero VOC and free of surfactant, it has great potentials in coating, adhesive and many other applications. This work represents a comprehensive study of CUP surface water which defines structural components and their effects on surface water in a detailed quantitative manner for the first time.

ACKNOWLEDGEMENTS

The authors would like to thank the Department of Chemistry for the use of the DSC and the Missouri S&T Coating Institute for financial support. Also Rachel Keppler for her assistance as an undergraduate researcher and Dave Satterfield for DSC calibration.

REFERENCES

1. Van De Mark, M. R.; Natu, A.; Gade, S. V.; Chen, M.; Hancock, C.; Riddles, C. Molecular Weight(Mn) and Functionality Effects on CUP Formation and Stability. *J. Coat. Technol. Res.* **2014**, *11*, 111-122.

2. Oncley, J. L. Evidence from Physical Chemistry Regarding the Size and Shape of Protein Molecules from Ultra-centrifugation, Diffusion, Viscosity, Dielectric Dispersion, and Double Refraction of Flow. *Annals of the New York Academy of Science*. **1941**, *41*, 121-150.

3. Pammenter, N. W.; Vertucci, C. W.; Berjak, P. Homeohydrous (Recalcitrant) Seeds: Dehydration, the State of Water and Viability Characteristics in Landolphiakirkii. *Plant Physiol.* **1991**, *96*, 1093-1098.

4. Yaghmur, A.; Aserin, A.; Tiunova, I.; Garti, N. Sub-zero temperature behaviour of non-ionic microemulsions in the presence of propylene glycol by DSC. *Journal of Thermal Analysis and Calorimetry*. **2002**, *69*, 163-177.

5. Jahnert, S.; Vaca, C. F.; Schaumann, G. E.; Schreiber, A.; Schonhoff, M.; Findenegg, G. H. Melting and freezing of water in cylindrical silica nanopores. *Phys Chem Chem Phys*. **2008**, *10*, 6039-6051.

6. Findenegg, G. H.; Jahnert, S.; Akcakayiran, D.; Schreiber, A. Freezing and Melting of Water Confined in Silica Nanopores. *ChemPhysChem*. **2008**, *9*, 2651-2659.

7. Riddles, C.; Zhao, W.; Hu, H. J.; Chen, M.; Van De Mark, M. R. Self-assembly of Water Insoluble Polymers into Colloidal Unimolecular Polymer (CUP) Particles of 3-9 nm. *Polymer*. **2013**, *55*, 48-57.

8. Chen, M., Riddles, C. Van De Mark, M. Gel point behavior of colloidal unimolecular polymer (CUP) particles. *Colloid Polym Sci*. **2013**, *291*, 2893–2901.

9. Vidulich, G. A.; Evans, D. F.; Kay, R. L. The Dielectric Constant of Water and Heavy Water between 0 and 40. degree. *J. Phys. Chem.* **1967**, *71*, 656-662.

10. Chen, M.; Van De Mark, M. R. Rheology Studies on Colloidal Unimolecular Polymer (CUP)Particles in Absence of NaCl. *Preprints.* **2011**, *52*, 336-337.

11. Natu, A.; Van De Mark, M. R. Synthesis and characterization of an acid catalyst for acrylic-melamine resin systems based on colloidal unimolecular polymer (CUP) particles of MMA-AMPS. *Progress in Organic Coatings.* **2015**, *81*, 35-46.

12. Aseyev, V. O.; Tenhu, H.; Klenin, S. I. Contraction of a Polyelectrolyte upon Dilution. Light-Scattering Studies on a Polycation in Saltless Water-Acetone Mixtures. *Macromolecules.* **1998**, *31*, 7717-7722.

13. Dobrynin, A. V.; Rubinstein, M.; Obukhov, S. P. Cascade of Transitions of Polyelectrolytes in Poor Solvents. *Macromolecules.* **1996**, *29*, 2974-2979.

14. Newton, R.; Gortner, R. A. A Method for Estimating Hydrophilic Colloid Content of Expressed Plant Tissue Fluids. *Bot. Gaz.* **1922**, *74*, 442-446.

15. Bockris, J. O.; Conway, B. E.; Yeager, E. Comprehensive Treatise of Electrochemistry. *Angewandte.* **1981**, *93*, 840.

16. Fawcett, W. R.; Levine, S.; deNobriga, R. M.; McDonald, A. C. A molecular model for the dielectric properties of the inner layer at the mercury/aqueous solution interface. *J. Electroanal. Chem.* **1980**, *111*, 163-180.

17. Lee, C.; McCammon, J. A.; Rossky, P. J. The structure of liquid water at an extended hydrophobic surface. *J. Chem. Phys.* **1984**, *80*, 4448-4455.

18. Patey, G. N.; Torrie, G. M. Water and salt water near charged surface: a discussion of some recent theoretical results. *Chemica Scripta.* **1989**, *29*, 39-47.

19. Schmickler, W.; Henderson, D. New model for the structure of the electrochemical interface. *Progr. Surf. Sci.* **1987**, *22*, 323-420.

20. Price, D.; Halley, J. W. Electronic structure of metal-electrolyte surfaces: Three-dimensional calculation. *Phys. Rev. B.* **1988**, *38*, 9357-9367.

21. Glosli, J. N.; Philpott, M. R. Molecular-dynamics simulation of adsorption of ions from aqueous media onto charged electrodes. *J. Chem. Phys.* **1992**, *96*, 6962-6969.

22. Spohr, E. Computer simulation of the water/platinum interface. *J. Phys. Chem.* **1989**, *93*, 6171-6180.

23. Raghavan, K.; Foster, K.; Berkowitz, M. Comparison of the structure and dynamics of water at the platinum(111) and platinum(100) interfaces: molecular dynamics study. *Chem. Phys. Lett.* **1991**, *177*, 426-432.

24. Nagy, G.; Heinzinger, K. A molecular dynamics study of water monolayers on charged platinum walls. *J. electroanalyt. Chem.* **1992**, *327*, 25-30.

25. Aloisi, G.; Foresti, M. L.; Guidelli, R. A Monte Carlo simulation of water molecules near a charged wall. *J. Chem. Phys.* **1989**, *91*, 5592-5596.

26. Erko, M.; Findenegg, G. H.; Cade, N.; Michette, A. G.; Paris, O. Confinement-induced structural changes of water studied by Raman scattering. *Phys. Rev.B.* **2011**, *84*, 104205.

27. Johnson, G. A.; Lecchini, S. M. A.; Smith, E. G.; Clifford, J.; Pethica, B. A. Role of water structure in the interpretation of colloid stability. *Discuss. Faraday Soc.* **1966**, *42*, 120-133.

28. Clifford, J. Properties of Micellar Solutions. Part 4.- Spin Lattice Relaxation Times of Hydrocarbon Chain Protons in Solutions of Sodium Alkyl Sulphates. *Transaction of the Faraday Society.* **1965**, *61*, 1276-1282.

29. Clifford, J.; Lecchini, S. State of Liquid Water near Solid Interfaces. *SCI Monograph.* **1967**, *25*, 174-195.

30. Katayama, S.; Fujiwara, S. NMR study of the spatial effect of polyacrylamide gel upon the water molecules confined in it. *J. Am. Chem. Soc.* **1979**, *101*, 4485-4488.

31. Van De Mark, M. R.; Zore, A.; Geng, P.; Zheng, F. Colloidal Unimolecular Polymer Particles: CUP. *In Single-Chain Polymer Nanoparticles.* **2017**, 259-312.

32. Mamontov, E. Dynamics of surface water in ZrO2 studied by quasielastic neutron scattering. *J. Chem. Phys.* **2004**, *121*, 9087-9097.

33. Toney, M. F.; Howard, J. N.; Richer, J.; Borges, G. L.; Gordon, J. G.; Melroy, O. R.; Wiesler, D. G.; Yee, D.; Sorensen, L. B. Voltage-dependent ordering of water molecules at an electrode-electrolyte interface. *Nature.* **1994**, *368*, 444-446.

34. Toney, M. F.; Howard, J. N.; Richer, J.; Borges, G. L.; Gordon, J. G.; Melroy, O. R.; Wiesler, D. G.; Yee, D.; Sorensen, L. B. Distribution of water molecules at Ag(111)/electrolyte interface as studied with surface X-ray scattering. *Surface Science.* **1995**, *335*, 326-332.

35. Ling, C. S.; Hansen, W. D. DTA Study of Water in Porous Glass. *Adsorption at Interface.* **1975**, *8*, 129-156.

36. Vidulich, G. A.; Evans, D. F.; Kay, R. L. The Dielectric Constant of Water and Heavy Water between 0 and 40. degree. *J. Phys. Chem.* **1967**, *71*, 656-662.

37. Lee, K. Y.; Ha, W. S. DSC studies on bound water in silk fibroin/S-carboxymethyl kerateine blend films. *Polymer.* **1999**, *40*, 4131-4134.

38. Higuchi, A.; Lijima, T. DSC investigation of the states of water in poly(vinyl alcohol) membranes. *Polymer.* **1985**, *26*, 1207-1211.

39. Ratto, J.; Hatakeyama, T.; Blumstein, R. B. Differential scanning calorimetry investigation of phase transitions in water/chitosan systems. *Polymer.* **1995**, *36*, 2915-2919.

40. Garti, N.; Aserin, A.; Ezrahi, S.; Tiunova, I.; Berkovic, G. Water Behavior in Nonionic Surfactant Systems I: Subzero Temperature Behaviour of Water in Nonionic Microemulsions Studied by DSC. *J. Colloid Interface Sci.* **1995**, *178*, 60-68.

41. Tahmasebi, A.; Yu, J.; Su, H.; Han, Y.; Lucas, H.; Zheng, H.; Wall, T. A differential scanning calorimetric (DSC) study on the characteristics and behaviour of water in low-rank coals. *Fuel.* **2014**, *135*, 243-252.

42. Monti, D.; Chetoni, P.; Burgalassi, S.; Najarro, M.; Saettone, M. F. Increased corneal hydration induced by potential ocular penetration enhancers: assessment by differential scanning calorimetry (DSC) and by desiccation. *Int. J. Pharm.* **2002**, *232*, 139-147.

43. Garti, N.; Aserin, A.; Tiunova, I.; Fanun, M. A DSC study of water behaviour in water-in-oil microemulsions stabilized by sucrose esters and butanol. *Colloids Surf. A.* **2000**, *170*, 1-18.

44. Ross, K. D. Differential scanning calorimetry of nonfreezable water in solute-macromolecule-water system. *J. Food Sci.* **1978**, *43*, 1812-1815.

45. Bushuk, W.; Mehrotra. V. K. Studies of water binding by differential thermal analysis. II. Dough studies using the melting mode. *Cereal Chem.* **1977**, *54*, 320-325.

46. Biswas, A. B.; Kumsah, C. A.; Pass, G.; Philips, G. O. The effect of Carbohydrates on the Heat of Fusion of Water. *J. Solution Chem.* **1975**, *4*, 581-590.

47. Berlin, E.; Kliman, P. G.; Anderson, B. A.; Pallansch, M. J. Water binding in whey protein concentrates. *J. Dairy Sci.* **1973**, *56*, 984-987.

48. Berlin, E.; Kliman, P. G.; Anderson, B. A.; Pallansch, M. J. Changes in state of water in proteinaceous systems. *J. Colloid Interface Sci.* **1970**, *34*, 488-494.

49. Hatakeyema, T.; Yamauchi, A. Studies on bound water in poly(vinyl alcohol) hydrogel by DSC and FT-NMR. *Eur. Polym. J.* **1984**, *20*, 61-64.

50. Ostrowska-Czubenko, J.; Pierog, M.; Gierszewska-Druzynska, M. State of water in noncrosslinked and crosslinked hydrogel chitosan membranes-DSC studies. *Pol. Tow. Chitynowe.* **2011**, *XVI*, 147-156.

51. Muffett, D. J.; Snyder, H. E. Measurement of unfrozen and free water in soy proteins by differential scanning calorimetry. *J. Agric. Food Chem.* **1980**, *28*, 1303-1305.

52. Kobayashi, Y.; Fukada, K. Characterization of swollen lamellar phase of dimyristoylphosphatidylcholine-gramicidin A mixed membranes by DSC, SAXS, and densimetry. *Biophys. Acta.* **1998**, *1371*, 363-370.

53. Standard Terminology Relating to Performance Validation in Thermal Analysis. *ASTM E2161-08*.

54. Standard Terminology Relating to Thermal Analysis and Rheology. *ASTM E473-08*.

55. Principles and Applications of Thermal Analysis. **2007**.

56. East, G. C.; Margerison, D.; Pulat, E. Variation of polymer density with molecular weight and consequences in dilatometric studies of addition polymerization. *Trans. Faraday Soc.* **1966**, *62* (5), 1301-1307.

57. Bosen, S. F.; Bowles, W. A.; Ford, E. A.; Person, B. D. Antifreezes. *Ullmann's Encyclopedia of Industrial Chemistry.* **1985**, *A3*, 5th ed.

58. Abdelwahed, W.; Degobert, G.; Stainmesse, S.; Fessi, H. Freeze-drying of nanoparticles: Formulation, process and storage considerations. *Adv. Drug Deliv. Rev.* **2006**, *58* (15), 1688-1713.

59. Jiang, S.; Nail, S. L. Effect of process conditions on recovery of protein activity after freezing and freeze-drying. *Eur. J. Pharm. Biopharm.* **1998**, *45*, 249-257.

60. Searles, J. A.; Carpenter, J. F.; Randolph, T. W. The ice nucleation temperature determines the primary drying rate of lyophilization for samples frozen on a temperature-controlled shelf. *J. Pharm. Sci.* **2001**, *90*, 860-871.

61. Auvillain, M.; Cave, G.; Fessi, H.; Devissaguet, J. P. Lyophilisation de vecteurs colloidaux submicroniques. *S.T.P. pharma.* **1989**, *5* (11), 738-744.

62. Chang, B. S.; Patro, S. Y. Freeze-drying Process Development for Protein Pharmaceuticals. Lyophilization of Biopharmaceuticals. Costantino, *H. R. and Pikal, M. J. ed.* **2004**, 113-138.

63. Manning, G. S. A limiting law for the conductance of the rod model of a salt-free polyelectrolyte solution. *J. Phys. Chem.* **1975**, *79*, 262-265.

64. Ninham, B. W.; Parsegian, V. A. Electrostatic Potential between Surfaces Bearing Ionizable Groups in Ionic Equilibrium with Physiologic Saline Solution. *J. Theor. Biol.* **1971**, *31* (3), 405−428.

65. Belloni, L. Private communication. Interdisciplinary laboratory of nanoscale and supramolecular organization. DSM/IRAMIS/SIS2M, CEA/Saclay, 91191 Gif-sur-Yvette Cedex, France.

66. Chen, M.; Riddles, C. J.; Van De Mark, M. R. Electroviscous contribution to the rheology of colloidal unimolecular polymer (CUP) particles in water. *Langmuir.* **2013**, *29* (46), 14034-14043.

67. de Kruif, C. G.; van Iersel, E. M. F.; Vrij, A. Hard sphere colloidal dispersions:viscosity as a function of shear rate and volume fraction. *J. Chem. Phys.* **1985**, *83* (9), 4717-4725.

68. van der Werff, J. C.; de Kruif, C. G.; Blom, C.; Mellema, J. Linear viscoelastic behavior of dense hard-sphere dispersions. *Phys. Rev. A.* **1989**, *39*, 795-807.

69. van de Werff, J. C.; de Kruif, C. G. Hard-sphere colloidal dispersions: the scaling of rheological properties with particle size, volume fraction, and shear rate. *J. Rheol.* **1989**, *33*, 421-454.

70. Pishvaei, M.; Grailat, C.; McKenna, T. F.; Cassagnau, P. Rheological behaviour of polystyrene latex near the maximum packing fraction of particles. *Polymer.* **2005**, *46*, 1235-1244.

71. Dames, B.; Morrison, B.; Willenbacher, N. An empirical model predicting the viscosity of highly concentrated, bimodal dispersions with colloidal interactions. *Rheol. Acta.* **2001**, *40*, 434–440.

72. Villa, S.; Riesco, N.; Garcia de la Fuente, I.; Gonzalez, J. A.; Cobos, J. C. Thermodynamics of mixtures with strongly negative deviations from Raoult's law: Part 5. Excess molar volumes at 298.15 K for 1-alkanols+dipropylamine systems: characterization in terms of the ERAS model. *Fluid Phase Equilib.* **2001**, *190* (1), 113-125.

73. Biswas, A. B.; Kumsah, C. A.; Pass, G.; Philips, G. O. The effect of carbohydrates on the heat of fusion of water. *J. Solution Chem.* **1975**, *4*, 581-590.

74. Kotz, J. C.; Treichel, P. M.; Weaver, G. C. Kinetic theory of gases, chemistry and chemical reactivity, 6th ed. Thomson, Brooks/Cole Publishers (Chapter 12).

75. March, J.; Advanced Organic Chemistry 4th Ed. J. Wiley and Sons, 1992. New York.

76. Palasantzas, G.; Svetovoy, V. B.; van Zwol, P. J. Influence of ultrathin water layer on the van der Waals/Casimir force between gold surfaces. *Phys. Rev. B.* **2009**, *79* (235434), 1-7.

77. Schufle, J. A.; Huang, C. T.; Drost-Hansen, W. Temperature dependence of surface conductance and a model of vicinal (interfacial) water. *J. Colloid Interface Sci.* **1976**, *54* (2), 184-202.

78. Ganta, D.; Dale, E. B.; Rosenberger, A. T. Measuring sub-nm adsorbed water layer thickness and desorption rate using a fused-silica whispering-gallery microresonator. *Meas. Sci. Technol.* **2014**, *25* (055206), 1-6.

79. Eisenberg, D.; Kauzmann, W. The structure and properties of water. *Oxford Univ. Press.* **1969**.

80. Opitz, A.; Scherge, M.; Ahmed, S. I.-U.; Schaefer, J. A. A comparative investigation of thickness measurements of ultra-thin water films by scanning probe techniques. *J. Appl. Phys.* **2007**, *101* (064310), 1-5.

81. Abbott, A. P.; Boothby, D.; Capper, G.; Davies, D. L.; Rasheed, R. K. Deep eutectic formed between choline chloride and carboxylic acids: versatile alternatives to ionic liquids. *J. Am. Chem. Soc.* **2004**, *126* (29), 9142-9147.

82. March, J.; Smith, D. Advanced organic chemistry, 5th ed. *Wiley: New York*, **2001**.

83. Demaison, J.; Herman, M.; Lievin, J. The equilibrium OH bond length. *J. Int. Rev. Phys. Chem.* **2007**, *26* (3), 391-420.

84. Huhne, G.; Hemminger, W.; Flammersheim, H. J. Differential scanning calorimetry. Berlin: *Springer*. **1996**.

II. INVESTIGATION OF THE EVAPORATION OF WATER FROM COLLOIDAL UNIMOLECULAR POLYMER (CUP) SYSTEMS BY ISOTHERMAL TGA

Peng Geng, Ashish Zore, Michael R. Van De Mark*

Department of Chemistry, Missouri S&T Coatings Institute, Missouri University of Science and Technology, Rolla, MO 65401, USA

ABSTRACT

Studies of the evaporation of aqueous nanoparticle solutions have been limited due to lack of homogeneity of the solution, difficulties in obtaining reproducible samples and stability of substrates, as well as the effect of other volatile components or contaminants such as surfactants. CUP is a spheroidal nanoparticle with charged hydrophilic groups on the surface, the particle size ranges from 3 to 9 nm. CUPs can be easily synthesized, the particle size can be designed by controlling molecular weight, offering a predictable and reproducible system. CUPs are thermodynamically stable in water, with zero VOC. CUP is a very promising model to investigate the factors that affect evaporation rate of ultra-small particles in solution or systems, like protein, micelle, colloidal, etc. In addition, a large amount of surface water was associated to the CUP surface, providing the opportunity to evaluate the evaporation of surface water. Six CUP systems were evaluated by TGA with respect to time and solids content. The evaporation rate of water was initially enhanced due to the deformation of the air-water interface at low to moderate concentration due to particle charge repulsive forces. At higher concentrations, above 20% surface charge condensation and increasing viscosity began to

dominate. At higher concentration where the CUP reached the gel point the rate of diffusion controlled the evaporation. The final drying point was the loss of three waters of hydration for each carboxylate on the CUP surface.

Keywords: Colloidal Unimolecular Polymer (CUP), nanoparticle, evaporation rate, Thermogravimetric analysis (TGA), counterion condensation, diffusion, deformation.

1. INTRODUCTION

In past decades, evaporation of aqueous nanoparticle solutions has been a topic of interest, it is one of the most important fundamental kinetic and thermodynamic characteristics, which offers an opportunity to investigate the basic concept in diffusion, surface behavior, polymer properties and solution dynamics [1,2]. In addition, the investigation of the water evaporation of aqueous nanoparticles solutions provide a great study model for DNA packing, protein drying processes and drug delivery, also its potential application in the drying of water borne coatings, water borne pesticides and biocides, herbicide, cosmetics and many others [3-5]. The evaporation rate of water has many significant economic impacts from efficacy for crop protection to drug production rates and even the drying of water borne coatings.

Boukherroub et al. reported an increase in the evaporation rate of water-based graphene nanofluids. It was proposed that graphene oxide functionalization with polyethylene glycol promoted the dispersion of graphene nanoparticles and increased the evaporation rate at constant temperature. The potential agglomeration and poor dispersion of graphene nanoparticles at high concentration could cause a decrease in the

evaporation rate [6]. Kim et al. found that the evaporation rate of nanofluid aqueous droplet was higher than pure water with the presence of 80 nm sized CuO powder under the same experimental condition. The increase in the evaporation rate was considered to be caused by the nanofluid having better thermal conductivity [7]. Aslani et al. investigated the evaporation rate of water from clay particles in aqueous solution under isothermal condition, with a particle size ranging from 25 to 30 nm. The experiment involved dispersion of nano-sized powder using an ultrasonic processor, and conducted by putting a heating vessel on a digital scale, which were all placed inside a wind tunnel to provide changing velocity. It was found that these particles were able to reduce the surface tension and therefore increased the evaporation rate, and with the increase of concentration, the evaporation efficiency was enhanced [8]. In general, most studies on evaporation rate were performed with metal oxide/metal nanoparticles, nanostructures of carbon and non-charged nanoparticles.

Colloidal Unimolecular Polymer (CUP) is a spheroidal nanoparticle with charged hydrophilic groups on the surface, and particle size ranging from 3 to 9 nm depending on the molecular weight [9]. Several advantages make CUP an ideal system to conduct evaporation studies. The surface area to volume ratio is ultra-high due to the small particle size, which significantly enhanced the properties of their aqueous solutions, like viscosity, surface tension, etc [10-12]. CUPs can be easily synthesized and obtained through a water reduction process [13]. The surface charge density and molecular weight of CUP can be designed to fit a need and the surface structure is predictable and reproducible, providing the possibility for system studies and avoiding the common issue for lacking of homogeneity of the solution/suspension and difficulty to obtain

reproducible samples [14]. In addition, CUP systems are truly zero VOC with no additives.

The lack of stability of substrates is another major issue for evaporation studies. When the percent solids reaches a high level, most nanoparticles tend to aggregate due to Van der Waals forces [15], and change the microstructure or configuration [16, 17]. CUP particles, once formed, are thermodynamically stable solutions in water, and can be dried and re-dissolve in water without aggregation. Therefore, CUPs are able to show the detailed process of how surface water is released in the drying process. Furthermore, CUP particles have charged hydrophilic groups on the surface that can associate with a large amount of surface water [18]. With the small particle size, CUPs offer an ultra-high surface water fraction [19], and therefore could significantly magnify the observation of the surface waters contribution in the evaporation process. Thus, CUP is considered an ideal particle to investigate the effect of charged nanoparticles and their associated surface water on evaporation.

TGA is the most common technique used for mass change, kinetic analysis [20-23]. This technique is based on the evaluation of mass loss of the studied sample in a specific gas stream at a given temperature or programmed temperature [24]. TGA allows small sample size while giving precise measurement of the mass change under isothermal condition. The continuous flow of inert gas can reduce the formation of thin moisture layer above the aqueous surface that may reduce the evaporation rate. In addition, by using TGA, it is possible to distinguish different water states by showing different mass loss rates at different stages of drying. Therefore, TGA is considered a very appropriate instrument for this study. This manuscript presents a primary study of the behavior of

free water and surface water in CUP systems during the evaporation of the water. The evaluation of molecular weight and surface charge density, in ions per nm^2, effects on the evaporation rate was quantified by TGA. A packing model for CUP particles during the evaporation process of water was proposed. Calculation of the vapor pressure of water in CUP solutions was done using a TGA fitted constant. The aim was to develop the knowledge of possible factors that affect the evaporation rate of CUP solutions so as to offer fundamental insight for how to design CUP particles which give the best properties for a given application avoiding a trial and error approach.

2. EXPERIMENTAL

2.1. MATERIALS AND SYNTHESIS

CUP particles used in this paper were synthesized, characterized, and formed into CUP particles and were reported in our earlier report [25]. Table 1 gives the critical data for these polymers.

2.2. THERMOGRAVIMETRIC ANALYSIS

Thermogravimetric analysis was performed on a TA instruments Q500. The experiments were performed at atmospheric pressure. A constant flow of inert gas (nitrogen, flow rate 40 ml/min) was maintained throughout the experiment. The same amount of the aqueous sample 30 μl was loaded to a tared platinum pan via micro-pipette in order to maintain the same depth of solution. The pan used has a 9.4 mm diameter platinum pan from TA instrument, and was suspended in the furnace. In order to avoid

evaporation before reaching temperature, the sample was heated to the experimental temperature 298.15 K at 100 K/min, the temperature of the sample was measured by a thermocouple placed aside the pan. The sample was held isothermally at the experimental temperature for 360 minutes and the weight percent change of the sample was recorded. Each CUP solution was run in triplicate. Seven solvents (water, ethylene glycol, 1,2-propylene glycol, 1-butanol,1-propanol, 2-methoxyethanol and 2-ethyoxyethanol) were measured at the same experimental condition for obtaining a TGA calibration constant for vapor pressure determination. The evaporation rate is very sensitive to the exposed surface area, any uneven or damage of the pan will cause unpredicted experimental error. The handling of the pan should be done very carefully, any damage to the pan will result in the need to replace the pan and do a recalibration. Pure water was run periodically to verify that the pan had not changed due to damage or contamination. It should also be noted that at pH 8.5 CO_2 may be absorbed and shift the pH and also alter the composition. Avoid exposure of the solution to ambient air and check pH periodically to ensure the system has not been compromised.

3. RESULTS AND DISCUSSION

3.1. POLYMER SYNTHESIS AND CHARACTERIZATION

Polymers 1-6 were previously synthesized and reduced in a study defining the amount and properties of surface water by DSC [25]. The polymers selected for this study were based on particle size and surface charge density issues which have been shown to dominate the properties of surface water, viscosity and density. The six

polymers' properties; molecular weight, polydispersity, acid number, particle size and density are given in Table 1. Polymers 1-3 had the same monomer ratio, the acid number was fairly constant, and the higher acid number for Polymer 4 is due to the higher monomer ratio of MAA. Polymer 5 has the lowest acid number because the monomer ratio is the lowest. The polydispersity indicates a relatively narrow size distribution unlike most nano particulate systems.

Table 1. Molecular weight, particle size, acid number and density of the polymers.

Sample ID	M_n/PD (g/mol)	Monomer ratio	Particle size (nm)	AN (mg KOH/g)	Density of dry CUP, ρ_p (g/ml)	charge density in ions per nm^2, ρ_v
Polymer 1	28.9k/1.8	9:1	4.22	56.8	1.2246±0.0018	0.52
Polymer 2	59.8k/1.7	9:1	5.38	57.0	1.2311±0.0014	0.66
Polymer 3	122.5k/1.7	9:1	6.83	56.9	1.2342±0.0018	0.84
Polymer 4	25.4k/2.3	6.8:1	4.04	73.2	1.2243±0.0018	0.66
Polymer 5	73.5k/1.7	9.8:1	5.76	52.6	1.2315±0.0018	0.66
Polymer 6	49.7k/1.8	14:1	5.06	37.7	1.2307±0.0016	0.42

3.2. METHOD FOR EVAPORATION RATE DETERMINATION

TGA was used to directly measure the total mass percent loss per unit time and was then converted to the actual mass loss per unit time and then the evaporation rate was calculated by Equation (1).

$$R = m \cdot (X_i - X_{i+1}) / \Delta t \quad (1)$$

where R is the evaporation rate of the measured sample, m is the mass of the sample, X_i is the weight fraction at time i, X_{i+1} is the weight fraction at time i+1, Δt is the time interval.

The evaporation rate of pure water was measured as the standard, shown in Figure 1. The first few hundred seconds exhibited an oscillation due to the thermal over run of the TGA and the system coming to equilibrium.

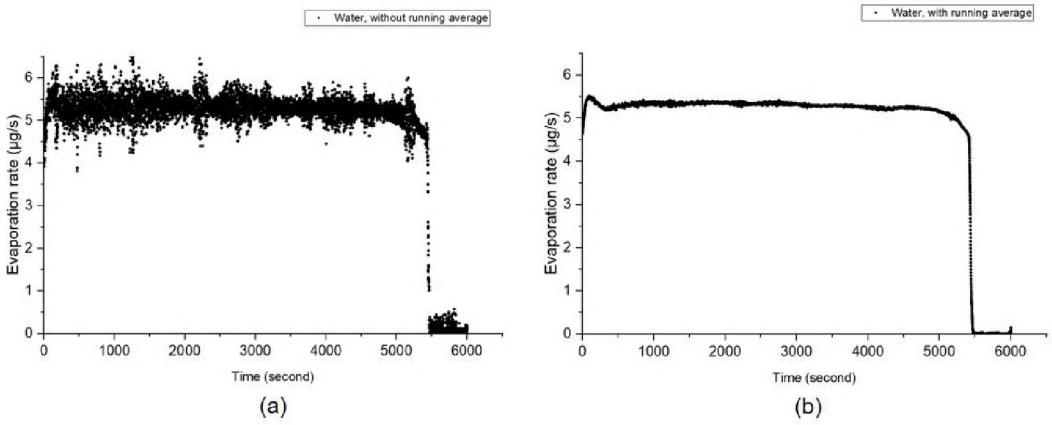

Figure 1. Evaporation rate of pure water, (a) raw data (b) with running average.

After an initial period of evaporation, the rate of mass loss of the sample remained constant with the plot of sample mass versus time resulting in a straight line. Data was collected every 0.6 second, with the very small amount of mass loss per second and a small amount of vibration, a significant amount of noise was observed in the data [24]. To reduce the noise in the TGA data, a running average method over 50 data points was used.

To reduce the noise in the TGA data, a running average method over 50 data points was used. A plot of the standard deviation of four different samples at each data point vs time, after running average is shown in Figure 2. In the very beginning of the measurement, a large standard deviation was observed. This noise is due to surface area

not being uniform initially and the temperature overshoot. Once the sample reaches a steady state the noise level drops to a very low level until about 5000 seconds.

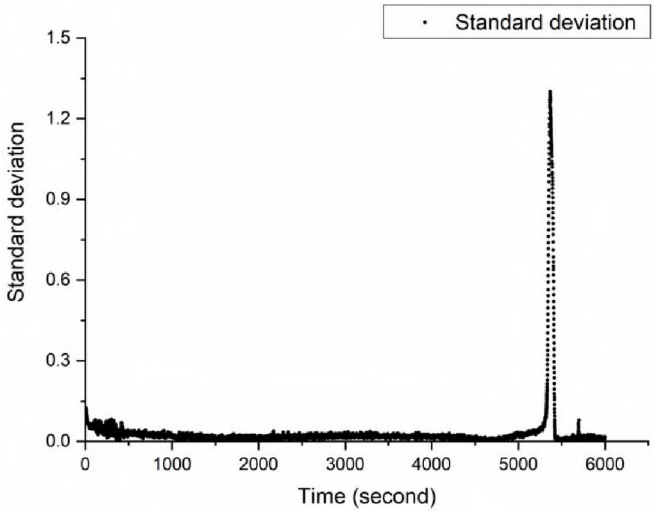

Figure 2. Deviation of evaporation rate of water.

As the pan nears dryness the water cannot cover the entire bottom of the pan, the surface area will exhibit a large random change. The data in the last part of the measurement cannot be trusted to represent the true evaporation rate for water. During the scan, for measurements between about 500 and 5,000 seconds, the deviations are very small making the data more reliable with minimal scatter.

3.3. EVAPORATION RATE OF FREE WATER FROM CUPS

The evaporation of both water and CUP solutions are highly dependent upon surface area. If the sample does not wet the platinum pan it can result in changing areas caused by the sample size and contact angle. To evaluate this, two platinum flags were cleaned and one had 15 microliters of deionized water placed on its surface and the other

had a 10% Polymer 4 CUP solution at the same volume placed on it. Figure 3 shows the image of the flags at time zero just after application and the third image after the CUP solution was dry. It can be seen that water wet the platinum partially but the CUP solution wet much better. Once dry the CUP sample formed a relatively even coating which cracked due to poor adhesion and low crystal lattice energy. This experiment indicates that the evaporation should be representative even to the end for CUP since it evaporates evenly.

Figure 3. Scheme of Photo of deionized water and CUP wetting and dry on platinum substrate.

In order to investigate the CUP particles' effect on the evaporation rate, a 5.47% Polymer 1 solution was measured following the same protocol as with water, and compared with deionized water, shown in Figure 4.

The Polymer 1 solution evaporated faster than deionized water in the beginning, and kept decreasing along the isothermal process, with multiple changes of evaporation rate reduction being observed. These complexities indicated that there were more than one factor involved during the isothermal process.

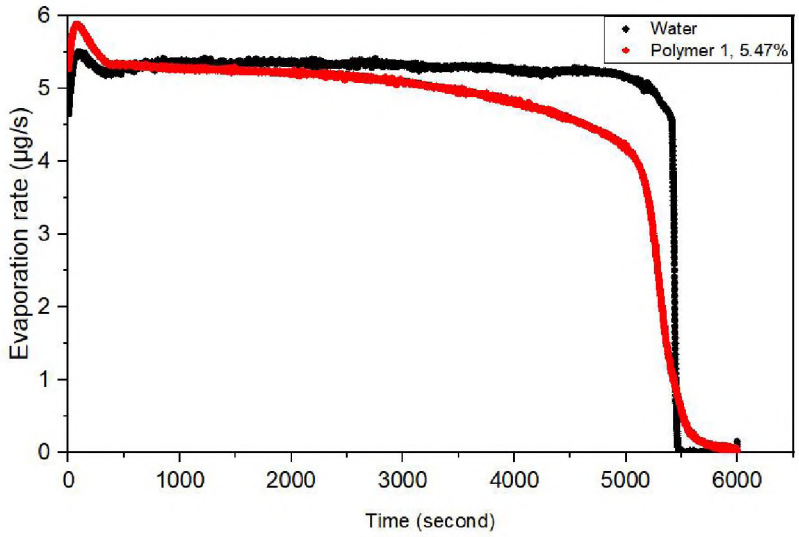

Figure 4. Evaporation rate of 5.47% Polymer 1 solution and water.

The study separated the evaporation process into five segments designated as I, II, III, IV and V, shown in Figure 5.

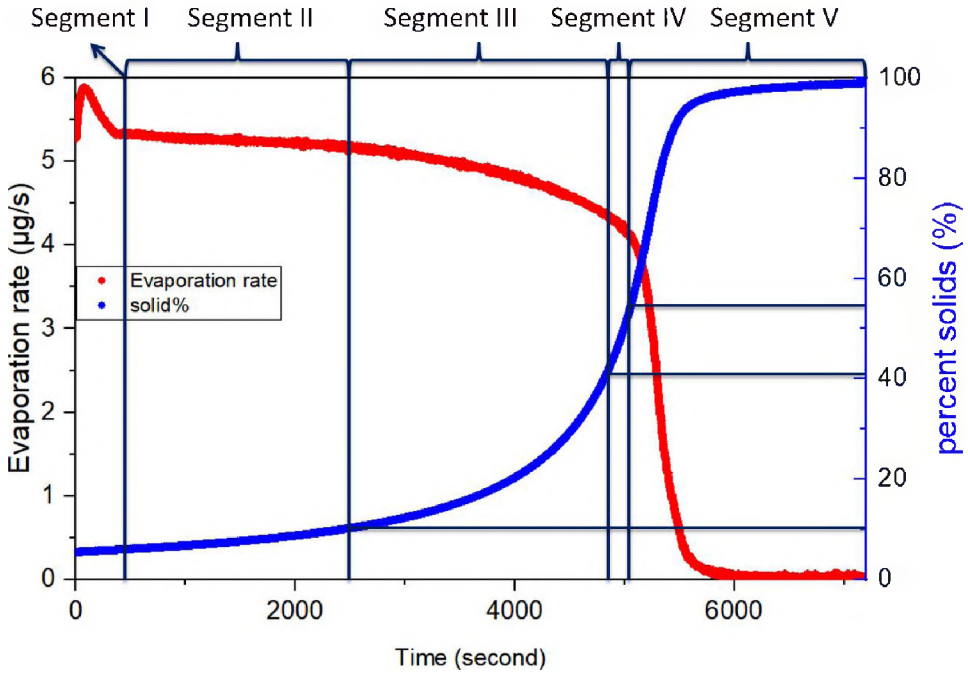

Figure 5. Segments I, II, III, IV and V during the isothermal process.

Segment I was the initial time frame of 480 seconds, before major compositional changes occurred. Segment II is for the range from Segment I until Manning condensation occurs. Segment III covers Manning condensation. Segment IV is the gelation of the solution and Segment V is the loss of the last water including surface water.

The evaporation rate of CUP solutions were not constant. Therefore, in order to investigate the CUP's effect on the evaporation rate in the beginning, the evaporation rate of various polymer solutions with multiple molarities were determined immediately after the pan settled down, at 480 seconds (Segment I), shown in Figure 6.

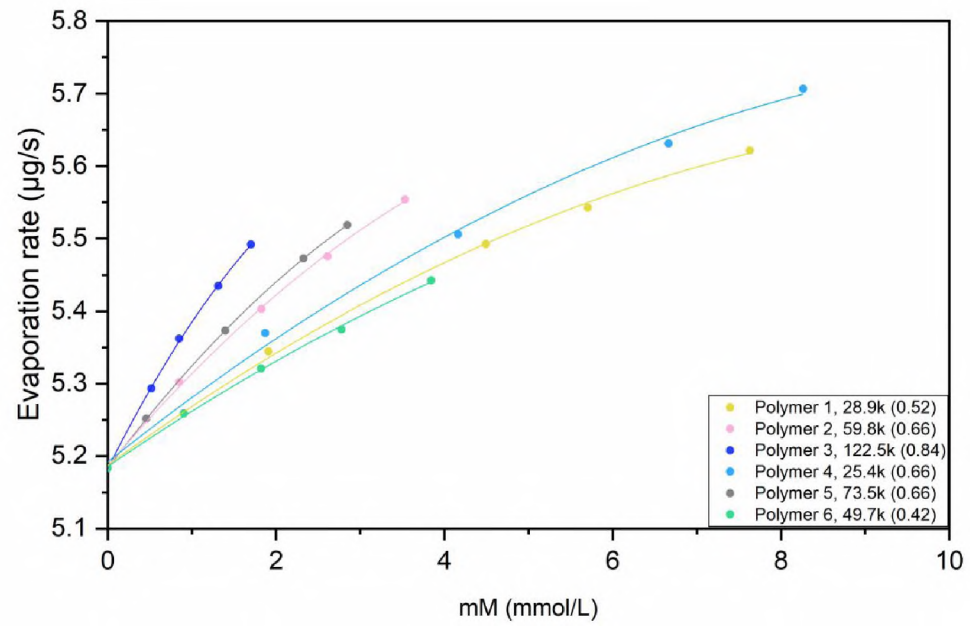

Figure 6. Evaporation rate of Polymer 1-6 solutions at various mM.

Polymer 1, 2 and 3 have the same monomer ratio but different surface charge density and molecular weight. It was observed that, with the same molarity, polymers

with higher molecular weight and surface charge density have higher evaporation rate. If comparing Polymer 2, 4 and 5, which have the same surface charge density, the polymer with larger molecular weight had a faster evaporation rate. Van De Mark et.al found that with the presence of CUP particles, the surface tension was lower than deionized water, and it was proportional to the number of charges on the particle surface [26]. The surface tension reduction was similar but smaller than that observed for typical surfactants [27]. This surface tension reduction was also observed for polyelectrolyte systems [28]. Polymer 3 evaporated faster than Polymer 2 and 1, due to more charges, which is the same for Polymer 2, 4 and 5. It was also observed that for each CUP solution, the evaporation rate was higher for the solutions with a higher initial molarity because the higher initial molarity having more charges. However, the effect of surface tension should not be a major factor for evaporation but it will have an effect on interfacial mobility. In order to further investigate the surface effect, the relation between surface tension and the evaporation rate of aqueous salts were examined, shown in Table 2.

Table 2. Comparison of surface tension and evaporation rate of sodium salts.

	water	NaCl	NaCl	NaAc	NaAc
Concentration	0	2%	5%	1M	2M
γ (mN/m)	72.2	73.9	75.6	70.2	69.2
$\Delta\gamma$	0	+1.7	+3.4	-2.0	-3.0
R (μg/s)	5.18	5.09	4.95	5.04	4.99
ΔR	0	-0.09	-0.23	-0.14	-0.19
$\lvert\Delta R/\Delta\gamma\rvert$	N/A	0.05	0.07	0.07	0.06

Sodium chloride was chosen since it causes an increase in the surface tension and sodium acetate, which has a carboxylate like CUP, causes a decrease in surface tension. The evaporation rate difference from water divided by the surface tension difference from water was used to evaluate the effect each had on the two, $\Delta R/\Delta\gamma$. It was shown that, with less surface tension, sodium acetate solution evaporated slower than deionized water, due to the salts [29, 30]. Also, the evaporation rate change was moderately lower than the change in surface tension for all four values. This data indicates that the primary effect on increasing the evaporation rate of CUPs is not surface tension.

Table 3 gives the surface tension and evaporation rate for CUP solutions of Polymer 1-6 at 2mM.

Table 3. Comparison of surface tension and evaporation rate of CUP solutions.

	Polymer 1 (28.9k) 0.52	Polymer 2 (59.8k) 0.66	Polymer 3 (122.5k) 0.84	Polymer 4 (25.4k) 0.66	Polymer 5 (73.5k) 0.66	Polymer 6 (49.7k) 0.42
Molarity(mmol/L)	2	2	2	2	2	2
γ (mN/m)	70.9	68.4	66.6	68.5	68.5	71.0
$\Delta\gamma$	-1.3	-3.8	-5.6	-3.7	-3.7	-1.2
R (μg/s)	5.32	5.42	5.548	5.37	5.44	5.34
ΔR	+0.14	+0.24	+0.37	+0.19	+0.26	+0.16
$\lvert\Delta R/\Delta\gamma\rvert$	0.11	0.06	0.07	0.05	0.07	0.13
n*acid	29.3	60.6	124.1	33.1	68.9	33.4
n*acid/n*ester (per CUP)	0.232	0.310	0.418	0.296	0.305	0.183

Notes: γ is surface tension, R is evaporation rate. $\Delta\gamma$ is the surface tension difference between water and the CUP solution, ΔR is the difference in evaporation rate for water vs CUP solution.

It should be noted that the change in the surface tension for these polymers are about 500 times higher than that for sodium acetate at the same concentration. Therefore, the molar concentration of CUP may not be a simple relationship. Table 3 also gives the number of carboxylate groups on each CUP. The number of carboxylates were partially responsible for the larger effect of both evaporation rate and surface tension. The chains of the CUP particle are not free to move and thus their relationship to each other define the "more hydrophobic" regions from the carboxylate. These hydrophobic regions are larger than those of the methyl group of the acetate ion. However, the more hydrophobic surface is dominated by the ester groups and likely some of the methyl groups of the backbone and ester. The surface tension of surfactant carboxylates become more effective as the aliphatic chain increases.

The use of percent solids as well as molarity and weight fraction, XCUP are relevant to different aspects of this study Equation (2) relates these terms.

$$X_{CUP} = \frac{M_W \cdot c \cdot 10^3}{\rho_s} \tag{2}$$

where M_w is the molecular weight of the polymer, ρ_s is the density of CUP solution, c is the molarity, X_{CUP} is the weight fraction of CUP solids.

When a very dilute CUP solution was at its equilibrium condition, the solution was homogeneous and CUP particles were randomly distributed and stabilized by the combination of Brownian motion, solvation by water and charge repulsion between particles. Assuming that each CUP occupies an average cubic volume in solution, which gives the largest distance between particles. At a given percent solids, the distance between two CUP particles was estimated by Equation (3).

$$r = \left(\sqrt[3]{\frac{M}{X_{CUP} \cdot \rho \cdot N_A}} \right) - d \tag{3}$$

where r is the distance between two particles, M is the molecular weight of CUP, X_{CUP} is the weight fraction of CUP, ρ is the density of solution, d is the size of the CUP particle, N_A is Avogadro constant.

The distance between two CUP particles was determined to be from 5.5 to 8.8 nm depending on the particle size at 5% solids. The electrostatic effective distance between two CUP particles can be estimated by Equation (4-6) [29-31].

$$\kappa^{-1} = \sqrt{\frac{\varepsilon_r \cdot \varepsilon_0 \cdot k_B \cdot T}{2 \cdot 10^3 \cdot N_A \cdot e^2 \cdot I}} \tag{4}$$

$$I = \frac{1}{2} \cdot (M \cdot 1 \cdot n_a \cdot 1) \tag{5}$$

$$d_{eff} = 2 \cdot (\kappa^{-1}) \tag{6}$$

where I is the ionic strength, M is the molarity of CUPs, n_c is the number of carboxylate groups per CUP, ε_0 is the permittivity of free space, ε_r is the dielectric constant for water, k_B is the Boltzmann constant, e is the elementary charge, k^{-1} is Debye length.

The assumption is that we have a single point charge separated by water. As Figure 7 shows, the effective distance was always larger than the estimated inter-particle distance, which indicated that the electrostatic repulsion force occurred at a CUP concentration of 1% and higher. At a constant percent solids the CUP with smaller particle size tends to have a larger difference between the effective distance and inter-particle distance, due to a higher number of particles that results in a higher repulsion

force. Polymer 1 has a higher effective distance to inter-particle distance ratio than Polymer 3, because of a larger number of particles at the same percent solids.

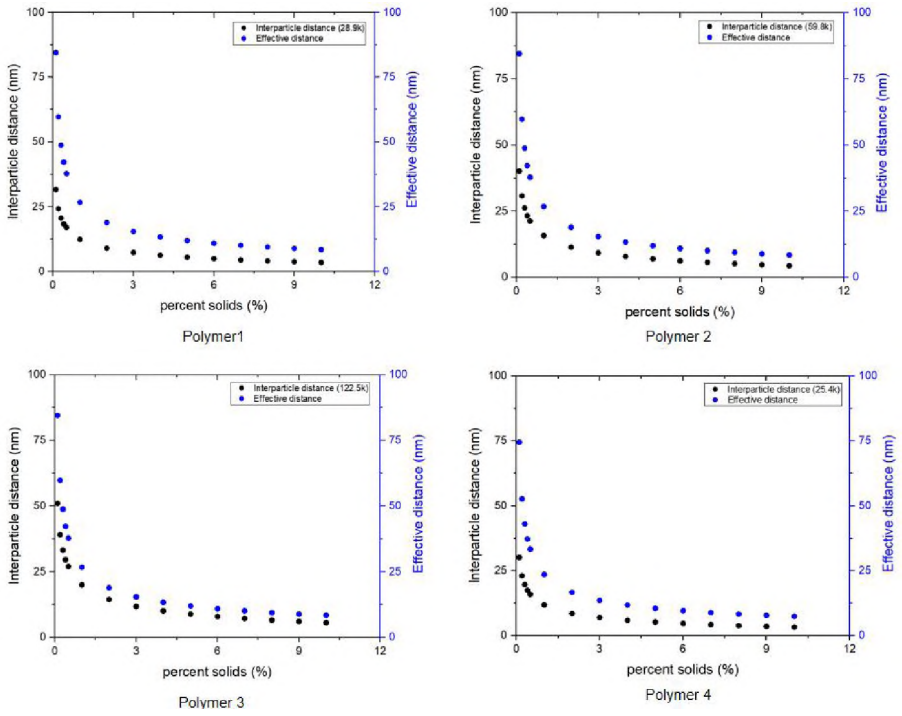

Figure 7. Comparison of effective distance and interparticle distance for Polymer 1-4.

Due to coulomb's law, the repulsion force is proportional to $1/r^2$ [34], where r is the distance between two charges. Consider each CUP particle as a point charge, and assume an r value of 9 nm, the electrostatic repulsion force for Polymer 1 is 2.85×10^{-12} N, while the surface tension of water is 7.22×10^{-11} N/nm and surface tension for 5.47% Polymer 1 solution is 7.08×10^{-11} N/nm. Since each CUP particle has multiple charges (29.3 to 124.1 charges per particle for Polymers 1 and 3 respectively), the actual repulsion force was expected to be much larger than 2.85×10^{-12} N. Therefore, at 5%

solids, the charge repulsion between CUP particles should be strong enough to cause deformation of the air-water interface as shown in Figure 8.

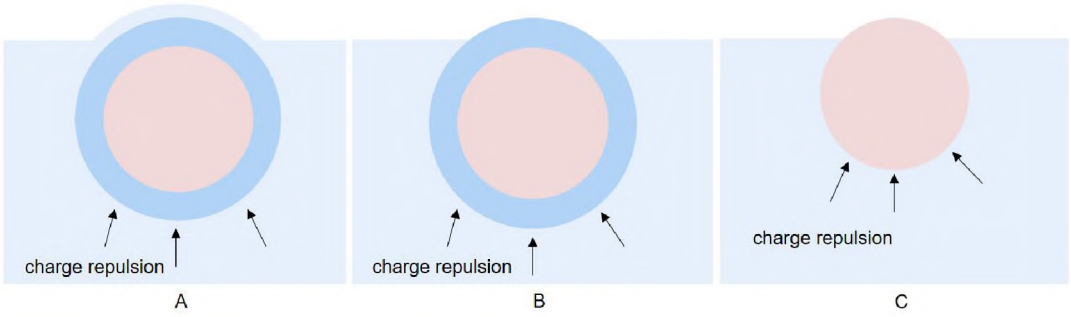

Figure 8. Scheme for deformation of water surface at air-water interface by CUP particles due to charge repulsion.

The three models indicate A: CUP with surface water and a layer of air/surface water, B: CUP with a layer of surface water, and C: Cup particle with no water. Model C can be eliminated, because CUP particles are highly hydrophilic on the surface, and have a layer of strongly associated surface water [25]. If model C were the case, all the evaporation rate would be due to edge effects on the surface tension and the loss of surface area occupied by the CUP particles would reduce the evaporation rate. Therefore, with the presence of CUP particles, the interface water deformed causing a decrease in surface tension, according to the Gibbs isotherm, and an increase in surface area. Assuming all the observed increase in the evaporation rate were contributed by increased surface area at the interface, the increased ratio of evaporation rate should be proportional to the increased surface area. At a given percent solids, the degree of interface water deformation (Figure 9) could be calculated by Equation (7).

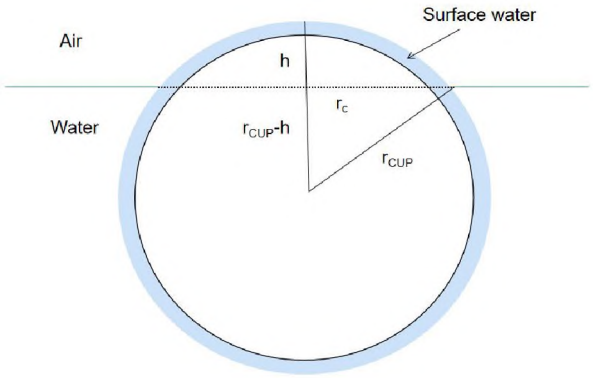

Figure 9. Scheme for deformation of water at air-water interface by CUP particles due to charge repulsion.

$$h = \sqrt{\frac{\Delta R}{R \cdot \pi}} \cdot \left(\sqrt[3]{\frac{M_w}{\rho \cdot X_{CUP}}} \right) \tag{7}$$

where h is the height of the interface water deformation, ΔR is the increased evaporation rate compared with water, R is the evaporation rate of the CUP solution, M_w is the molecular weight of CUP, ρ is the density of the solution, X_{CUP} is the weight fraction of CUP.

The h was calculated to be from 0.70 to 1.27 nm with the range of about 5% to 20% solids, h depends on the percent solids and molecular weight of CUP particles. The particle size of CUPs ranges from 4.02 to 6.83 nm, due to the moderate repulsive force, interfacial water deformation may be the major contributor. The surface tension on the deformational region may be lower than normal water and the circumference region will have a significantly lower surface tension. It is most likely that Model A or B is the correct one and that contribution from the increased surface area is the cause of the enhanced evaporation at low concentrations. It is well known that polymers in solution

reduce the vapor pressure of the solvent. This would in general reduce the evaporation rate of a CUP solution. The increased area must overcome this small reduction in vapor pressure also.

In the Segment I, the main factor that dominated the evaporation rate was the increased surface area which increased the rate. At a given molarity, the CUP with larger particle size has shorter inter-particle distance, resulting in a higher charge repulsion force, that increases the amount of interfacial water deformation, h. In addition, more charges on the CUP surface caused more surface tension reduction, the combination of these two effects showed a higher evaporation rate. Looking back to Figure 4, 25.4k, Polymer 4 has a similar particle size as 28.9k, Polymer 1 and the CUP surface tension was lower for Polymer 4 and the interfacial deformation was greater due to the larger charge repulsion, therefore it showed a higher evaporation rate. Polymer 6, 49.7k has the lowest charge density but a higher molecular weight, particle size, than Polymer 1. The surface tensions for Polymer 1 and 6 are similar and the evaporation rate for Polymer 6 is slightly higher. This is because with the same molarity, Polymer 6 has a shorter inter-particle distance due to the larger particle size, that resulted in a higher charge repulsion. The interfacial water deformation for Polymer 6 would be expected to be greater thus showing a higher evaporation rate.

As water continuously evaporated during the isothermal process, the temperature at the interface decreased due to the lost heat of vaporization and the surface molarity/percent solids of CUP particles at the interface became higher than the bulk solution, Segment II. As the surface molarity/percent solids increases, it sets up an osmotic gradient with the bulk solution. The osmotic gradient draws water to the surface

to dilute the CUPs [35,36]. The movement of water to the surface not only dilutes the CUP at the air interface but also brings heat to reestablish equilibrium. At the same time, CUP particles experience a higher charge repulsion and move toward the bottom through translational diffusion at low concentration. The reduced temperature at the interface decreases the evaporation rate, and the increased molarity provided higher charge repulsion to create an increase in the interfacial water deformation that will increase the water evaporation rate. However, the evaporation rate largely depends on the diffusion rate of water molecules to the interface [37]. The viscosity in the interfacial region will be increasing with the increasing of CUP molarity/percent solids, due to the secondary electroviscous effect[38], which was demonstrated by Van De Mark et al. [39]. The increased viscosity slowed movements of both the water and CUP particles, which explains a slower observed evaporation rate.

The diffusion coefficient could be determined by Stokes-Einstein equation [40].

$$D = \frac{K_B \cdot T}{6 \cdot \pi \cdot \eta \cdot r} \tag{8}$$

where K_B is Boltzmann constant, T is the absolute temperature, η is the viscosity of the solution, r is the radius of CUP particle.

Table 4 gives the diffusion coefficient for the six polymers at 5% and 10% at 298.15K.

Table 4. Diffusion coefficient of CUP particles at 298.15 K ($\times 10^{-6}$ cm^2/s)

Polymer ID / %Solids	Polymer 1 28.9k	Polymer 2 59.8k	Polymer 3 122.5k	Polymer 4 25.4k	Polymer 5 73.5k	Polymer 6 49.7k
5%	1.59	1.16	0.74	1.69	1.10	1.31
10%	1.15	0.83	0.45	1.24	0.78	0.92

The evaporation rate of Polymer 4 solution with initial percent solids of 4.71%, 10.34%, 16.92% and 20.16% in the first 2500 seconds were evaluated as an example, shown in Figure 10.

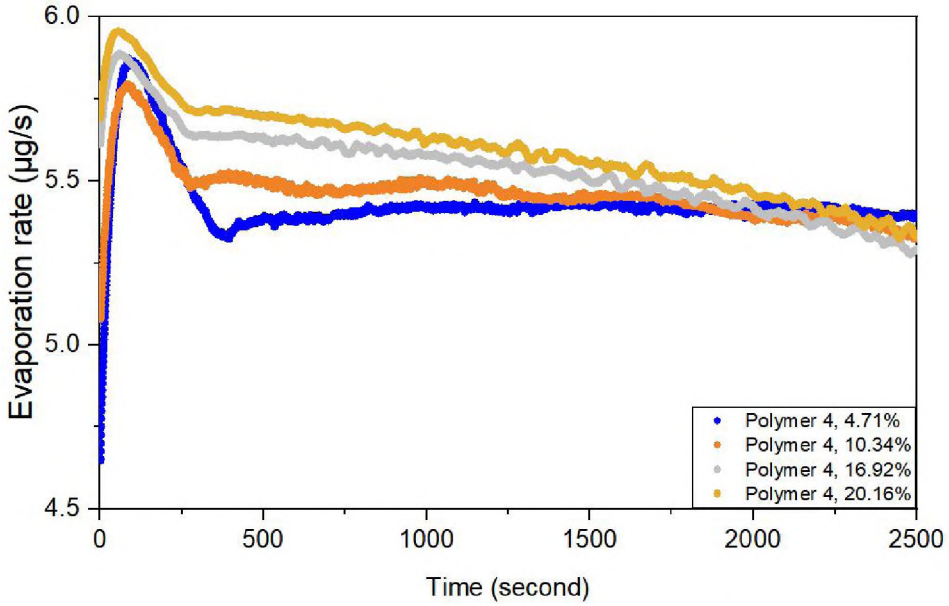

Figure 10. Evaporation rate of Polymer 4 solution at 4.71%, 10.34%, 16.92% and 20.16% in the first 2500 seconds.

It was shown that, the higher initial percent solids of CUP solution, the faster the initial evaporation rate was, due to the increased surface area, Segment I. However, when the water started to evaporate, the evaporation rate of all CUP solutions decreased, except the 4.71% which retained its evaporation rate for a longer time before decreasing. The change was more obvious for higher initial percent solids CUP solutions. Because the higher percent solids solution has higher viscosity, that resulted in a slower movement of particles and water molecules in Segment II. The 4.71% solution was dilute enough that the translational diffusion and osmotic flow kept the surface CUP concentration lower for

a longer time as the evaporation progressed. The low mobility of particles and water molecules further enhanced the CUP particles stacking at interface, increasing the viscosity and reducing the evaporation rate. This observation was further investigated by comparing the evaporation rate when two different initial percent solids solution were evaporated to the same percent solids. The evaporation rate of Polymer 1 and Polymer 4 solutions with different initial percent solids were evaluated during the drying process at the same solids content as shown in Figure 11.

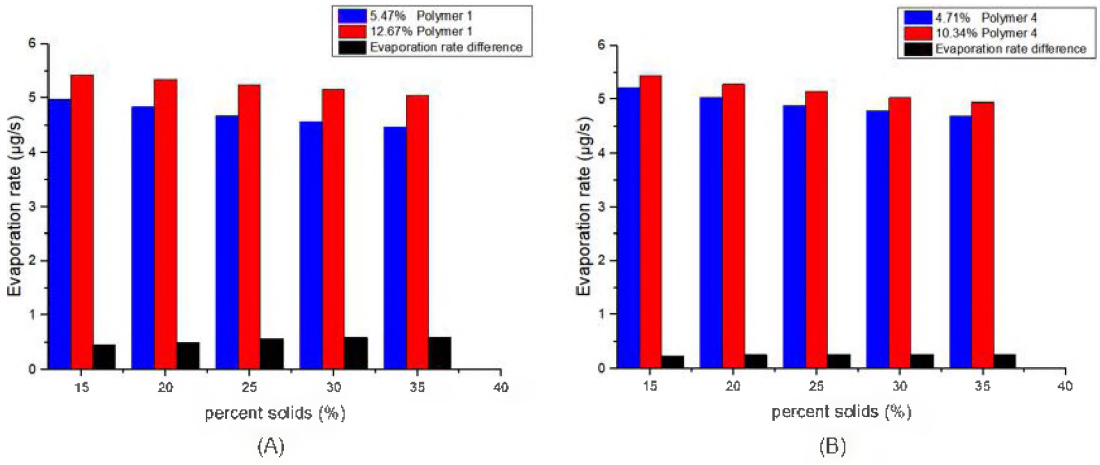

Figure 11. Evaporation rate of Polymer 1 and Polymer 4 solutions with different initial %solids concentrations.

It was seen that when concentrated to the same percent solids, the evaporation rate of the low initial percent solids solution was lower. The low solids sample must first loose significant water which creates a higher concentration of CUP particles at the surface which increases the viscosity lessening the diffusion of water to the surface and slowing the movement of CUP particles away from the surface as well as lowering the surface temperature. For the lower concentration the total solution thickness is decreasing

with time as does the higher concentration, however the rate of change in the thickness is almost twice as much for the lower concentration. The shorter distance will also influence the result by reducing the osmotic flow since the liquid thickness increases the opportunity to set up osmotic gradients. Polymer 1 shows a greater difference in evaporation rate than Polymer 4. The rate differences may be due to the higher charge density of Polymer 4 forcing the particles to rearrange positions more rapidly and increasing viscosity. Polymer 4 has slightly lower mass which makes the charge effect even more meaningful.

As evaporation progressed in Segment II, the movement of water molecules and CUP particles caused by osmotic pressure and charge repulsion were the dominant driving forces in this segment. As the concentration increased the viscosity reduced the osmotic flow which in turn allowed the temperature of the surface to fall lower since the rate of warm water being transferred to the surface slowed.

The ionic force between particles forces CUP particles down from the surface by each one pushing down the particle below it, which helped to minimize osmotic differences. The ionic force also increases the vertical displacement of the CUP particles at the air interface as the CUP concentration increases. The air surface area with free water decreases and the area of CUP surface water increases and dominates evaporation as the solids content rises. When the concentration at or near the surface hits about 20% solids the CUP surface ions begin to undergo Manning type condensation which lowers the effective charge. When this condensation begins to occur the CUP particles can increase their packing concentration and reduce the repulsion on their neighbor as well as limit the CUP penetration through the air interface.

In addition, particle size is another important factor, because it directly influences the diffusion rate of CUP particles. The Polymer 2 and Polymer 4 solutions with similar molarity were compared, shown in Figure 12.

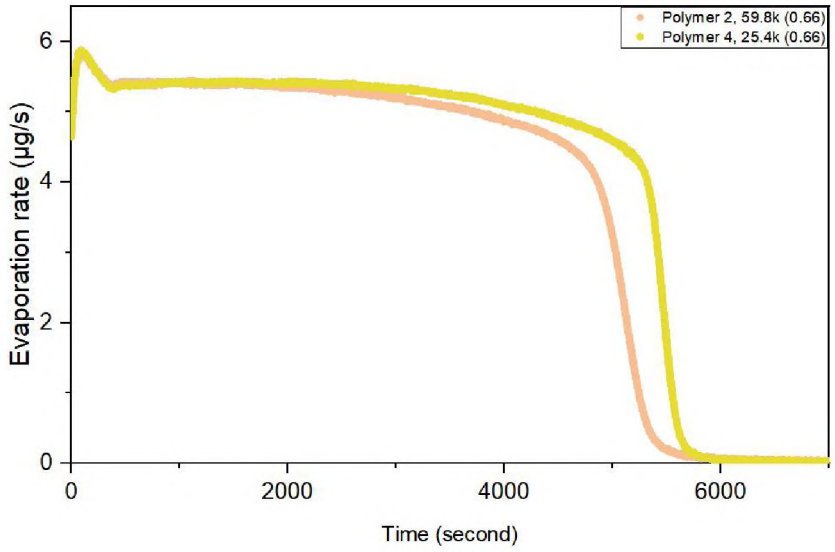

Figure 12. Evaporation rate of Polymer 2 (1.83 mmol/L) and Polymer 4 (1.87 mmol/L).

It was seen that, in Segment I, the Polymer 2 solution evaporated slightly faster due to more charges per particle than Polymer 4. However, Polymer 2 solution started to show a larger and larger evaporation rate reduction as compared to Polymer 4 solution through Segment II. This reduction was due to a larger particle size diffusing slower, which caused more particles to stack up at the air-water interface. This also increased the viscosity at the interface, and further decreased the diffusion rate of particles, and therefore, Polymer 2 presented a slower evaporation rate through Segment II.

Previous studies have demonstrated that when the percent solids increased above 20%, inter-molecular counterion condensation occurred, segment III [25]. Increasing the

CUP percent solids also increased the counterion concentration, which condensed on the CUP surface reducing its effective charge [27]. The phenomenon known as Manning condensation (counterion condensation) is widely accepted in charge stabilized colloidal suspensions [41]. The inter-molecular counterion condensation causes the effective charge to be lower than the bare surface charge and allows more CUP particles with better packing at the air-water interface. At the same time, the total number of charged groups at the air-water interface increases because only a small fraction of the charged groups on the CUP surface undergo Manning condensation. The inter-molecular counterion condensation decreases the charge repulsion effect to a degree, therefore, decreases the mobility of CUP particles to the bottom as a result of charge repulsion.

Using Polymer 6 as an example, it was shown that with the increasing of the initial percent solids, the inter-molecular counterion condensation occurs earlier in the time frame. This drop in the rate can be observed in Figure 10. The darker line drops to an evaporation rate of 4 micrograms per second first while the 4.35% occurs much later. Segment III begins with inter-molecular counterion condensation and ends with gelation as random close packing, RCP, which is marked with a red line in Figure 10. Starting at low concentration it requires more time to reach RCP as well as the start of Manning condensation. Once gelled the CUP particles cannot move translational but they can move as a unity shrinking all the spaces between particles uniformly to avoid significant stress development. Rapid evaporation has been noted to cause crack development in a drying sample with the surface shrinking due to drying before the system can reestablish equilibrium.

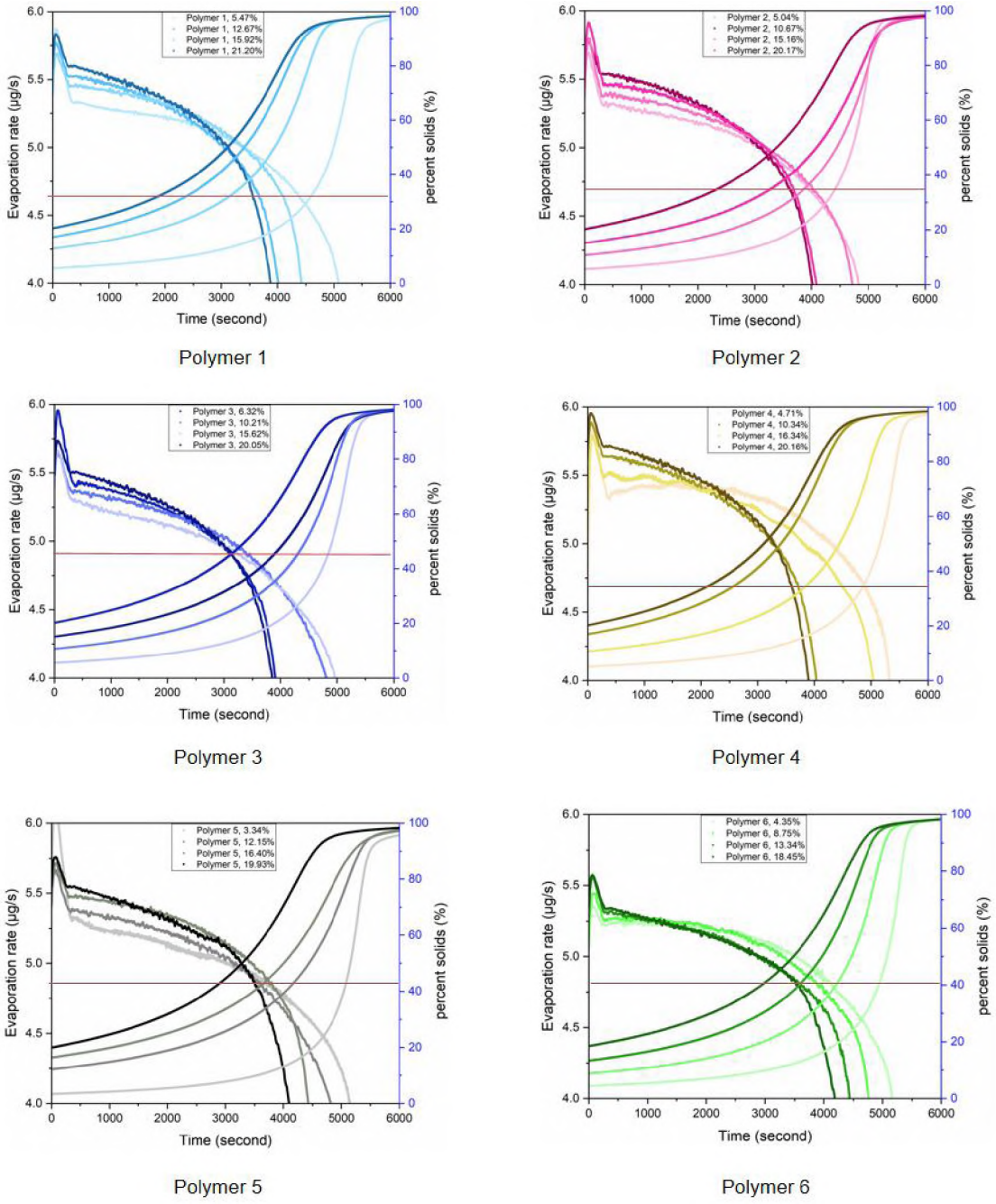

Figure 13. Evaporation rate at various percent solids for Polymer 1-6.

The evaporation of water, as it approaches the end of Segment III, slowed as the percent solids of the bulk solution increased, this reduced the distance between particles in the bulk portion. The particles reached a pseudo random close packing state which was

defined as the gel point of CUP, and then with a small additional loss of water became pseudo hexagonal close packing, Segment IV. The term pseudo HCP was used since the particles have a distribution of diameters and charges so it will not be a perfect HCP lattice. As the particles formed an organized structure where each particle occupied a lattice position even in the bulk solution, the mobility of water molecules and CUP particles were highly limited [39]. Thus, the evaporation rate decreased even faster. All water diffusion was either through the CUP surface water or through the voids between the spheres occupied by free water with the state of surface deformation having little meaning since the surface is now occupied by CUP particles with their surface water only.

3.4. EVAPORATION RATE OF SURFACE WATER

As water molecules continuously escaped from the interface, the particles approach each other, and the increased electrostatic repulsion tends to arrange them in positions with equal distance from the nearby particles. There are two types of packing models for spheroidal materials when the percent solids are very high, random close packing and hexagonal close packing. CUP particles will first approach random close packing as the concentration increases and slowly, through movements driven by the repulsive forces between particles approach hexagonal close packing. At this point the particles are only surrounded by surface water with a small amount of free water occupying the space in the voids, Segment IV. Many previous studies have shown that surface water has a much lower mobility, higher density [42], and tighter association with the hydrophilic groups [43]. Therefore, the evaporation rate of surface water is expected to show very different behavior from free water. The viscosity of the solution is close to

infinity at this point and free water has to move primarily through the surface water layer. The rate of water diffusion is therefore very small and significantly reduces the rate of evaporation. There are potentially three possibilities for each packing model, shown in Figure 14. CUP with surface water and free water, CUP with free water and CUP only with surface water. Previous studies have eliminated models III and VI since the existence of surface water layer has been demonstrated [44].

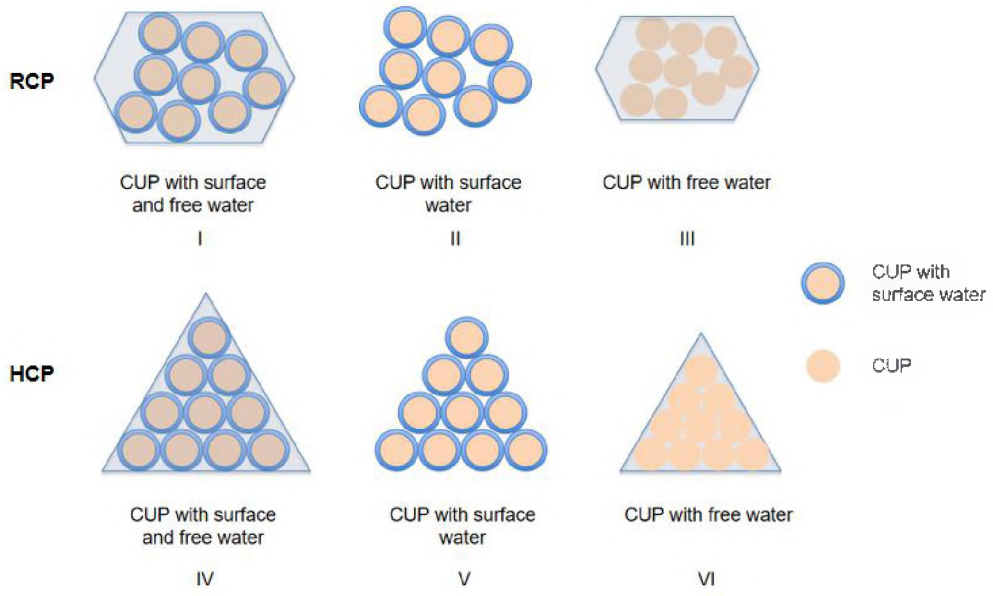

Figure 14. Scheme for possibilities during surface water evaporation process.

In order to evaluate the evaporation process of the surface water and the last trace of free water in the voids, the percent solids of CUP particles for each packing model can be calculated by knowing the max volume fraction of random close packing which is 0.634, and 0.7405 for hexagonal close packing [45-49], by Equation (9-11).

$$\phi = \frac{\rho_s \cdot X_{CUP}}{\rho_p} \tag{9}$$

$$\phi_{R-\max}(1+\lambda/r)^3 = 0.634 \tag{10}$$

$$\phi_{H-\max}(1+\lambda/r)^3 = 0.7405 \tag{11}$$

where ϕ is the CUP volume fraction, ρ_s is the density of CUP solution, ρ_p is the density of CUP particle, $\phi_{H\text{-max}}$ is the maximum volume fraction for hexagonal close packing, $\phi_{R\text{-max}}$ is the maximum volume fraction for random close packing, l is the thickness of surface water, r is radius of the CUP particle.

The percent solids of CUP for the possibilities of each packing model were calculated and are shown in Table 5. The amount and thickness of CUP surface water has been determined by DSC [25]. As it was discussed in Figure 1, for the last water loss, a large reduction in the evaporation rates were observed near the end. One possible reason for this issue was an insufficient amount of solution to cover the pan bottom. In this case, 5.04% Polymer 2 and 4.35% Polymer 6 solutions were used as examples. Knowing the diameter of the pan being 9.4 mm, it was calculated that even when there is only CUP solids existing in the pan, the bottom of the pan is still fully covered with a 0.02 mm depth. By applying the results from Table 5 to the evaporation curve, Figure 3 indicates that CUP solutions dry relatively uniform wetting the platinum pan. The CUP solution surface tension decreases with increasing concentration making it more wetting of the pan. Therefore, in Segment V, the evaporation rate reduction was not because of the lack of sufficient solution to cover the pan. It is reasonable to consider that the lowered evaporation rate is due to the low mobility of surface water and tighter association to the CUP surface.

Table 5. Percent solids for CUP Polymer 2&6 for HCP and RCP.

Possibility / Packing	2 layer of surface water with free water	1 layer of surface water with free water	2 layers of surface water	1 layer of surface water	Solids only	Last three water molecules
RCP (59.8k)	32.56	45.53	60.94	77.47	100	94.92
HCP (59.8k)	46.71	54.90	60.94	77.47	100	
RCP (49.7k)	39.50	51.31	59.39	76.42	100	96.55
HCP (49.7k)	45.84	58.92	59.39	76.42	100	

Figure 15 shows the plot of Polymer 2 and Polymer 6 as an example.

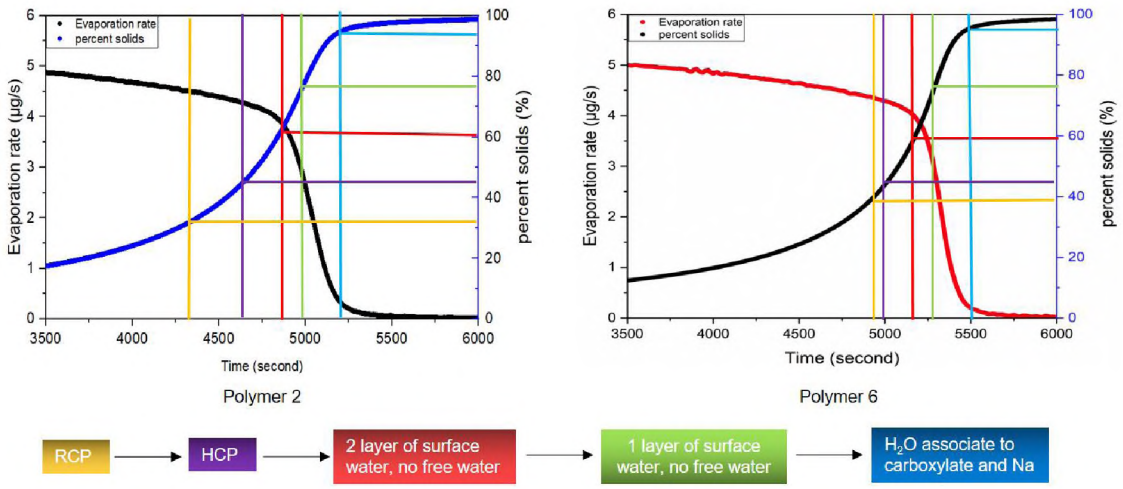

Figure 15. Evaporation rate of water at different solid%, (a) 5.04% Polymer 2, (b) 4.35% Polymer 6.

By comparing the percent solids of CUP at each slope change of the evaporation rate curve with the results in the Table 2, we illustrate the process of how surface water

and free water in the voids evaporate. The results showed that evaporation rate sharply decreased when the percent solids passes the HCP, due to the highly limited mobility of particles and water molecules. Another big evaporation rate reduction occurred at about 53%, where there is no free water between the CUP particles and two layers of surface water around CUP particles, that implied surface water doesn't evaporate until all free water is released. The next step was at about 72% solid, where there was only one layer of surface water, due to the inner layer being more tightly hydrogen bounded to the CUP surface. Furthermore, at about 96% solid, there was another evaporation rate change.

The results imply that free water completely evaporated before surface water started to evaporate, and water molecule associated to carboxylate group are released in the end. This was demonstrated for CUP solutions with different molecular weight and surface charge density, and indicated it is molecular weight and surface charge density independent. Sodium acetate hydrate has three waters of hydration which are held relatively strongly. Based on Table 4, Polymer 2 and Polymer 4 should have 94.92% and 96.55% solids respectively if it had 3 waters of hydration also. As can be seen in Figure 15 the two polymers are very close to these values. Therefore, it is highly likely that the last three waters to leave are those associated with the surface carboxylates.

4. CONCLUSIONS

The TGA method is a useful screening method for evaporation rate measurements with only small amounts of substance required. The experiments are quick and easy and yet provide accurate results for comparing different substances. Results indicated that

CUP was able to cause interfacial water deformation due to inter-particle charge repulsion, which increases the surface area and reduces surface tension, that increases the evaporation rate. In addition, the viscosity, in other words, the mobility of CUP particles and water molecules are also important factors for the evaporation rate. The CUP solution with higher initial percent solids has a higher evaporation rate in the beginning of the isothermal process than deionized water, due to more interfacial deformation and increased surface area as a result. During the isothermal process, the evaporation rate decreased, because of the combination of the effect of decrease in air-water interface temperature and limited mobility of water molecules and CUP particles by the increased viscosity. When reaching RCP and HCP, the movement of free water molecules were highly retarded, that caused significant evaporation rate reduction. Surface water didn't evaporate until all free water evaporated, and presented a slower evaporation rate. Water molecules associated with the carboxylate groups on CUP surface evaporated last.

AUTHOR CONTRIBUTIONS

Performed all TGA work and co-wrote the paper, P.G.; CUP solutions surface tension measurement, A.Z.; Theory development, co-wrote and supervised the project, M.R.V.D.M. All authors have read and agreed to the published version of the manuscript.

FUNDINGS

This research received no external funding.

ACKNOWLEDGEMENTS

The authors would like to thank the Department of Chemistry and the Missouri S&T Coatings Institute for financial support. Also Rachel Keppler for her assistance as an undergraduate researcher.

CONFLICTS OF INTEREST

The authors declare no conflict of interest.

REFERENCES

1. Somasundaram, S.; Anand, T. N. C.; Bakshi, S. Evaporation-induced flow around a pendant droplet and its influence on evaporation. *Phys. Fluids.* **2015**, *27*, 112105.

2. Harikrishnan, A.R.; Purbarun, Dhar; Sateesh, Gedupudi; Sarit, K. Das. Oscillatory solutothermal convection-driven evaporation kinetics in colloidal nanoparticle-surfactant complex fluid pendant droplets. *PHYSICAL REVIEW FLUIDS.* **2018**, *3*, 073604.

3. Erbil, H. Y. Evaporation of pure liquid sessile and spherical suspended drops: A review. *Adv. Colloid Interface Sci.* **2012**, *170*, 67-86.

4. Deegan, R. D. Pattern formation in drying drops. *Phys. Rev. E.* **2000**, *61*, 475.

5. Sefiane, K.; Wilson, S. K.; David, S.; Dunn, G. J.; Duffy, B. R. On the effect of the atmosphere on the evaporation of sessile droplets of water. *Phys. Fluids.* **2009**, *21*, 062101.

6. Chen, P.; Harmand, S.; Szunerits, S.; Boukherroub, R. Evaporation behavior of PEGylated graphene oxide nanofluid droplets onheated substrate. *International Journal of Thermal Sciences.* **2019**, *135*, 445-458.

7. Kim,Y.C. Evaporation of nanofluid droplet on heated surface. *Advances in mechanical engineering*. **2015**, 8.

8. Moghiman, M.; Aslani, B. Influence of nanoparticles on reducing and enhancing evaporation mass transfer and its efficiency. *Int. J. Heat Mass Transfer*. **2013**, *61*, 114.

9. Van De Mark, M. R.; Natu, A.; Gade, S. V.; Chen, M.; Hancock, C.; Riddles, C. Molecular Weight(Mn) and Functionality Effects on CUP Formation and Stability. *J. Coat. Technol. Res*. **2014**, *11*, 111-122.

10. Lee, S.; Choi, S. U.-S.; Li, S.; Eastman, J. A. Measuring thermal conductivity of fluids containing oxide nanoparticles. *J Heat Transfer*. **1999**, *121*(2), 280-289.

11. Murshed, M. S.; Leong, K.C; Yang, C. A combined model for the effective thermal conductivity of nanofluids. *Appl. Therm. Eng*. **2009**, *29* (11), 2477-2483.

12. Duangthongsuk, W.; Wongwises, S. Measurement of temperature-dependent thermal conductivity and viscosity of TiO2–water nanofluids. *Therm. Fluid Sci*. **2009**, *33* (4), 706-714.

13. Vidulich, G. A.; Evans, D. F.; Kay, R. L. The Dielectric Constant of Water and Heavy Water between 0 and 40. degree. *J. Phys. Chem*. **1967**, *71*, 656-662.

14. Prime, R.B.; Bair, H.E.; Vyazovkin, S.; Gallagher, P.K.; Riga, A. Thermogravimentricanalysis (TGA), in: *J. Menczel, R. Prime (Eds.)*, Thermal Analysis of Polymers:Fundamentals and Applications, John Wiley & Sons, Inc., New Jersey, **2009** (Chapter 3).

15. Zareei, M.; Yoozbashizadeh, H.; Hosseini, H.R. M. Investigating the effects ofpH, surfactant and ionic strength on the stability of alumina/water nanofluids using DLVO theory. *J. Therm. Anal. Calorim*. **2019**, *135*, 1185–1196.

16. Martins, P.; Lopes, A. C.; Lanceros-Mendez, S. Electroactive phase of poly(vinylidene fluoride): Determination, processing and application. *Prog. Polym. Sci*. **2014**, *39*, 683 –706.

17. Wachtler, M.; Wagner, M. R.; Schmied, M.; Winter, M.; Besen-hard, J. O. The effect of the binder morphology on the cycling stability of Li-alloy composite electrodes. *J. Electroanal. Chem*. **2001**, *510*,12–19

18. Chen, M., Riddles, C. Van De Mark, M. Gel point behavior of colloidal unimolecular polymer (CUP) particles. *Colloid Polym Sci*. **2013**, *291*, 2893–2901.

19. Riddles, C.; Zhao, W.; Hu, H. J.; Chen, M.; Van De Mark, M. R. Self-assembly of Water Insoluble Polymers into Colloidal Unimolecular Polymer (CUP) Particles of 3-9 nm. *Polymer*. **2013**, *55*, 48-57.

20. Cai, J.; Liu, R. New distributed activation energy model: Numerical solution and application to pyrolysis kinetics of some types of biomass. *Bioresour. Technol.* **2007**, *99*, 2795-2799.

21. Brown, M. E. Introduction to Thermal Analysis: Techniques and Applications; Kluwer Academic Publishers: Boston, **2001**.

22. Rahman, Md. R.; Hamdan, S.; Hui, J. L. C. Differential Scanning Calorimetry (DSC) and Thermogravimetric Analysis (TGA) of Wood polymer nanocomposites. *Chemical Engineering*. **2017**, *87*, 03013.

23. Forouharshad, M.; Montazer, M.; Moghadam, M.B.; Saligheh, O. Flame retardant wool using zirconium oxychloride in various acidic media optimized by RSM. *Thermochim. Acta*. **2011**, *516*, 29-34.

24. Cao, R.; Naya, S.; Artiaga, R.; García, A.; Varela, A. Logistic approach to polymer degradation in dynamic TGA. *Polym. Degrad. Stab*. **2004**, *85*, 667–674.

25. Geng, P.; Zore, A.; Van De Mark, M.R. Thermodynamic Characterization of free and surface water of Colloidal Unimolecular Polymer (CUP) Particles utilizing DSC. *Polymers*. accepted.

26. Van De Mark, M.R.; Chen, M.; Norman, S.G. Surface tension of colloidal unimolecular polymer particles at air/water interface. The Waterborne Coatings Symposium. **2013**.

27. Natu, A.; Van De Mark, M. R. Synthesis and characterization of an acid catalyst for acrylic-melamine resin systems based on colloidal unimolecular polymer (CUP) particles of MMA-AMPS. *Progress in Organic Coatings*. **2015**, *81*, 35-46.

28. Okubo, T. Surface tension of synthetic polyelectrolyte solutions at the air-water interface. *J. Colloid Interf. Sci.* **1988**, *125*, 386-398.

29. King, M. D.; Yang, J. C.; Chien, W. S.; Grosshandler, W. L. Proceedings of the ASME National Heat Transfer Conference, Baltimore, 1997.

30. Mysels, K. J. Vapor Pressure Lowering, Osmotic Pressure, and the Elementary Pseudo-Gas Model. J. Phys. Chem. B. 1997, 101, 1893-1896.

31. International Standard ISO 13099-1, **2012**, "Colloidal systems – Methods for Zeta potential determination- Part 1: Electroacoustic and Electrokinetic phenomena".

32. Characterization of liquids, nano-and micro-particulates and porous bodies using Ultrasound, 3rd ed. Dukhin, A. S.; Goetz, P. J. **2017**.

33. Russel, W.B.; Saville, D.A.; Schowalter, W. R. *Colloidal Dispersions*, Cambridge University Press, **1989**.

34. Sadiku, M. *Elements of electromagnetics, 5th ed.* **2009**, 104.

35. Fundamentals of Biochemistry, Rev. ed. Voet, D.; Judith A.; Charlotte, W. Pratt. **2001**. New York: Wiley. p30.

36. Physical Chemistry, 9th ed. *Oxford University Press*. Atkins, P. W.; de Paula, J. **2010**. "Section 5.5 (e)".

37. Prime, R.B.; Bair, H.E.; Vyazovkin, S.; Gallagher, P.K.; Riga, A.; Thermogravimentric analysis (TGA), in: *J. Menczel, R. Prime (Eds.)*, Thermal Analysis of Polymers:Fundamentals and Applications, John Wiley & Sons, Inc., New Jersey, **2009** (Chapter 3).

38. Russel, W.B. Bulk stresses due to deformation of the electrical double layer around a charge sphere. *J. Fluid Mech.* **1978**, *85*, 673-683.

39. Chen, M.; Riddles, C. J.; Van De Mark, M. R. Electroviscous contribution to the rheology of colloidal unimolecular polymer (CUP) particles in water. *Langmuir*. **2013**, *29* (46), 14034-14043.

40. Zeghbroeck, V. Principles of Semiconductor Devices. Chapter 2.7. 2011.

41. Manning, G.S. Limiting laws and counterion condensation in polyelectrolyte solutions. I. Colligative properties. *J. P. Chem.* **1969**, *51*, 924-933.

42. Mamontov, E. Dynamics of surface water in ZrO_2 studied by quasielastic neutron scattering. *J. Chem. Phys.* **2004**, *121*, 9087-9097.

43. Velazquez, G.; Herrera-Gomez, A.; Martin-Polp, M.O. Identification of bound water through infrared spectroscopy in methylcellulose. J. Food Eng. 2003, 59 (1), 79-84.

44. Van De Mark, M. R.; Zore, A.; Geng, P.; Zheng, F. Colloidal Unimolecular Polymer Particles: CUP. In *Single-Chain Polymer Nanoparticles*. Pomposo, J. A. **2017**, 259-312.

45. de Kruif, C. G.; van Iersel, E. M. F.; Vrij, A. Hard sphere colloidal dispersions:viscosity as a function of shear rate and volume fraction. *J. Chem. Phys.* **1985**, *83* (9), 4717-4725.

46. van der Werff, J. C.; de Kruif, C. G.; Blom, C.; Mellema, J. Linear viscoelastic behavior of dense hard-sphere dispersions. *Phys. Rev. A*. **1989**, *39*, 795-807.

47. van de Werff, J. C.; de Kruif, C. G. Hard-sphere colloidal dispersions: the scaling of rheological properties with particle size, volume fraction, and shear rate. *J. Rheol.* **1989**, *33*, 421-454.

48. Pishvaei, M.; Grailat, C.; McKenna, T. F.; Cassagnau, P. Rheological behaviour of polystyrene latex near the maximum packing fraction of particles. *Polymer*. **2005**, *46*, 1235-1244.

49. Dames, B.; Morrison, B.; Willenbacher, N. An empirical model predicting the viscosity of highly concentrated, bimodal dispersions with colloidal interactions. *Rheol. Acta*. **2001**, *40*, 434–440.

III. DSC AND TGA CHARACTERIZATION OF FREE AND SURFACE WATER OF COLLOIDAL UNIMOLECULAR POLYMER (CUP) PARTICLES FOR COATINGS APPLICATIONS

Peng Geng, Sagar Vijay Gade, and Michael R. Van De Mark*

Department of Chemistry, Missouri S&T Coating Institute, Missouri University of Science and Technology, Rolla, Missouri 65409 USA

*Corresponding Author: Michael Roy Van De Mark, Director Missouri S&T Coatings Institute, Missouri University of Science & Technology, Rolla, MO 65409
mvandema@mst.edu

ABSTRACT

Colloidal Unimolecular Polymer (CUP) particles are spheroidal nano-scale and 3-9 nm that can be easily designed and controlled. The formation of CUP involves simple synthesis and water reduction. These nano particles have charged hydrophilic groups on the surface and are surrounded by a layer of surface water that does not freeze until very low temperature. CUPs have very high surface area per gram which gives them a high non-freezing water content. The CUP system is free of surfactant and has zero VOC that exhibit great potential in coatings applications. The amount and thickness of the surface water was determined by DSC using the heat of fusion. The solution density and knowledge of the resin density and the composition of the CUP solution was used to determine the density of surface water. The evaporation rate of free water and surface water in CUP solutions were investigated by thermogravimetric analysis, and showed the effect of CUP on the evaporation rate. CUP as an additive to give freeze thaw stability, wet edge retention and open time improvements were explored. Excellent performance in

freeze thaw, wet edge time improvement and more open time was found. The CUP system offers an excellent alternative to form zero VOC water borne coatings.

Keywords: Colloidal Unimolecular Polymer (CUP), nano-scale, surface water, freeze thaw stability, wet edge retention.

1. INTRODUCTION

In the recent years, due to the capacity of nanotechnology to have enhanced physical and chemical properties, application of nanotechnology has become more and more important. The term nano commonly refers to anything smaller than 1000 nm, and nanoparticles with particle size smaller than 10 nm. These nanoparticles often exhibit significant increases in properties due to the ultra-small particle size or higher surface area per gram.[1] Most existing nanoparticles smaller than 10 nm are inorganic nanoparticles. It is difficult to make polymeric nanoparticles with particle size less than 10 nm. Colloidal Unimolecular Polymer (CUP) particles are a new type of spheroidal nanoscale material (3-9 nm). The polymer can be simply synthesized and made into CUP through a water reduction process,[2] which is shown in Figure. 1.

The process of CUP formation for the carboxylate example was as follows. The polymers were dissolved in THF, the solvent must be low boiling and water miscible, and then neutralized to pH 8.5 based on the acid number using a peristaltic pump. It is critical that the polymer concentration be low enough to avoid chain chain entanglement at the point of collapse. The carboxylate groups repelled each other due to the increasing of dielectric constant (80.1 for water and 7.6 for THF) caused by the added water and the

chain extends toward linearity which increased the viscosity.[3] Through continuously adding water to the system, the Mark-Houwink parameter, a, will reach the highest value as does the viscosity, where $[\eta]=KM^a$. The parameter a is typically 0.5 for a random coil, 2.0 for a ridged rod and zero for a hard sphere shape.[4] CUPs presented a random coil shape when firstly dissolved in THF, and had the parameter value ranging from 0.6 to 0.7. As water was slowly added, the parameter approached 2.0 and increased the viscosity of the solution, due to the inter-particle charge repulsion.

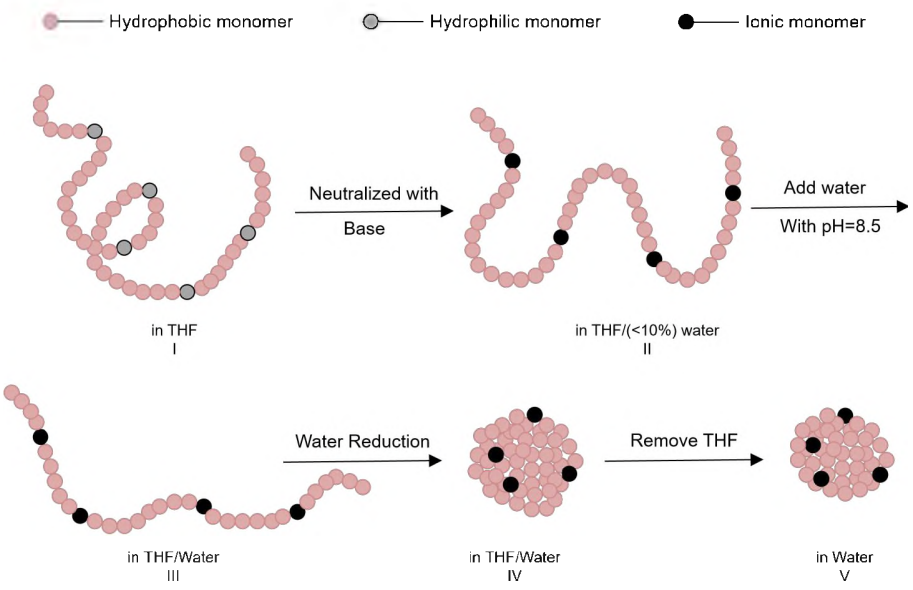

Figure 1. Water reduction process, formation of CUP.

Further addition of water caused the polymer-polymer interactions to become greater than the polymer-solvent interaction, and the carboxylate groups oriented into the water phase as collapse occurs. At which point, the parameter became nearly zero while the viscosity of the solution was kept high due to the inter-particle charge repulsion. The polymer was organized to produce maximum separation of charge. Hence, water released

from the polymer backbone entropically drives the particle formation similar to that of a surfactant forming a micelle. The presence of ionic groups on the surface is the driving force to prevent particles from aggregating, and the formation of the spherical shape. Once formed, these colloidal solutions are thermodynamically stable.[4] The ratio of hydrophobic to hydrophilic monomer units making up the backbone is important and defined similar to the ratio in surfactants.[1,6,7]

CUP particles generally have charged hydrophilic groups on the surface and a collapsed hydrophobic backbone. The charged surface can associate with a layer of surface or bound water, that does not freeze until very low temperature,[8] illustrated in Figure 2.

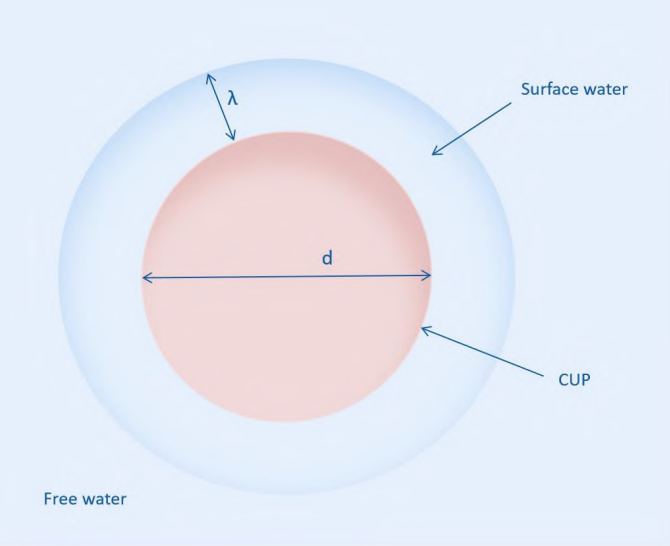

Figure 2. CUP with surface water and free water.

Due to its ultra-small particle size, the surface area per unit mass and surface area per unit volume of CUP is very high. Also, the CUP surface functionality can be utilized

and controlled. Many coatings applications have been made in publications by Van De Mark et al.[8-12]

Freeze thaw stability is a major issue for coatings during transportation and storage at low temperature. The lack of an efficient freeze-thaw stabilizer will often result in failure of the paint. When the temperature is lower than 0 °C, the water in the paint starts to freeze and increases the concentration of latex particles in the remaining liquid, pushing them closer together. This lower liquid volume leads to particle-particle contact that cause aggregating and coagulating problems during thawing.[12] For low Tg latex particles, the polymer flow and coalescence occurs at low temperature. In this case the freeze-thaw stabilizer is even more critical. The most widely used freeze-thaw stabilizers are ethylene and propylene glycol, which can inhibit part of the water from freezing and maintain a layer of non-frozen fluid around the latex particles that stabilize the paint.[13] However, due to the stricter environmental regulations, in order to achieve zero VOC in paint, the glycols in paint has to be eliminated.

Limited open time or wet edge retention has also been a common issue for waterborne coatings causing skinning as well as lap marks. Wet edge is defined as the period of time during which there is no visible edge between freshly applied and a previously applied paint area.[14] Normally the open time for waterborne coatings is only around 6-5 minutes, while the wet edge time is as short as 2-6 minutes. Many studies have been made to extend the wet edge time and open time for waterborne coatings, mostly by delaying the coalescence of the paint by adding a glycol, or grafting hydrophilic compounds to latex particles. Also, a surface-active evaporation suppressing agent has been used, forming of the hydrophobic barrier at water-air interface can reduce

the water evaporation rate to a certain extent.[15-17] No solution to this problem has been found that is generally applicable and zero VOC.

CUP has a diameter ranging from 3 to 9 nm that is determined by the molecular weight and its density. With small particle size, CUP offers a large surface area with a large amount of non-freezable surface water. For example, a 4.22 nm CUP particle with one layer of water associated with the particle surface would have a 27.8% volume fraction of surface water, which is significantly greater than a typical latex particle which is about 100 nm diameter and has a 1.08% volume fraction of surface water. The presence of non-freezable surface water makes CUP a great candidate for a freeze-thaw stabilizer to replace traditional glycols and wet edge retention additives for architectural paint. In addition, CUP has zero VOC due to the complete removal of the organic solvent, which potentially solves the issue that many manufactures have to compromise the performance of paint by eliminating the glycol to reach zero VOC.

CUP also has many other potential applications in coatings. An EA-AA co-polymer was synthesized with 9:1 ratio, then the carboxylic acid groups were reacted with 2-methylaziridine to produce an amine functional co-polymer, using acetic acid to form the salt and then forming a CUP. The amine salt CUP is a highly effective cross-linker for epoxy with near zero VOC and very low viscosity.[12] CUP was also synthesized from MMA and AMPS, the sulfonate amine salt CUP has the potential to be used as an acid catalyst for water-borne acrylic-melamine resin systems.[11] It gives significantly better results for pencil and indentation hardness compared with standard toluene sulfonic acid catalyst.[18,19] Unlike the standard pTSA catalyst, the CUP catalyst will become chemically incorporated by reacting the ester groups with the melamine and rendering the

catalyst immobile unlike pTSA which can, over time, migrate in the coating. CUPs can be used as a water borne lacquer or air dry system with the small particle size allowing for more rapid coalescence since the polymer chain only needs to migrate a few nanometers to form a film. The coalescence time for CUPs are typically in hours where the latex resins are usually 7-10 days.[18] In addition, the nano-scale CUP particles may deliver breakthroughs for coating performance such as barrier properties and mechanical properties.[20-25]

This work presents a preliminary study of the CUPs surface water properties, utilizing differential scanning calorimetry (DSC) as well as thermogravimetric analysis (TGA) to define the importance of surface water on coating applications.

2. EXPERIMENTAL

2.1. POLYMER SYNTHESIS

Polymers were synthesized by a free radical polymerization in THF with a nitrogen atmosphere, monomer ratio was 9:1 for MMA:MAA copolymer, and 9:1 for EA:AA copolymer, the amount of initiator AIBN and chain transfer agent were determined based on the desired molecular weight, the amount used was shown in Table 1. The reaction was carried out under nitrogen. The mixture was heated slowly to reflux under stirring for 24 hours. The polymer solutions were then cooled to room temperature, and part of the THF removed by rotovap. The polymer was precipitated in cold deionized water under high shear rate, and dried in a 50 °C oven under vacuum for 24 hours.[2]

Table 1. Polymer synthesis, the amount of materials used.

Polymer	Molecular weight (g/mol)	Monomer 1	Monomer 2	Initiator	Chain transfer agent	Solvent
		Methyl methacrylate (g)	Methacrylic acid (g)	AIBN (g)	1-Dodecanethiol (g)	Tetrahydrofuran (g)
Polymer 1	28,900	225.25	21.5	0.2911	1.5394	750
Polymer 2	59,800	225.25	21.5	0.2911	1.4274	750
Polymer 3	122,500	225.25	21.5	0.2911	0.3546	750
		Ethyl acrylate (g)	Acrylic acid (g)	AIBN (g)	1-Butanethiol (g)	Tetrahydrofuran (g)
Polymer 4	31,000	90.1	7.1	0.1362	0.0898	250

2.2. ABSOLUTE MOLECULAR WEIGHT OF COPOLYMERS

By using gel permeation chromatography (Viscotek model 305 manufactured by Malvern Corp.), the absolute molecular weight and distribution of copolymers were measured. The GPC was equipped with a triple detector array TDA305 that included refractive index detector, low and right angle light scattering detector, and intrinsic viscosity detector, thus yielding absolute molecular weight. Column PAM-505 from PolyAnalytik with size 7.5 mm (ID)×300 mm (L) was used. Polymers solutions were ran at 2 mg/cc in THF with a 0.5 ml/min flow rate.

2.3. DENSITY OF DRY CUPS

The solutions of CUPs were dried in a vacuum oven at 50 °C with the presence of solid sodium hydroxide to absorb carbon dioxide. After the clear material formed, the sample was then heated to 110 °C until constant weight was obtained. The densities of

the dry CUPs were measured by a gas displacement pycnometer (Micrometritics AccuPycII 1340). Equilibrium flow rate of helium gas was 0.005 psig/min, temperature was controlled at 25.89±0.04 °C. Twenty five readings were made for each sample, and the results were reported by its average and standard deviation.

2.4. DENSITY OF CUP SOLUTIONS

Densities of CUP solutions were directly measured by density meter (DDM 2911 plus by Rudolph Research Analytical) at various weight fractions at 25 °C. The accuracy is 0.00001 g/cm^3.

2.5. ACID NUMBER (AN)

The acid number of the copolymers were determined by the titration method (ASTM D 974), and reported in mg of KOH/g of polymer sample. The method was modified by using potassium hydrogen phthalate (KHP) in place of hydrochloric acid and phenolphthalein in place of methyl orange. THF was used as the solvent for the titration.

2.6. VISCOSITY OF CUP SOLUTIONS

Viscosity of CUP solutions were measured by Ubbelohde capillary viscometer J-340 from Cannon instrument company, according to ASTM D445, ASTM-D446 and ISO 3104, 3105. The viscosity of CUP solutions were determined at 25 °C and 29 °C. Before each measurement, CUP solution was transferred to the Ubbelohde capillary viscometer and kept in a constant temperature water bath at 25±0.1 °C for 20 minutes with plastic wrap covering on top of the viscometer to prevent potential evaporation and carbon

dioxide contamination of the solution. A stop watch with 0.01 second precision was used to monitor the elution time and each measurement was repeated for at least three times and the error being less than 0.5%. Absolute viscosity was then calculated by Equation 1.

$$\eta = t \cdot d \cdot c \tag{1}$$

where η is the viscosity of CUP solution (cP), t is the elution time (s), d is the density of CUP solution (g/ml) and c is the Ubbelohde capillary viscometer constant (0.009749 mm^2/s).

2.7. PARTICLE SIZE OF CUP

Particle size was measured by dynamic light scattering using Microtrac Nanotrac 250. The viscosities of solutions were used due to the high concentration of CUP having strong charge repulsion between particles. The CUP particles are very small, and result in very poor signal of the scatted light requiring high (10%) concentrations.[1] The CUPs solutions were diluted to 10% concentration by Mili-Q ultra-pure water with resistance of 18.3 MΩ adjusted to pH 8.5. The laser diode was 780 nm wavelength, and 180° measuring angle.

$$D = \frac{k_B T}{6\pi\eta r} \tag{2}$$

where k_B is Boltzman constant, T is absolute temperature of the solution, η is the viscosity of solution, r is the radius of particle. Viscosity measurements were done by Ubbelohde viscometer method. Additional viscosity measurements, when needed, were made with an LV DVIII rheometer with spindle CP-40 from Brookfield Engineering.

2.8. DIFFERENTIAL SCANNING CALORIMETRY

Differential scanning calorimetry from TA instruments Q2000 was used to measure the heat of fusion of CUP solutions. About 30 mg of CUP solutions were sealed in the Tzero Hermetic pan, then cooled to -40 °C at the rate of 10 °C/min, isothermal for 10 minutes, and heated to 40 °C at the rate of 3 °C/min. The mass was measured before and after the measurement to determine if a proper seal was obtained. If the mass difference exceeded 0.001 mg the data was not used due to the leak.

2.9. PAINT FORMULATION

To avoid variation of raw materials in the paint formulations, a master grind batch was prepared, 3 levels of CUP were used as a partial replacement of the Encor 379G resin during the letdown process at low shear rate (800RPM) and mixed for 20 minutes. All the testing was done after at least 24 hours after preparation of the paint formulations. Use of a freeze-thaw stabilizer and coalescing aid was deliberately avoided to investigate the actual effect of CUP on the paint formulations. The U.S. Environmental Protection Agency has officially removed AMP 95 from the Clean Air Act's list of VOC making these paints truly zero VOC systems.

2.10. FREEZE THAW STABILITY

Testing was done based on ASTM 2243-95, by separating paints into two pint-size (500 ml) resin lined can. One can was stored at room temperature as a standard while the other can went through cycles of freezing and thawing process, as the test specimen. The test specimen was kept at -18 °C for 17 hours and then allowed to stand at room

temperature for 7 hours. After these cycles, the coating was examined for any changes in viscosity and visual film properties.

2.11. WET EDGE RETENTION

A 3 mil draw down of paint was made on an AG-5390 Leneta card, and seven "X" marks were made on the drawndown using a wide curved end of paint brush. After every two minute interval, paint was brushed back and forth across the film for ten cycles, according to ASTM D7488-11. The time at which the edge of the drawn down can no longer be worked into the body of the paint was referred to as the wet edge time, while the time at which the "X" began to show through the paint was deemed the open time.

2.12. PAINT VISCOSITY

A KU-1 viscometer from Brookfield was used to measure the viscosity. Paint was kept at 25 °C, when the temperature reached equilibrium, the paint was stirred vigorously to avoid entrapping air. The container of paint was immediately placed on the platform of the viscometer and the paddle-type rotor was immersed in the paint, according to ASTM D562-10.

2.13. THERMOGRAVIMETRIC ANALYZER

Thermogravimetric analyzer from TA instruments Q500 was used to measure the evaporation rates of the water. The experiments were performed at atmospheric pressure. A constant flow of inert gas (nitrogen, flow rate 40 ml/min) was maintained throughout the experiment. A small amount of the aqueous sample (about 30 mg) was placed in a

platinum sample pan and suspended in the furnace of the thermogravimetric analyzer. In order to avoid excess evaporation, the sample was heated to the experimental temperature 25 °C at 100 °C/min, the temperature of the sample was measured by a thermocouple placed aside the sample pan. The sample was held isothermally at the experimental temperature for 360 minutes and the weight percent change of the sample was recorded.

3. RESULTS AND DISCUSSION

Table 2 shows the characterization of the four polymers studied.

Table 2. Molecular weight, particle size, acid number and density of the polymers.

Sample	M_n (g/mol)	Monomer ratio	Particle diameter (nm)	Acid Number (mg KOH/g)	Density of dry CUP ρ_p (g/cc)	charge density in ions per nm^2
Polymer 1	28,900	9:1	4.22	56.8	1.2246±0.0018	0.52
Polymer 2	59,800	9:1	5.38	57.0	1.2311±0.0014	0.66
Polymer 3	122,500	9:1	6.83	56.9	1.2342±0.0018	0.84
Polymer 4	31,000	9:1	4.26	56.4	1.2255±0.0018	0.56

Four polymers with a monomer ratio of 9 to 1 and different molecular weights were synthesized. Molecular weight, acid number, particle size and density of the polymers are listed. These polymers were selected for this initial study based upon earlier work.25 They represent a stable and well-studied CUP system. Polymer 4 was targeted as

a room temperature coalescing resin with a low Tg , -16.2 °C, for use in the paint for freeze thaw and wet edge testing.

3.1. HEAT OF FUSION

The heat of fusion of a given sample can be directly determined by differential scanning calorimetry, which is represented by the area of the endothermic peak, shown in Figure 3 for water. Here all the water freezes and is melted during the endothermic scan.

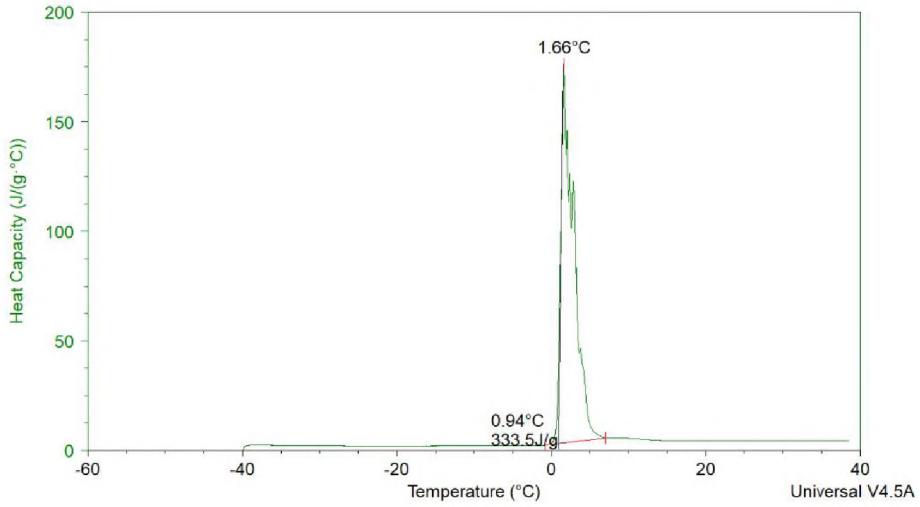

Figure 3. Heat of fusion of water.

Figure 4 shows the endotherm for a 10.35% Polymer 2 CUP solution. The solution contains only CUP particles and pH adjusted water. The difference between the heat of fusion of water and the CUP solution indicates that there is water in the CUP system that does not freeze until well below -40 °C.

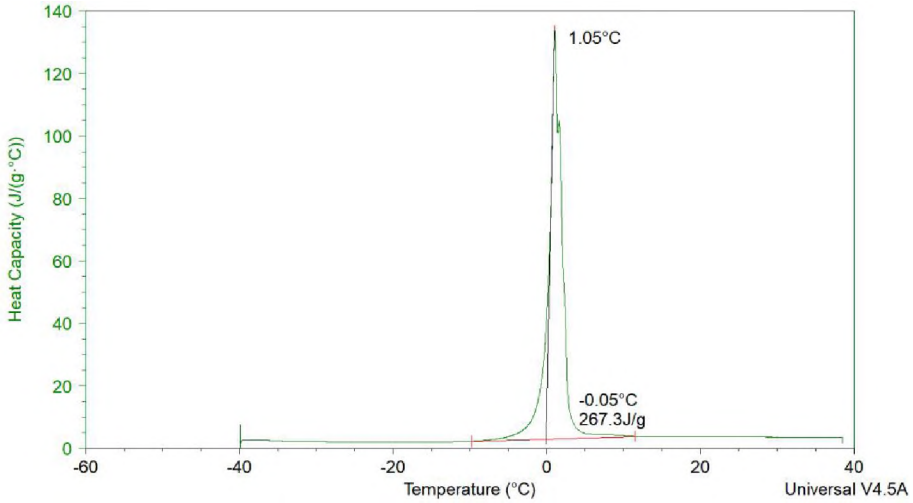

Figure 4. Heat of fusion of 10.35% Polymer 2.

Using the heat of fusion of water as the standard, the weight fraction of free and surface water in CUP solution can be determined by Equations 3-5.

$$X_{FW} = \frac{\Delta H_{FW}}{\Delta H_W} \tag{3}$$

$$X_{SW} = 1 - X_{FW} - X_{CUP} \tag{4}$$

$$X_{SW} = 1 - X_{CUP} - \left(\frac{\Delta H_{FW}}{\Delta H_W}\right) \tag{5}$$

where X_{FW} is the weight fraction of freezable water, ΔH_{FW} is the heat of fusion of freezable water obtained from DSC, ΔH_W is the heat of fusion of water, 333.5 J/g.

In addition, in order to understand the effect of molecular weight and ions per nm2 (surface charge density) on the surface water properties, the charge density was determined by Equation 6.

$$\rho_v = \frac{M_W}{4\pi r^2 (n_1 \cdot M_{monomer1} + n_2 \cdot M_{monomer2})} \tag{6}$$

where ρ_v is the charge density in ions per nm^2, M_w is the molecular weight of CUP, r is the radius of the CUP particle, n_1 is the moles of MMA and n_2 is the moles of MAA used per average repeat unit, $M_{monomer1}$ is the molecular weight of monomer 1, $M_{monomer2}$ is the molecular weight of monomer 2.

The charge density in ions per nm^2 and the weight fraction of surface water were calculated for a group of CUPs with different molecular weights, shown in Table 3. At the same solid percent, higher molecular weight CUP tends to have a lower amount of surface water. This lower value is mainly due to the smaller particle size CUP having a larger surface area per gram that can associated with more water if the surface layer was of constant thickness.

Table 3. Weight fraction of free water and CUP polymers.

CUP	Solid percent	X_{SW}	CUP	Solid percent	X_{SW}
Polymer 1 28.9k (0.52)	5.85%	6.00%	Polymer 2 59.8k (0.66)	4.83%	4.42%
	9.57%	9.85%		10.35%	9.51%
	13.32%	13.70%		11.35%	10.43%
	16.55%	17.00%		18.72%	17.25%
Polymer 3 122.5k (0.84)	4.53%	3.32%			
	10.12%	7.32%			
	13.72%	10.10%			
	18.10%	13.19%			

In order to gain a deeper understanding of CUP's surface water, the density of CUP solutions were measured by high precision density meter at various solid percent, and the $1/\rho_s$ values were plotted against solid percent of CUP solutions, shown in Figure

5. The density of the surface water is linearly dependent upon the solids content up to 15% solids. This indicates that the surface water is of constant thickness over this range.

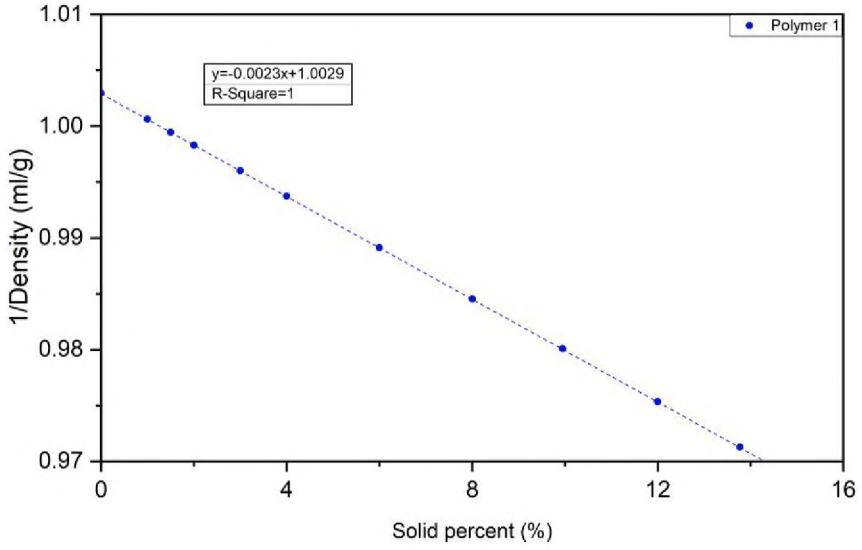

Figure 5. 1/density vs solid% of Polymer 1.

In a given CUP solution, the volume of CUP solution includes: volume of CUP particles, volume of surface water and volume of free water. By knowing the weight fraction and the density of each component, the density of surface water can be determined by Equation 7.

$$\frac{1}{\rho_S} = \frac{X_{FW}}{\rho_{FW}} + \frac{X_{SW}}{\rho_{SW}} + \frac{X_{CUP}}{\rho_{CUP}} \tag{7}$$

where ρ_s is the density of the CUP solution, ρ_{sw} is the density of surface water, ρ_{FW} is the density of free water, ρ_{CUP} is the density of the CUP particle.

The density of the surface water of each CUP system was considered to be constant at the studied range, where the surface water density for Polymer 1, 2 and 3 are

1.0412 g/ml, 1.0509 g/ml and 1.0558 g/ml. The difference of the density of surface water is due to the different charge densities in ions per nm^2. The higher charge density is capable of associating with more water molecules. The surface of CUP is primarily occupied by two functionalities, the carboxylate and the ester. The carboxylate will have more and stronger hydrogen bonds to water than the ester. As the charge density increases the ratio of carboxylates to esters will increase on the surface. The difference in hydrogen bond strength and amount of water associated with the carboxylate may be a significant contributor to the density difference. This aspect will be further investigated in the future.

Since the density of surface water is known, as well as the weight fraction of surface water, the thickness of the water layer could be calculated by Equation 8.

$$\frac{4}{3}\pi(\lambda+\frac{d}{2})^3-\frac{4}{3}\pi(\frac{d}{2})^3=\frac{X_{SW}M}{X_{CUP}N_A\rho} \tag{8}$$

where λ is the thickness of surface water, d is the diameter of CUP particle, X_{SW} is the weight fraction of surface water, X_{CUP} is the weight fraction of CUP particle, M is the molecular weight of CUP, N_A is Avogadro constant, ρ_{sw} is the density of surface water.

The surface water thickness for Polymer 1 was 0.636, Polymer 2 was 0.734 and Polymer 3 was 0.766 nm. The higher charge density, the thicker surface water is clearly shown by the data. This can be explained by the effective charge density: the larger CUP particle has more charges on the surface per unit area, which forms a thicker electrical double layer, giving more counter-ions and associate with more water molecules. This hypothesis assumes that all the charges are on the surface of the CUP as they are in micelles.

Previous studies[4,10] have observed that, when CUP solid percent is high, the surface water thickness was lower due to Manning condensation.[26] However, in this study the concentration is below that needed to cause Manning condensation. Further studies will be focused on understanding the charge density effects on the surface water properties, as well as the effect of each functional group on the surface at all concentrations below the gel point of the CUP solutions.

3.2. FRZEEZE/THAW STABILITY

When the temperature of a coating goes below the freezing point during transportation and storage, water in latex paint freezes like pure water. Ice crystals form and grow causing less and less water to be in liquid form. The formation of ice causes an increase in the solid percent of the remaining latex system. The loss of water increases the potential contact between latex particles during the freezing cycle. Traditional freeze thaw stabilizers such as propylene glycol give freeze thaw stability even below -10 °C by forming a liquid hydration layer around latex particles at low temperature, minimizing the particle contacts with each other which prevents aggregation.

Figure 6 shows the heat of fusion of 9.96% propylene glycol in water, the weight fraction of non-freezable water is only 4.70%, which is about half of the weight fraction of propylene glycol. Thus, the liquid portion around a latex particle with propylene glycol would be very thin. It should be noted that when a latex paint freezes the can contents becomes frozen solid. The glycol only prevents a very small amount of the water from freezing.

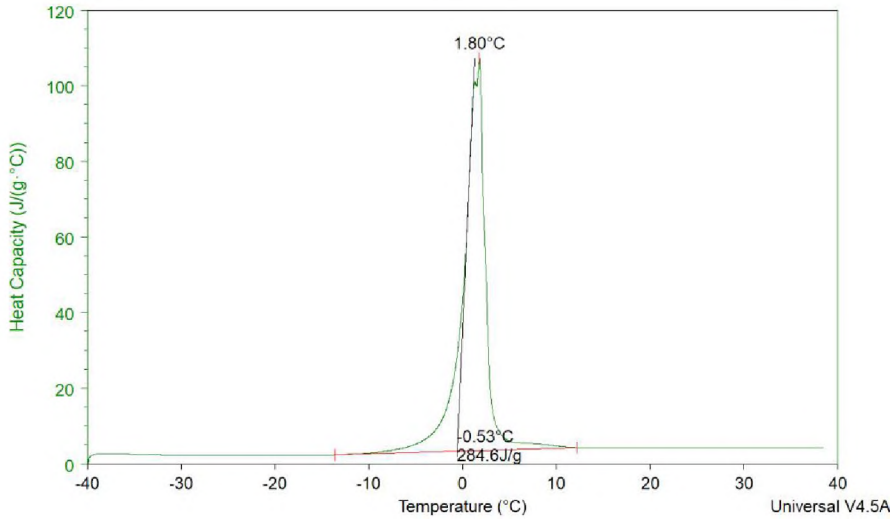

Figure 6. Heat of fusion of propylene glycol 9.96% in water.

In the CUP solution for example, using 9.57% solids Polymer 1, the CUP solution has 9.85% surface water (non-freezable water) by weight. The surface water is about the same as the weight fraction of CUP particles which is significantly larger than for propylene glycol. CUPs should have a better chance to keep latex particle separated when paints are exposed to low temperature conditions.

In this study, a freeze thaw unstable latex paint formulation was prepared with different CUP amounts. Part of the latex resin, UCAR 379G, was replaced by Polymer 4 CUPs with molecular weight of 31,000 g/mol in the paint formulation. The replaced amount of CUP particles were 20 lbs, 30 lbs and 40 lbs per 100 gallons of paint as shown in the letdown in Table 4. The glass transition temperature of Polymer 4 is -16.2 °C, that allows CUP particles to coalesce with the latex and other CUP particles. The CUP resin is essentially a normal resin binder.

Table 4. Paint formulation of the master batch.

			Formula		Solids	
%NV	Wt/Gal	Material	Pounds	Gallons	Pounds	Gallons
0	8.33	Water	227.41	27.30	0.00	0.00
0	7.85	AMP 95 pH Modifier	2.00	0.25	0.00	0.00
100	8.83	Triton X-100	3.76	0.43	3.76	0.43
100	8.33	Byk 22 defoamer	1.33	0.16	1.33	0.16
60	8.90	Tamol 731A	28.20	3.17	16.92	1.81
100	33.32	Kronos 2101 TiO_2	250.00	7.50	250.00	7.50
25	8.70	RM 825	12.00	1.38	3.00	0.30
	Let down for control					
55	9.00	UCAR 379G	436.36	48.48	240.00	24.91
0	8.33	Water	94.38	11.33	0.00	0.00
		Total	1055.44	100.00	515.01	35.11
	Let down UCAR 379G with 20 lbs CUP solids					
55	9.00	UCAR 379G	400.00	44.44	220.00	22.84
23.5	8.77	CUP	85.10	9.70	20.00	1.96
0	8.33	Water	47.23	5.67	0.00	0.00
		Total	1057.03	100.00	515.01	35.00
	Let down UCAR 379G with 30 lbs CUP solids					
55	9.00	UCAR 379G	381.83	42.43	210.01	21.80
23.5	8.77	CUP	127.65	14.56	30.00	2.93
0	8.33	Water	23.49	2.82	0.00	0.00
		Total	1057.67	100.00	515.02	34.93
	Let down UCAR 379G with 40 lbs CUP solids					
55	9.00	UCAR 379G	363.63	40.40	200.00	20.76
23.5	8.77	CUP	170.21	19.41	40.00	3.91
0	8.33	Water	0.00	0.00	0.00	0.00
		Total	1058.54	100.00	515.01	34.87

The weight per gallon, percent solids by weight, percent solids by volume, PVC and the amount of CUP surface water of the paint were determined, shown in Table 5.

Table 5. Weight per gallon, % solids by weight, % solids by volume and PVC of the paint.

	Control (no CUP)	20 lbs CUP/100 gal	30 lbs CUP/100 gal	40 lbs CUP/100 gal
WPG	10.55	10.57	10.58	10.59
% Solids (Wt)	48.80	48.72	48.69	48.65
% Solids (Vol)	35.11	35.00	34.93	34.87
PVC	21.36	21.43	21.47	21.51
Amount of surface water of CUP (lbs)	0	20.51	30.77	41.02

To determine the paints stability with and without CUPs and at what level it would give good stability, a set of freeze thaw stability tests were performed according to ASTM 2243-95,[11] shown in Table 6.

Table 6. Freeze thaw stability (KU viscosity).[11]

Replaced Latex*	Initial	FT Cycle 1	FT Cycle 2	FT Cycle 3	FT Cycle 4	FT Cycle 5
Without CUP	67	Failed	-	-	-	-
20 lb	60	62	65	86	115	-
30 lb	58	58	58	58	60	60
40 lb	58	58	58	58	58	58

*Replacing pounds of Latex solids with CUP solids based on 100 gal formulation.

The evaluation shows that with the addition of CUP, the freeze thaw stability was improved dramatically. The paint with the lowest level (20 lbs) of CUP failed on the second freeze thaw cycle, but did not coagulate. The viscosity of the paint of medium

level (30 lbs) increased by 2 KU after three freeze thaw cycles. With the highest level (40 lbs) of CUP, the viscosity remained stable even after 5 freeze thaw cycles. It was observed that the higher loadings of EA-AA CUP could maintain a stable viscosity during the freeze thaw process. By replacing part of the resin by 20 lbs, 30 lbs and 40 lbs CUP in the formulation, which is only 7.71%, 12.11% and 16.91% of the resin based on volume percent solids major improvement is seen. If taking surface water into consideration of the volume, that's approximately 2.98%, 4.47% and 5.94% of CUP based on volume; while the volume percent of latex is 22.84%, 21.80% and 20.76%. Therefore, the number of particles of CUP to latex is about 389.43, 612.02 and 854.47 to 1 latex particle. Thus, when all free water freezes, the existence of a large amount of CUP can maintain sufficient non-frozen fluid that it prevents the latex particles from contacting each other, and therefore increases the freeze thaw stability as shown in Figure 7.

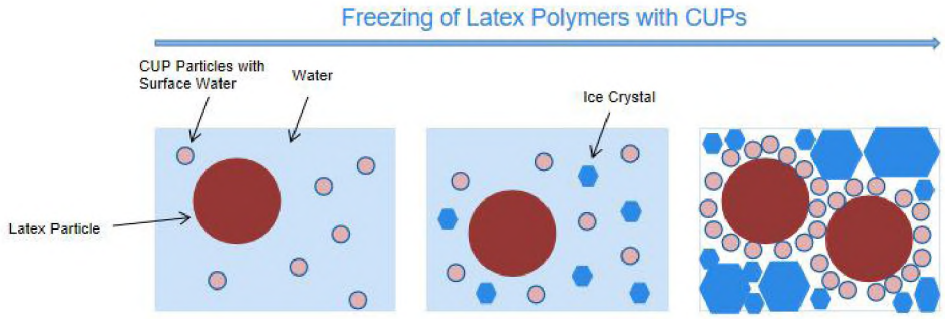

Figure 7. Freezing of Latex Polymers with CUP.

These results indicate that CUP is a very promising replacement for the current anti-freeze. CUPs provide a zero VOC option with no need to compromise the freeze

thaw stability. CUPs can be used as a co-resin for latex and polyurethane dispersions, as well as the cross-linker for waterborne epoxy and other aqueous systems, only the CUP monomers need to be changed to accommodate the system. With the large amount surface water, there is no need to use additional anti-freeze. It should be noted that the Tg of the CUP can be readily changed by using different hydrophobic monomers.

3.3. EVAPORATION RATE

In a previous study it was shown that when water in a CUP solution evaporates, as the volume fraction of CUP increases, the viscosity increases.[27] This increase is due to the repulsive force between particles increasing as the volume fraction of CUP particles increases. Initially CUPs are in a random disordered state at low concentration. As the concentration increases the charged CUP particles begin to repel each other due to common charge. When the CUP concentration increases high enough the system will gel as a pseudo-lattice forms.[28] The water evaporation rate was evaluated to gain an understanding of its effect on the drying process of paint. The evaporation of CUP solutions was determined by using a thermogravimetric analyzer (TGA). Samples were set at a fixed temperature, and held isothermal until there is no more weight loss. The weight percent loss per unit time can be directly given by the measurement. By knowing the actual mass loss of the sample (m), the weight loss per unit time (evaporation rate) can be determined by Equation 9.

$$\vartheta = \frac{m \cdot \Delta weight\%}{\Delta t} \tag{9}$$

Figure 8 is given as an example of the evaporation of water and CUP samples. Initially, free water in CUP solutions evaporate faster than pure water in region I. The

CUP functions like a surfactant and lowers the surface tension. The lowering of surface tension may be responsible for the increase in evaporation rate. As the water evaporates the concentration increase at the surface and will also cause an osmotic flow to be set up bringing water to the surface. When more water evaporates from the air-water interface, the solid percent of CUP particles builds up and the counter-ion concentration also increases.

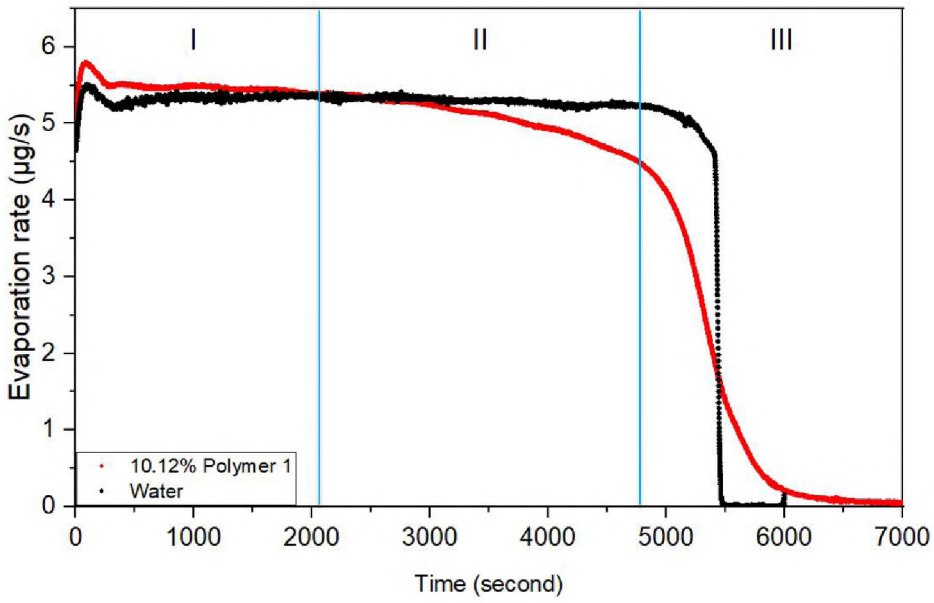

Figure 8. Evaporation rate of water in 10.12% Polymer 1 CUP solution and pure water.

Some of the ions condense on the CUP surface reduce the effective charge on the surface,[29] which allows more CUP particles to pack at the air-water interface increasing the viscosity and reducing the rate of diffusion of water and the water evaporation rate, shown in region II. When the solid percent enters region III the CUP starts to gel, at which point the particles are fixed in location and the surface water highly reduces water

movement. Thus, the evaporation rate dropped drastically due to the much slower water molecule diffusion and the hydrogen bonding to the ions on the CUP surface.

The evaporation rate of water in 10.12% CUP solution is shown in Figure 9 as an example. The evaporation in region I allows a quick dry allowing a paint to normally flow and level but the slowing of the evaporation in regions II&III would give a paint more open time without any flow or sag. The existence of a large amount of surface water can further extend the wet edge time and open time.

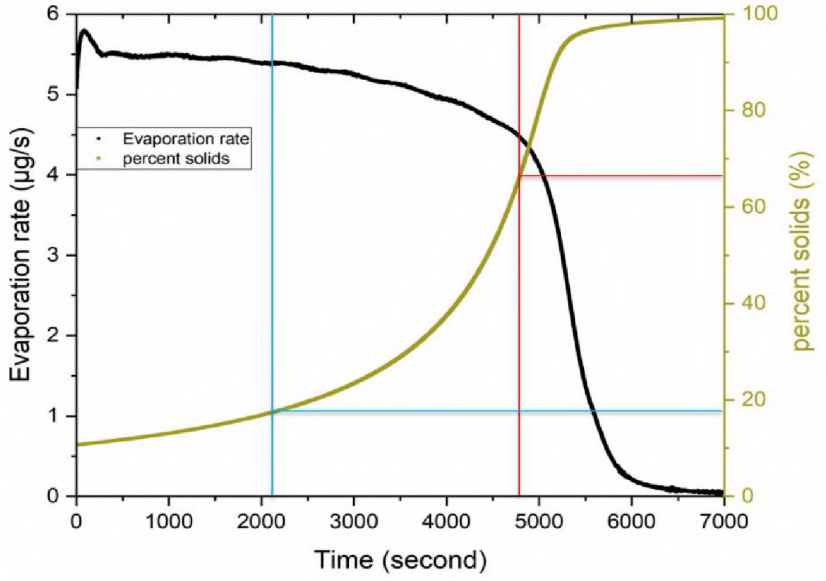

Figure 9. Evaporation rate of water in 10.12% Polymer 1 CUP solution.

The demonstration of using CUP as an additive in a paint to improve wet edge retention and open time was is shown in Table 7. With CUP as an additive in the paint, the evaporation rate data in Figure 8&9 and the effects in regions II&III clearly indicate the effect and mechanism for their mode of action. CUPs may have the potential to be use

as film formation inhibitor that can improve the open time and wet edge time for waterborne dispersion paints.

Table 7. Wet edge retention and open time.

CUP	Wet edge (second)	Open time (second)
0 lbs	240	360
20 lbs	360	480
30 lbs	360	480
40 lbs	480	600

The doubling of the wet edge and almost doubling of the open time are very impressive especially if it were being used as a freeze thaw additive. CUPs are the first wet edge and open time additive that offers a no VOC solution for this problem.

4. CONCLUSIONS

This work discussed the thermal properties of surface water in CUP systems. Based on the heat of fusion determined by DSC, it was found that surface water occupied a significant amount of CUP solutions, and surface water doesn't freeze even at -40 °C, making CUP a great candidate as a new type of freeze thaw stabilizer. In addition, TGA evaluation of the drying of cup solutions indicate a more rapid dry initially followed by a decrease in the rate of evaporation resulting in early viscosity build reducing pigment mobility and an even slower dry at the end giving more open time and better wet edge retention. All are excellent properties for a water borne coating and at zero VOC.

ACKNOWLEDGEMENTS

The authors would like to thank the Department of Chemistry for use of the DSC and the Missouri S&T Coatings Institute for financial support.

REFERENCES

1. Van De Mark, MR, Natu, A., Chen, M, Hancock, C, Riddles, C, "Molecular Weight(Mn) and Functionality Effects on CUP Formation and Stability." *J. Coat. Technol. Res.*, 11 (2) 111-122 (2014)

2. Riddles, C, Zhao, W, Hu, HJ, Chen, M, Van De Mark, MR, "Self-assembly of Water insoluble Polymers into Colloidal Unimolecular Polymer (CUP) Particles of 3-9 nm." *Polymer*, 55 48-57 (2013)

3. Vidulich, GA, Evans, DF, Kay, RL, "The Dielectric Constant of Water and Heavy Water between 0 and 40 °C." *J. Phys. Chem.*, 71 (3) 656-662 (1967)

4. Millich, F, Hellmuth, EW, Huang, SY, "Rigid rod-random coil transformation, Mark-Houwink constants, and Millich's intrinsic isoviscosity, [η]M, and isohydrodynamic volume, [η]MMM." *J. Polym. Sci. A.*, 13 (9) 2143-2150 (1975)

5. Geng, P, Zore, A, Van De Mark, MR, "Thermodynamic Characterization of Free and Surface Water of Colloidal Unimolecular Polymer (CUP) Particles Utilizing DSC." *Polymers.*, 12 (6) 1417 (2020)

6. Aseyev, VO, Tenhu, H, Klenin, SI, "Contraction of a Polyelectrolyte upon Dilution. Light-Scattering Studies on a Polycation in Saltless Water-Acetone Mixtures." *Macromolecules.*, 31 7717-7722 (1998)

7. Dobrynin, AV, Rubinstein, M, Obukhov, SP, "Cascade of Transitions of Polyelectrolytes in Poor Solvents." *Macromolecules.*, 29 2974-2979 (1996)

8. Alabarse, FG, Haines, J, Cambon, O, Levelut, C, Bourgogne, D, Haidoux, A, Granier, D, Coasne, B, "Freezing of Water Confined at the Nanoscale." *Phys. Rev. Lett.*, 109 035701 (2012)

9. Mistry, JK, Van De Mark, MR, "Aziridine Cure of Acrylic Colloidal Unimolecular Polymers(CUPs)." *J. Coats. Technol. Res.*, 10 (4) 453-463 (2013)

10. Mistry, JK, Natu, A, Van De Mark, MR, "Synthesis and Application of Acrylic Colloidal Unimolecular Polymers as a Melamine Thermoset System." *J. Appl. Polym. Sci.*, 40916 (2014)

11. Natu, A, Van De Mark, MR, "Synthesis and Characterization of an Acid Catalyst for Acrylic-melamine Resin System based on Colloidal Unimolecular Polymer(CUP) Particles of MMA-AMPS." *Progress in Organic Coatings*, 81 35-46 (2015)

12. Gade, SV, "Application of Colloidal Unimolecular Polymer(CUP) Particles in Coatings." Doctoral Dissertation, 2446 (2015)

13. Bosen, SF, Bowles, WA, Ford, EA, Person, BD, "Antifreezes." *In: Ullmann's Encyclopedia of Industrial Chemistry*, A3, 5th ed. (1985)

14. Reuvers, AJ, "Control of Rheology of Water-born Paints Using Associative Thickeners." *In: Proceedings of the International Conference on Organic Coating:Water-borne, High Solids, Powder Coating,* 24th ed. (1998)

15. Cooke, P, Delatycki, O, Kershaw, R, Sang, W, "The Brushing Characteristics of Latex Paints." *J. Oil Col. Chem. Assoc.*, 55 275-284 (1972)

16. Collins, MJ, Taylor, JW, Martin, RA, "Zero and Near-Zero VOC Interior Glossy Architectural Coatings." *213th ACS National Meeting*, San Francisco 1997

17. Storfer, S, DiPiazza, J, Moran, R, "Isoparaffins Impart Beneficial Properties to Coatings." Journal of Coating Technology, 60 37-43 (1988)

18. Kan, CS, "Role of Particle Size on Latex Deformation During Film Formation." *Journal of Coating Technology*, 71 89-97 (1999)

19. Radičević, RZ, Budinski-Simendić, JK, "The Effects of Alkyd/Melamine Resin Ratio and Curing Temperature on the Properties of the Coatings." *J. Serb. Chem. Soc.*, 70 593-599 (2005)

20. Li, F, Larock, RC, "New Soybean Oil-Styrene-Divinylbenzene Thermosetting Copolymers. III. Tensile Stress-Strain Behavior." *J. Polym. Sci.*, 39 60-77 (2001)

21. Laferte, VO, "All Layers Count: Silica Nanopartilces in the Optimisation of Scratch and Abrasion Resistance of High Performance UV Multi-Layer Coatings." *European Coatings Journal*, 6 34-36 (2006)

22. Schaller, EJ, "Critical Pigment Volume Concentration of Emulsion Based Paints." *Journal of Paint Technology*, 40 433-438 (1968)

23. Craver, JK, Tess, RW, "Applied Polymer Science." *Organic Coatings and Plastics Division*, ACS. 1975

24. Repenning, D, "Nanodispersed Hardened Chrome Coatings. Variable Properties for a Wide Range of Applications." *Galvanotechnik*, 91 2878-2883 (2000)

25. Fernando, R, "Nanomaterial technology applications in coatings." *JCT Coatings Tech.*, 1 (5) 32-38 (2004)

26. Van De Mark, MR, Zore, A, Geng, P, Zheng, Fei, "Colloidal Unimolecular Polymer Particles: CUP." *In: Single-Chain Polymer Nanoparticles*, pp. 259-312. Wiley Publishers, (2017)

27. Chen, M, Riddles, CJ, Van De Mark, MR, "Electroviscous Contribution to the Rheology of Colloidal Unimolecular Polymer(CUP) Particles in Water." *Langmuir*, 29 (46) 14034-14043 (2013)

28. Hales, TC, "A Proof of the Kepler Conjecture." *Annals of Mathematics*, 162 1065-1195 (2005)

29. Alexander, S, Chaikin, PM, Grant, P, Morales, GJ, Pincus, P, Hone, D, "Charge Renormalization, Osmotic Pressure, and Bulk Modulus of Colloidal Crystals:Theory." *J. Chem. Phys.*, 5776-5781 (1984)

SECTION

1. CONCLUSIONS AND FUTURE WORK

1.1. CONCLUSIONS

In this dissertation, the thermal properties of CUPs with different molecular weight, monomer ratio and CUP surface charge density (ions per nm^2) were investigated based on the heat of fusion, specific heat and melting point depression aspects. It was found that surface water occupied a significant amount of volume in CUP solutions, that doesn't freeze even at 258.15 K. Rapid cooling of CUP solutions will result in larger amount of surface water due to more rapid ice crystal growth and less time for CUP particles to migrate and undergo Manning condensation. The effect of cooling rate is less on the higher weight fraction solutions due to charge charge repulsion which lowers mobility. The density of surface water was calculated and ranged from 1.023 g/ml to 1.056 g/ml depending on the surface charge density. The thickness of surface water was calculated, showing a dependency with surface charge density. However, as the weight fraction of CUP particles increased to above approximately 20%, inter-molecular counterion condensation occurs and decreases surface water layer thickness. The melting point depression was found to linearly dependent upon molality of CUPs with the slope being related to the number of ions on the surface of CUPs. The average area of carboxylate and ester groups were determined, based on the measured melting point depression, and its results are independent of the molecular weight. The specific heat of surface water was found to be 3.07 to 3.09 J/g·K at 293.15 K and 3.04 to 3.07 J/g·K at

253.15 K, which was between ice and free water and exhibited a small dependency with the surface charge density.

Furthermore, evaporation rate of CUP solutions were determined using TGA. Results indicated that CUP was able to cause interface water deformation due to inter-particle charge repulsion, which increases the surface area and reduces surface tension, that increases the evaporation rate. The particle size, the viscosity, in another word, the mobility of CUP particles and water molecules are also important factors for the evaporation rate. The CUP solution with higher initial percent solids has a higher evaporation rate in the beginning of the isothermal process, due to more surface tension reduction and increased surface area as a result. During the isothermal process, the evaporation rate decreased, because of the combination of the effect of decrease in air-water interface temperature, limited mobility of water molecules and CUP particles by the increased viscosity. When reaching RCP and HCP, the movement of free water molecules were highly retarded, that caused significant evaporation rate reduction. Surface water didn't evaporate until all free water evaporated, and presented a slower evaporation rate. Water molecules associated with the carboxylate groups on CUP surface evaporated last. In addition, TGA was capable of determination of the vapor pressure of CUP samples by measuring the evaporation rate of CUP solutions.

In addition, with the significant amount of non-freezable surface water, CUP can be considered as a great candidate for a new type of freeze thaw stabilizer. TGA evaluation of the drying of cup solutions indicate a more rapid dry initially followed by a decrease in the rate of evaporation resulting in early viscosity build reducing pigment

mobility and an even slower dry at the end giving more open time and better wet edge retention. All are excellent properties for a water borne coating and at zero VOC.

1.2. FUTURE WORK

Van De Mark et al. successfully synthesized CUP particles from [2-(methacryloyloxy)ethyl]trimethylammonium chloride, and sulfonate functional CUPs. The surface water behavior in these systems need to be investigated. CUPs could also be modified to have intra-CUP crosslinking. To evaluate the HCP model, Neutron Scattering is expected to investigate the microscopic dynamic properties and static structure of CUP system with high concentration (at or above the gel point) and at low temperature, near zero, to minimize movement.

BIBLIOGRAPHY

[1] Van De Mark, M. R.; Natu, A.; Gade, S. V.; Chen, M.; Hancock, C.; Riddles, C. Molecular Weight(Mn) and Functionality Effects on CUP Formation and Stability. *J. Coat. Technol. Res.* **2014**, *11*, 111-122.

[2] Chen, M., Riddles, C. Van De Mark, M. Gel point behavior of colloidal unimolecular polymer (CUP) particles. *Colloid Polym Sci*. **2013**, *291*, 2893–2901.

[3] Vidulich, G. A.; Evans, D. F.; Kay, R. L. The Dielectric Constant of Water and Heavy Water between 0 and 40. degree. *J. Phys. Chem.* **1967**, *71*, 656-662.

[4] Chen, M.; Van De Mark, M. R. Rheology Studies on Colloidal Unimolecular Polymer (CUP)Particles in Absence of NaCl. *Preprints*. **2011**, *52*, 336-337.

[5] Natu, A.; Van De Mark, M. R. Synthesis and characterization of an acid catalyst for acrylic-melamine resin systems based on colloidal unimolecular polymer (CUP) particles of MMA-AMPS. *Progress in Organic Coatings*. **2015**, *81*, 35-46.

[6] Wilenbacher, J.; Altintas, O.; Roesky, P. W.; Barner-Kowollik, C. Single-Chain Self-Folding of Sythetic Polymers Induced by Metal-Ligand Complexation. *Macromol. Rapdi Commun*. **2014**, *35*, 45-51.

[7] Cheng, L.; Hou, G.; Miao, J.; Chen, D.; Jiang, M.; Zhu, L. Efficient Synthesis of Unimolecular Polymeric Janus Nanoparticles and Their Unique Self-Assembly Behavior in a Common Solvent. *Macromolecules*. **2008**, *41*, 8159-8166.

[8] Perez-Baena, I.; Asenjo-Sanz, I.; Arbe, A.; Moreno, A. J.; Verso, F.; Colmenero, J.; Pomposo, J. A. Efficient Route to Compact Single-Chain Nanoparticles: Photoactivated Synthesis via Thiol-Yne Coupling Reaction. *Macromolecules*. **2014**, *47*, 8270-8280.

[9] Terashima, T.; Sugita, T.; Fukae, K.; Sawamoto, M. Synthesis and Single-Chain Folding of Amphiphilic Random Copolymers in Water. *Macromolecules*. **2014**, *47*, 589-600.

[10] Aseyev, V. O.; Tenhu, H.; Klenin, S. I. Contraction of a Polyelectrolyte upon Dilution. Light-Scattering Studies on a Polycation in Saltless Water-Acetone Mixtures. *Macromolecules*. **1998**, *31*, 7717-7722.

[11] Dobrynin, A. O.; Rubinstein, M.; Obukhov, S. P. Cascade of Transitions of Polyelectrolytes in Poor Solvents. *Macromolecules*. **1996**, *29*, 2974-2979.

[12] Geng, P.; Zore, A.; Van De Mark, M. R. Thermodynamic Characterization of Free and Surface Water of Colloidal Unimolecular Polymer (CUP) Particles Utilizing DSC. *Polymers*. Accepted.

[13] Geng, P.; Gade, S. V.; Van De Mark, M. R. DSC and TGA Characterization of Free and Surface Water of Colloidal Unimolecular Polymer (CUP) Particles for Coatings Applications. *J. Coat. Technol. Res*. Accepted.

[14] Roy, R. K.; Lutz, J. Compartmentalization of Single Polymer Chains by Stepwise Intramolecular Cross-Linking of Sequence-Controlled Macromolecules. *J. Am. Chem. Soc*. **2014**, *136*, 12888-12891.

[15] Newton, R.; Gortner, R. A. A Method for Estimating Hydrophilic Colloid Content of Expressed Plant Tissue Fluids. *Bot. Gaz*. **1922**, *74*, 442-446.

[16] Bockris, J. O.; Conway, B. E.; Yeager, E. Comprehensive Treatise of Electrochemistry. *Angewandte*. **1981**, *93*, 840.

[17] Fawcett, W. R.; Levine, S.; deNobriga, R. M.; McDonald, A. C. A molecular model for the dielectric properties of the inner layer at the mercury/aqueous solution interface. *J. Electroanal. Chem*. **1980**, *111*, 163-180.

[18] Lee, C.; McCammon, J. A.; Rossky, P. J. The structure of liquid water at an extended hydrophobic surface. *J. Chem. Phys*. **1984**, *80*, 4448-4455.

[19] Patey, G. N.; Torrie, G. M. Water and salt water near charged surface: a discussion of some recent theoretical results. *Chemica Scripta*. **1989**, *29*, 39-47.

[20] Schmickler, W.; Henderson, D. New model for the structure of the electrochemical interface. *Progr. Surf. Sci*. **1987**, *22*, 323-420.

[21] Price, D.; Halley, J. W. Electronic structure of metal-electrolyte surfaces: Three-dimensional calculation. *Phys. Rev. B*. **1988**, *38*, 9357-9367.

[22] Glosli, J. N.; Philpott, M. R. Molecular-dynamics simulation of adsorption of ions from aqueous media onto charged electrodes. *J. Chem. Phys*. **1992**, *96*, 6962-6969.

[23] Spohr, E. Computer simulation of the water/platinum interface. *J. Phys. Chem*. **1989**, *93*, 6171-6180.

[24] Raghavan, K.; Foster, K.; Berkowitz, M. Comparison of the structure and dynamics of water at the platinum(111) and platinum(100) interfaces: molecular dynamics study. *Chem. Phys. Lett*. **1991**, *177*, 426-432.

[25] Nagy, G.; Heinzinger, K. A molecular dynamics study of water monolayers on charged platinum walls. *J. electroanalyt. Chem*. **1992**, *327*, 25-30.

[26] Aloisi, G.; Foresti, M. L.; Guidelli, R. A Monte Carlo simulation of water molecules near a charged wall. *J. Chem. Phys.* **1989**, *91*, 5592-5596.

[27] Ling, C. S.; Hansen, W. D. DTA Study of Water in Porous Glass. *Adsorption at Interface*. **1975**, *8*, 129-156.

[28] Toney, M. F.; Howard, J. N.; Richer, J.; Borges, G. L.; Gordon, J. G.; Melroy, O. R.; Wiesler, D. G.; Yee, D.; Sorensen, L. B. Voltage-dependent ordering of water molecules at an electrode-electrolyte interface. *Nature*. **1994**, *368*, 444-446.

[29] Toney, M. F.; Howard, J. N.; Richer, J.; Borges, G. L.; Gordon, J. G.; Melroy, O. R.; Wiesler, D. G.; Yee, D.; Sorensen, L. B. Distribution of water molecules at Ag(111)/electrolyte interface as studied with surface X-ray scattering. *Surface Science*. **1995**, *335*, 326-332.

[30] Katayama, S.; Fujiwara, S. NMR study of the spatial effect of polyacrylamide gel upon the water molecules confined in it. *J. Am. Chem. Soc.* **1979**, *101*, 4485-4488.

[31] Van De Mark, M. R.; Zore, A.; Geng, P.; Zheng, F. Colloidal Unimolecular Polymer Particles: CUP. In *Single-Chain Polymer Nanoparticles.* Pomposo, J. A. **2017**, 259-312.

[32] Mamontov, E. Dynamics of surface water in ZrO2 studied by quasielastic neutron scattering. *J. Chem. Phys.* **2004**, *121*, 9087-9097.

[33] Hatakeyema, T.; Yamauchi, A. Studies on bound water in poly(vinyl alcohol) hydrogel by DSC and FT-NMR. *Eur. Polym. J.* **1984**, *20*, 61-64.

[34] Ostrowska-Czubenko, J.; Pierog, M.; Gierszewska-Druzynska, M. State of water in noncrosslinked and crosslinked hydrogel chitosan membranes-DSC studies. *Pol. Tow. Chitynowe*. **2011**, *XVI*, 147-156.

[35] Oncley, J. L. Evidence from Physical Chemistry Regarding the Size and Shape of Protein Molecules from Ultra-centrifugation, Diffusion, Viscosity, Dielectric Dispersion, and Double Refraction of Flow. *Annals of the New York Academy of Science*. **1941**, *41*, 121-150.

[36] Erko, M.; Findenegg, G. H.; Cade, N.; Michette, A. G.; Paris, O. Confinement-induced structural changes of water studied by Raman scattering. *Phys. Rev.B.* **2011**, *84*, 104205.

[37] Lee, K. Y.; Ha, W. S. DSC studies on bound water in silk fibroin/S-carboxymethyl kerateine blend films. *Polymer*. **1999**, *40*, 4131-4134.

[38] Higuchi, A.; Lijima, T. DSC investigation of the states of water in poly(vinyl alcohol) membranes. *Polymer*. **1985**, *26*, 1207-1211.

[39] Ratto, J.; Hatakeyama, T.; Blumstein, R. B. Differential scanning calorimetry investigation of phase transitions in water/chitosan systems. *Polymer*. **1995**, *36*, 2915-2919.

[40] Garti, N.; Aserin, A.; Ezrahi, S.; Tiunova, I.; Berkovic, G. Water Behavior in Nonionic Surfactant Systems I: Subzero Temperature Behaviour of Water in Nonionic Microemulsions Studied by DSC. *J. Colloid Interface Sci*. **1995**, *178*, 60-68.

[41] Tahmasebi, A.; Yu, J.; Su, H.; Han, Y.; Lucas, H.; Zheng, H.; Wall, T. A differential scanning calorimetric (DSC) study on the characteristics and behaviour of water in low-rank coals. *Fuel*. **2014**, *135*, 243-252.

[42] Monti, D.; Chetoni, P.; Burgalassi, S.; Najarro, M.; Saettone, M. F. Increased corneal hydration induced by potential ocular penetration enhancers: assessment by differential scanning calorimetry (DSC) and by desiccation. *Int. J. Pharm*. **2002**, *232*, 139-147.

[43] Garti, N.; Aserin, A.; Tiunova, I.; Fanun, M. A DSC study of water behaviour in water-in-oil microemulsions stabilized by sucrose esters and butanol. *Colloids Surf. A*. **2000**, *170*, 1-18.

VITA

Peng Geng was born in Xuzhou, Jiangsu Province, China. He received his Bachelor's degree in Chemical Engineering from Jiangsu Normal University in July 2010. Peng Geng received his Doctor of Philosophy degree in Chemistry from Missouri University of Science and Technology in August 2020.